

EXPERIMENTAL VERIFICATION OF CH<sub>4</sub>-CO<sub>2</sub> SWAP IN METHANE-  
PROPANE-CARBON DIOXIDE MIXTURE HYDRATES

A THESIS SUBMITTED TO  
THE GRADUATE SCHOOL OF NATURAL AND APPLIED SCIENCES  
OF  
MIDDLE EAST TECHNICAL UNIVERSITY

BY

ABBAS ABBASOV

IN PARTIAL FULFILLMENT OF THE REQUIREMENTS  
FOR  
THE DEGREE OF MASTER OF SCIENCE  
IN  
PETROLEUM AND NATURAL GAS ENGINEERING

AUGUST 2014



Approval of the thesis:

**EXPERIMENTAL VERIFICATION OF CH<sub>4</sub>-CO<sub>2</sub> SWAP IN METHANE-  
PROPANE-CARBON DIOXIDE MIXTURE HYDRATES**

submitted by **ABBAS ABBASOV** in partial fulfillment of the requirements for the degree of **Master of Science in Petroleum and Natural Gas Engineering Department, Middle East Technical University** by,

Prof. Dr. Canan Özgen

Dean, Graduate School of **Natural and Applied Sciences** \_\_\_\_\_

Prof. Dr. Mahmut Parlaktuna

Head of Department, **Petroleum and Natural Gas Engineering** \_\_\_\_\_

Prof. Dr. Mahmut Parlaktuna

Supervisor, **Petroleum and Natural Gas Engineering Dept., METU** \_\_\_\_\_

**Examining Committee Members:**

Asst. Prof. Dr. Çağlar Sınayuç

Petroleum and Natural Gas Engineering Dept., METU \_\_\_\_\_

Prof. Dr. Mahmut Parlaktuna

Petroleum and Natural Gas Engineering Dept., METU \_\_\_\_\_

Asst. Prof. Dr. Ismail Durgut

Petroleum and Natural Gas Engineering Dept., METU \_\_\_\_\_

Dr. Sevtaç Bülbül

Petroleum Research Center, METU \_\_\_\_\_

Uğur Karabakal, M.Sc.

Research Center, Turkish Petroleum Corporation \_\_\_\_\_

Date: 21.08.2014

**I hereby declare that all information in this document has been obtained and presented in accordance with academic rules and ethical conduct. I also declare that, as required by these rules and conduct, I have fully cited and referenced all material and results that are not original to this work.**

Name, Last name: Abbas Abbasov

Signature:

## ABSTRACT

### EXPERIMENTAL VERIFICATION OF CH<sub>4</sub>-CO<sub>2</sub> SWAP IN METHANE- PROPANE-CARBON DIOXIDE MIXTURE HYDRATES

Abbasov, Abbas

M.S., Department of Petroleum and Natural Gas Engineering

Supervisor: Prof. Dr. Mahmut Parlaktuna

August 2014, 101 pages

Significant interest has been given to unconventional hydrocarbon resources in recent years. Natural gas hydrates are one of the key components of unconventional hydrocarbon resources to be addressed. However, energy utilization from hydrate reservoirs is challenging and related researches are still being carried out. Recently, a method in which methane gas (CH<sub>4</sub>) is recovered from natural gas hydrate formations by injection of carbon dioxide (CO<sub>2</sub>) has been proposed. This method is considered to be a promising solution to simultaneously access an unconventional fossil fuel reserve and reduce atmospheric CO<sub>2</sub> increase.

In this study, formation of natural gas hydrate in porous media at laboratory conditions was carried out by using a mixture of gases: methane (CH<sub>4</sub>), propane (C<sub>3</sub>H<sub>8</sub>) and carbon dioxide (CO<sub>2</sub>). Composition of the gas mixture was obtained from the results of the investigations of the Black Sea hydrate depositions, carried out by “The Institute of Marine Sciences and Technology” of Dokuz Eylul University in Izmir, Turkey. The following mole percent of the gases was used throughout experiments in order to simulate hydrate reservoir conditions of the Black Sea: CH<sub>4</sub> (95%), C<sub>3</sub>H<sub>8</sub> (3%) and CO<sub>2</sub> (2%).

It was shown that CH<sub>4</sub>-CO<sub>2</sub> swap process takes place in CH<sub>4</sub>-C<sub>3</sub>H<sub>8</sub>-CO<sub>2</sub> mixture hydrates as in the case of pure methane hydrates. Based on the results of this study,

it was also observed that injection of CO<sub>2</sub> into hydrate media caused release of propane which exhibits sII type hydrate structure.

**Keywords:** Natural gas hydrates, CH<sub>4</sub>-CO<sub>2</sub> swap, unconventional hydrocarbon resources, CO<sub>2</sub> sequestration.

## ÖZ

### METAN-PROPAN-KARBON DİOKSİT KARIŞIM HİDRATLARINDA CH<sub>4</sub>-CO<sub>2</sub> YER DEĞİŞİMİNİN DENEYSEL DOĞRULANMASI

Abbasov, Abbas

Yüksek Lisans, Petrol ve Doğal Gaz Mühendisliği Bölümü

Tez Yöneticisi: Prof. Dr. Mahmut Parlaktuna

Ağustos 2014, 101 sayfa

Son yıllarda geleneksel olmayan hidrokarbon kaynaklarına yüksek önem verilmektedir. Geleneksel olmayan hidrokarbon kaynaklarının en önemlilerinden biri de doğal gaz hidratlarıdır. Ancak, hidrat rezervuarlarından enerji elde edilmesi oldukça zordur ve ilgili araştırmalar hala sürdürülmektedir. Son zamanlarda, doğal hidrat oluşumlarındaki metan (CH<sub>4</sub>) gazının, karbondioksit (CO<sub>2</sub>) enjeksiyonu yöntemiyle üretilmesi önerilmiştir. Bu yöntem aynı zamanda geleneksel olmayan bir fosil yakıt rezervine erişmek ve atmosferdeki CO<sub>2</sub> artışını azaltmak için bir çözüm olarak kabul edilmektedir.

Bu çalışmada, gözenekli ortamda doğal gaz hidratının oluşumu, laboratuvar koşullarında metan (CH<sub>4</sub>), propan (C<sub>3</sub>H<sub>8</sub>) ve karbondioksit (CO<sub>2</sub>) gaz karışımları kullanılarak gerçekleştirilmiştir. Gaz karışım kompozisyonu, İzmir Dokuz Eylül Üniversitesi 'Deniz Bilimleri ve Teknolojisi Enstitüsü' tarafından Karadeniz'de hidrat kaynaklarını araştırmak amacıyla yürütülen çalışmaların sonuçlarına göre belirlenmiştir. Buna göre gaz karışımı CH<sub>4</sub> (95 %), C<sub>3</sub>H<sub>8</sub> (3 %) ve CO<sub>2</sub> (2 %) olarak hazırlanmıştır ve tüm karışım hidrat deneylerinde belirtilen mol yüzdeleri kullanılmıştır.

CH<sub>4</sub>-CO<sub>2</sub> yer değişiminin metan hidratında olduğu gibi CH<sub>4</sub>-C<sub>3</sub>H<sub>8</sub>-CO<sub>2</sub> karışım hidratında mümkün olduğu gösterilmiştir. Ayrıca, bu çalışmanın sonuçları hidrat

ortamının ierisine CO<sub>2</sub> enjeksiyonunun sII tip hidrat yapısına sahip olan propanın aıęa ıkmasına neden olduęunu gstermiřtir.

**Anahtar Kelimeler:** Doęal gaz hidratları, CH<sub>4</sub>-CO<sub>2</sub> yer deęiřimi, geleneksel olmayan hidrokarbon kaynakları, CO<sub>2</sub> depolama.



To My mother Tamella Abbasova, father Ismayil Abbasov, and brother Tural  
Abbasov

## ACKNOWLEDGEMENT

Foremost, I would like to express my sincere gratitude to my advisor Prof. Mahmut Parlaktuna for his continuous support during my MSc study and research, for his patience, motivation, enthusiasm, and immense knowledge. Prof. Mahmut Parlaktuna helped me not only in my thesis, but in guiding through my two year education at the department of Petroleum and Natural Gas Engineering. Also I would like to thank Prof. Parlaktuna for his support in getting MSc scholarship from BP Caspian for my studies, and helping me to get acquainted with the working environment at the department. Opportunity provided by him to carry out my experimental studies and whole work in the department is invaluable.

Secondly, I would like to express my great thankfulness to Şükrü Meray, who is currently a PhD student at the department of Petroleum and Natural Gas Engineering. Şükrü helped me a lot during experiments, shared his knowledge. We became friends very quickly after getting acquainted and time we spent in laboratory, in the department, and in the campus of METU will never be forgotten. I wish him a great success throughout his journey of becoming an academic staff in the area of Petroleum Engineering. Hope to see you soon, Şükrü!

Special thanks go to the technical staff of the department, namely; Murat Akın, Naci Doğru and Murat Çalışkan. The assistance by chemistry technician, Murat Akın during experiments, and his friendship is highly appreciated.

I am grateful to the thesis committee members for their valuable comments and recommendations.

I would like to thank METU Petroleum Research Center for carrying out Gas Chromatography analyses. The help of Mr. Mutlu Ugurlu is highly appreciated.

I would like to express my gratitude to my family for their continuous support during my entire life including undergraduate and graduate years at METU and

friends for their motivation including Ali Etemadi, Arman Afrasiyabi, Yashar Osguie, Arash Ebrahimi and others.

I would like to express my gratitude to my cousin Zeka Fataliyev, who helped me during my visits to Baku. I wish him and his family, his wife Aytekin, his son Nihat and daughter Nermin great happiness and joy throughout their life.

## TABLE OF CONTENTS

ABSTRACT .....	v
ÖZ.....	vii
ACKNOWLEDGEMENT.....	x
TABLE OF CONTENTS .....	xii
LIST OF TABLES .....	xiv
LIST OF FIGURES.....	xv
CHAPTERS	
1. INTRODUCTION.....	1
2. NATURAL GAS HYDRATES.....	5
2.1 Structural Characteristics of Natural Gas Hydrates .....	6
2.2 Chemical and Physical Properties of Natural Gas hydrates .....	11
2.3 Formation of Marine Natural Gas Hydrates.....	12
2.3.1 Gas Origin .....	12
2.3.2 Effect of Temperature and Pressure on Hydrate Stability.....	14
2.4 Characteristics of Hydrate Distribution and Reserves .....	15
2.4.1 Characteristics of Distribution.....	15
2.4.2 Resource Reserves Prediction .....	19
2.5 Prospecting Techniques.....	20
2.5.1 Seismic Technique .....	20
2.5.2 Drilling to Get Cores .....	22
2.5.3 Logging Methods .....	22
2.5.4 Geochemical Exploration .....	23
3. A REVIEW ON RESEARCH ON CH <sub>4</sub> REPLACEMENT BY CO <sub>2</sub> IN NATURAL GAS HYDRATES.....	25
3.1 Thermodynamics and Fundamentals.....	25
3.2 Kinetics of Replacement Mechanism.....	28
3.3 Accomplished Experimental Studies on Replacement Reaction .....	31
3.3.1 Replacement of CH <sub>4</sub> Hydrate by Gaseous CO <sub>2</sub> .....	32

3.3.2 Replacement of CH <sub>4</sub> Hydrate by Liquid CO <sub>2</sub> .....	35
3.3.3 Replacement of CH <sub>4</sub> Hydrate by CO <sub>2</sub> Emulsion.....	39
4. STATEMENT OF THE PROBLEM .....	45
5. EXPERIMENTAL SET-UP AND PROCEDURE .....	47
5.1 Experimental Equipment.....	47
5.2 Experimental Procedures .....	53
6. EXPERIMENTAL RESULTS AND DISCUSSION.....	57
6.1 Pure Methane Hydrate Formation (Run #1).....	59
6.2 “Memory Effect” of Pure Methane Hydrate (Run #2).....	61
6.3 CH <sub>4</sub> -C <sub>3</sub> H <sub>8</sub> -CO <sub>2</sub> Mixture Hydrate Formation (Run #3) .....	65
6.4 “Memory Effect” of CH <sub>4</sub> -C <sub>3</sub> H <sub>8</sub> -CO <sub>2</sub> Mixture Hydrates (Run #4).....	70
6.5 CO <sub>2</sub> Injection from Constant Pressure Supply (Run #5) .....	73
6.6 Replacement of Free Gas with CO <sub>2</sub> (Run #6).....	79
6.7 Repeatability of Replacement of Free Gas with CO <sub>2</sub> Experiment (Run #7).....	84
7. CONCLUSION .....	91
8.RECOMMENDATION .....	93
REFERENCES.....	95

## LIST OF TABLES

### TABLES

Table 2-1: Comparison of crystal structure of gas hydrate (Ye and Liu, 2013).....	8
Table 2-2: Ratio of molecular diameters to cavity diameters for Natural Gas Hydrate formers and a few others (Sloan, 1998).....	10
Table 2-3: Comparison of properties of methane hydrate and ice (Ye and Liu, 2013) .....	11
Table 5-1: Specification of the apparatus used in experimental studies .....	50
Table 5-1: Specification of the apparatus used in experimental studies (Cont.) .....	51
Table 6-1: List of the experiments performed throughout this study.....	58
Table 6-2: Experimental parameters for Run #1 .....	59
Table 6-3: Experimental parameters of Run #3 .....	66
Table 6-4: Composition of the prepared gas mixture.....	66
Table 6-5: Sample 1 results .....	68
Table 6-6: Sample 2 results .....	71
Table 6-7: Experimental data for Run #5 .....	73
Table 6-8: Composition of the gas mixture at the end of hydrate formation .....	74
Table 6-9: Composition of the gas mixture at the end of CO <sub>2</sub> injection .....	79
Table 6-10: Experimental parameters for Run #6 .....	79
Table 6-11: Composition of the gas mixture during and after free gas replacement.....	82
Table 6-12: Experimental parameters for Run #7 .....	84
Table 6-13: Results for the replacement process of the free gas with CO <sub>2</sub> for “Repeatability Experiment” .....	86
Table 6-14: Trial 3 results for the replacement process of the free gas with CO <sub>2</sub> ...	88

## LIST OF FIGURES

### FIGURES

Figure 1-1: Four example study results which show varying CH <sub>4</sub> recovery percent from hydrate imposed to the injection of CO <sub>2</sub> (Schicks <i>et al.</i> , 2011) .....	3
Figure 2-1: Crystalline hydrate structure (Sloan, 1998).....	6
Figure 2-2: Unit structures of hydrate crystal (Sloan, 1998): (a) sI (b) sII, and (c) sH .....	7
Figure 2-3: Global distribution of natural gas hydrates (Ye and Liu, 2013).....	17
Figure 2-4: Gas hydrate samples from sediments of Hydrate Ridge. (a) Layered distribution. (b) Massive distribution (Ye and Liu, 2013) .....	18
Figure 3-1: CH <sub>4</sub> -CO <sub>2</sub> -H <sub>2</sub> O phase equilibrium diagram (Zhao <i>et al.</i> , 2012) .....	26
Figure 3-2: Schematic diagram of replacement of the guest molecule in the M-cage and the re-occupation of S-cage by CH <sub>4</sub> (Zhao <i>et al.</i> , 2012) .....	29
Figure 3-3: Schematic diagram of the experimental apparatus (Zhao <i>et al.</i> , 2012). .....	32
Figure 3-4: Amount of the decomposed CH <sub>4</sub> hydrate (Q <sub>CH<sub>4</sub>, Dec</sub> ) versus time (Ota <i>et al.</i> , 2005) .....	34
Figure 3-5: Amount of the formed CO <sub>2</sub> hydrate (Q <sub>CO<sub>2</sub>, Form</sub> ) versus time (Ota <i>et al.</i> , 2005) .....	34
Figure 3-6: Mole fraction of CH <sub>4</sub> and CO <sub>2</sub> in the hydrate phase as a function of time (Ota <i>et al.</i> , 2005) .....	37
Figure 3-7: CH <sub>4</sub> ratios replaced from the hydrate of the two different experiments (Zhou <i>et al.</i> , 2008).....	37
Figure 3-8: Evolution of CH <sub>4</sub> in the M-cages, S-cages and hydrate with time (Ota <i>et al.</i> , 2005) .....	38
Figure 3-9: Ratios of CH <sub>4</sub> replaced from the hydrate with different forms of CO <sub>2</sub> (Zhou <i>et al.</i> , 2008).....	41
Figure 3-10: CH <sub>4</sub> replacement rates with different forms of CO <sub>2</sub> (Zhou <i>et al.</i> , 2008) .....	41

Figure 3-11: Amount of the replaced CH <sub>4</sub> gas by gaseous CO <sub>2</sub> against time (Zhou <i>et al.</i> , 2008).....	42
Figure 3-12: Amount of the replaced CH <sub>4</sub> gas by CO <sub>2</sub> emulsion against time (Zhou <i>et al.</i> , 2008).....	42
Figure 5-1: High pressure cell used in experiments .....	48
Figure 5-2: Schematic representation of the experimental set-up .....	49
Figure 5-3: Experimental set-up (profile view).....	52
Figure 5-4: Experimental set-up (front view).....	52
Figure 6-1: Response of the system after first 118 hours .....	60
Figure 6-2: Segment of the increase in temperature at the point of hydrate formation .....	60
Figure 6-3: Investigation of “memory effect” .....	61
Figure 6-4: Illustration of hydrate formation for “Case 1” .....	62
Figure 6-5: Illustration of hydrate formation for “Case 2” .....	62
Figure 6-6: <i>P-T</i> diagram for two cases .....	63
Figure 6-7: Combination of responses for two cases after first 2 hours from the start of sharp decrease in slope in pressure, <i>i.e.</i> , observation of formation of first hydrate .....	65
Figure 6-8: Behavior of the system for the first 120 hours .....	67
Figure 6-9: Clear picture of formed hydrate in sand sediments .....	69
Figure 6-10: Inflammation of hydrate formed in sand sediments .....	70
Figure 6-11: Illustration of the system response until the end of “memory effect” ..	71
Figure 6-12: Combination of responses for two cases after first 2 hours from the start of sharp decrease in slope of pressure, <i>i.e.</i> , observation of formation of first hydrate .....	72
Figure 6-13: Combination of responses for two cases after first 6 hours from the start of sharp decrease in slope of pressure, <i>i.e.</i> , observation of formation of first hydrate .....	72
Figure 6-14: Illustration of hydrate formation for the first 104 hours.....	73
Figure 6-15: Schematic representation of constant carbon dioxide injection process .....	75



Figure 6-16: Response of the system from the start of CO <sub>2</sub> injection for 112 hours	75
Figure 6-17: Response of the system after another 145 hours .....	77
Figure 6-18: Response of the system upon injection of CO <sub>2</sub> from the top part of the cell after 50 hours.....	78
Figure 6-19: Schematic representation of replacement process.....	80
Figure 6-20: Total response of the system for the case of simultaneous CO <sub>2</sub> injection and free gas withdrawal .....	81
Figure 6-21: Response of the system during the first 4 hours from the start of the process of CO <sub>2</sub> injection and free gas removal .....	81
Figure 6-22: Detailed illustration of the effects of replacement process on the hydrate media .....	82
Figure 6-23: P-T diagram for mixture of gases during replacement (Run#6) .....	83
Figure 6-24: P-T diagram for mixture of gases after replacement (Run#6) .....	84
Figure 6-25: Response of the system during repeatability experiment.....	85
Figure 6-26: Detailed illustration of the effects of replacement of free gas by CO <sub>2</sub> in the case of repeatability experiment.....	85
Figure 6-27: P-T diagram for mixture of gases during replacement (Run#7) .....	87
Figure 6-28: P-T diagram for mixture of gases after replacement (Run#7) .....	87



## CHAPTER 1

### INTRODUCTION

Gas hydrate deposits which are found in deep seas and in permafrost region are supposed to be a fossil fuel reserve for the future. Methane gas is trapped inside these deposits of hydrate in the order of at least all conventional reservoirs (Collett, 2002; Max *et al.*, 2006). The estimates of methane gas in hydrate form fluctuate, subject to the assumptions made, numerical values for the estimates range between  $0.2 \times 10^{15} \text{ Sm}^3$  (standard temperature, standard pressure) and  $120 \times 10^{15} \text{ Sm}^3$  (Soloviev, 2002; Klauda and Sandler, 2005). When compared to conventional gas reserves of  $0.2 \times 10^{15} \text{ Sm}^3$  (Radler, 2000), the volume of gas in hydrate form is quite enormous. However, gas production from hydrate-bearing sediments is a challenging issue. Decomposition of gas hydrate is necessary in order to release gas from hydrate-bearing sediments. Hypothetically, decomposition can be realized by distorting mechanical equilibrium, thermal equilibrium or chemical equilibrium. Mechanical equilibrium distortion includes pressure reduction; thermal equilibrium distortion can be realized by heating, chemical equilibrium distortion can be achieved by injection of inhibitors or  $\text{CO}_2$  (in gaseous or liquid form). On the other hand, the phenomenon, known as  $\text{CH}_4\text{-CO}_2$  exchange or  $\text{CH}_4\text{-CO}_2$  replacement, creates a distinctive opportunity to recover an energy source, methane, and sequester  $\text{CO}_2$  in hydrate form. The difference in chemical potential between  $\text{CH}_4$  and  $\text{CO}_2$  hydrate reveals that  $\text{CH}_4\text{-CO}_2$  gas exchange is thermodynamically favorable. Also, the stability of a hydrate field can be maintained in order to avoid

potential slope slides and subsidence by replacing CH<sub>4</sub> with CO<sub>2</sub> (Beeskow-Strauch and Schicks, 2012).

It has been explained in theory that the exchange process between CH<sub>4</sub> in hydrate form and CO<sub>2</sub> is possible because of the fact that CO<sub>2</sub> is a very good hydrate forming molecule. Resultant CO<sub>2</sub> hydrate is secure at even higher temperatures at particular pressure conditions as compared to pure CH<sub>4</sub> case. However, in practice there are several other aspects which must be considered and their consideration were not carried out in the past. One example of such aspects is the formation of natural gas hydrates from a mixture of gases including CH<sub>4</sub>, CO<sub>2</sub>, C<sub>2</sub>H<sub>6</sub>, C<sub>3</sub>H<sub>8</sub>, H<sub>2</sub>S and etc. because it is very hard to encounter pure CH<sub>4</sub> hydrates in natural environments (Milkov, 2005). In reality, almost all natural gas hydrate deposits, which were encountered up to now, contain certain amount of some other hydrocarbons or other gases (Beeskow-Strauch and Schicks, 2012). Gas hydrates which exhibit structure I (sI) are usually rich in CH<sub>4</sub> molecules, but may also be rich in CO<sub>2</sub> and H<sub>2</sub>S. Biogenic CH<sub>4</sub> production is the origin for these hydrates and they are the most ample hydrate structure on earth (Kvenvolden, 1995). Gas molecules of thermo-genic origin build up structure II (sII) and structure H (sH) hydrates. They contain compounds starting from CH<sub>4</sub> up to butane and up to hexane for sII and sH, respectively (Sassen *et al.*, 1999; Lu *et al.*, 2007).

Several groups and institutions studied the replacement of CH<sub>4</sub> in the hydrate phase by CO<sub>2</sub> under lab conditions. It has been noted in the literature that the higher stability of CO<sub>2</sub> hydrate compared to CH<sub>4</sub> hydrate is supposed to be the driving force for the exchange reaction. Also, several studies have been carried out recently to investigate the exchange kinetics and to optimize the swapping process with respect to the recovery rate of CH<sub>4</sub> (Beeskow-Strauch and Schicks, 2012). Four example results of recovery rates as a result from CH<sub>4</sub>-CO<sub>2</sub> swapping processes from the literature are shown in Figure 1-1. The studies illustrated in Figure 1-1 were performed under different experimental conditions and can be described in more details as follows: approximately 560 cm<sup>3</sup> of water (31 moles) were filled by Hirohama *et al.* (1996) into a pressure vessel of volume 3.2 L, the cell was pressurized with CH<sub>4</sub> and conversion of 24 moles of water into a bulk CH<sub>4</sub> hydrate

phase was implemented. Liquid CO<sub>2</sub> replaced CH<sub>4</sub> gas phase afterwards. After about 800 hours the conversion of remaining free water (7 moles) and the transformation of about 15% CH<sub>4</sub> hydrate into CO<sub>2</sub> hydrate were observed. Much smaller hydrate samples prepared from powdered ice (size of particles and resulting hydrates: 5-50 μm) were investigated by Lee *et al.* (2003) in porous silica gel (pore size: 15 nm). Liquid CO<sub>2</sub> was offered in their study to the CH<sub>4</sub> hydrate phase and 50% CH<sub>4</sub> recovery was achieved after observation of a steady state conditions after 5 hours. The effect of additional N<sub>2</sub> on the swapping process was studied by Park *et al.* (2006). CH<sub>4</sub> hydrate form powdered ice together with CH<sub>4</sub> gas in a stirred reactor were synthesized by them before exposing the small amount of formed pure methane hydrate (approximately 1 cm<sup>3</sup>) to a N<sub>2</sub>/CO<sub>2</sub> gas mixture (80% N<sub>2</sub>, 20% CO<sub>2</sub>). Recovery of about 85% of CH<sub>4</sub> from hydrate phase after 24 hours was achieved in their experiments. Kvamme *et al.* (2007) investigated the process of CH<sub>4</sub>-CO<sub>2</sub> swap by forming hydrates in sand sediments. At the initial stage CH<sub>4</sub> hydrate was formed in sandstones and thereafter it was exposed to liquid CO<sub>2</sub>. Almost 60% of CH<sub>4</sub> was recovered from the hydrate phase within a time range of approximately 300 hours.

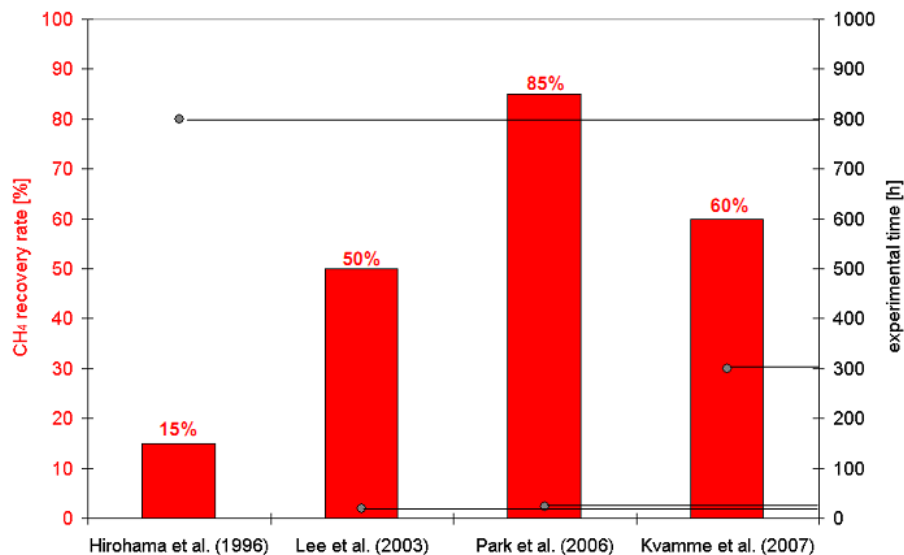


**Figure 1-1:** Four example study results which show varying CH<sub>4</sub> recovery percent from hydrate imposed to the injection of CO<sub>2</sub> (Schicks *et al.*, 2011)

In the study performed by Ors (2012) interaction of CO<sub>2</sub> and CH<sub>4</sub> hydrates were investigated together with sealing efficiency of CH<sub>4</sub> hydrate for determination of feasibility for CO<sub>2</sub> storage in the Black Sea sediments. In his study various experiments were performed such as formation of pure CH<sub>4</sub> hydrate both in bulk and porous media, permeability measurement of porous media at 30% and 50% hydrate saturation, and injection of gaseous CO<sub>2</sub> into the CH<sub>4</sub> hydrate. It was found that presence of hydrate significantly causes a decrease in porous media permeability and if 50% or higher hydrate saturation is achieved, the porous media can act as an impermeable cap. His investigation was concluded with the remark that it would be safe to store CO<sub>2</sub> in the hydrate stability region in deep sea sediments of the Black Sea.

But the investigation of forming hydrates from a mixture of gases and the effect of CO<sub>2</sub> upon injection into the system has not been studied thoroughly. The majority of studies which were carried out included only formation of pure CH<sub>4</sub> hydrate at laboratory conditions and injection of pure CO<sub>2</sub>. Investigation of the process of swapping of structure II CH<sub>4</sub>-C<sub>2</sub>H<sub>6</sub> mixed hydrates with CO<sub>2</sub> and CO<sub>2</sub>-N<sub>2</sub> gas mixtures was done by Park *et al.* (2006). According to the derived results, the recovery percentage of CH<sub>4</sub> is 92-95% and C<sub>2</sub>H<sub>6</sub> recovery percentage is 93%.

In this study formation of pure methane hydrate in porous media at laboratory conditions was carried out. Pressure and temperature versus time graphs were drawn during formation process as well, which were used to discuss properties of pure methane hydrate formation. Then, formation of natural gas hydrate in porous media by using mixture of gases (CH<sub>4</sub> + C<sub>3</sub>H<sub>8</sub> + CO<sub>2</sub>) was performed. Evaluation of its properties was implemented by taking samples for gas chromatography analysis and also by investigation of pressure and temperature versus time graphs.

Also, in this research, investigation of CH<sub>4</sub>-CO<sub>2</sub> swap in case of CH<sub>4</sub>-C<sub>3</sub>H<sub>8</sub>.CO<sub>2</sub> mixture hydrates and possible affection of other compounds in the mixture by the injected carbon dioxide was carried out experimentally. During experiments samples for gas chromatography analysis were taken as well in order to study the effects of injected CO<sub>2</sub>.

## CHAPTER 2

### NATURAL GAS HYDRATES

Natural gas hydrate, or clathrate, is a nonstoichiometric ice-like crystalline composite that is established by water and gas molecules (Figure 2-1). The formation of natural gas hydrate requires certain conditions. These conditions can be listed as follows:

- Temperature
- Pressure
- Gas saturation
- Water salinity
- pH

Natural gas hydrate is sometimes called as “flammable ice” or “combustible ice” because it can burn upon ignition. Polyhedral cages are the result of combination of water molecules in the hydrate through hydrogen bonds, and there is an accumulation of gas molecules inside the cages. Usually, natural gas hydrate is expressed as  $M \cdot nH_2O$ . The gas molecule in hydrate is represented by “M”, on the other hand “n” is the hydration number (number of water molecules). Example gases which arrange themselves in cages are methane ( $CH_4$ ), ethane ( $C_2H_6$ ), propane ( $C_3H_8$ ), carbon dioxide ( $CO_2$ ), nitrogen ( $N_2$ ), and hydrogen sulfide ( $H_2S$ ) (Ye and Liu, 2013).

The most common “guest” molecule which forms natural gas hydrate in nature is methane. When methane percentage as guest molecule reaches 99% in a hydrate structure, the natural gas hydrate is generally called as methane hydrate. Upon ignition methane or other hydrocarbon gas always burns and leaves few residues after combustion. Therefore, gas hydrate can be regarded as a relatively clean energy for the future compared to other fossil fuels known, including coal and oil. This fuel is made of colorless hydrocarbon and water molecules. But, it can be colorful and not always white in nature. As an example, there have been cases when yellow, orange and even red gas hydrate samples were identified from Gulf of Mexico. Hydrates found in the Atlantic are identified to be gray or blue. The reason for that difference in color has not been reached, but most probably the cause is the existence of some other substances (minerals, bacteria, or oil) (Ye and Liu, 2013).

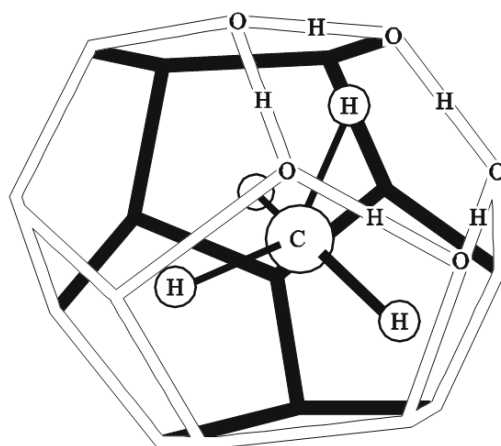


**Figure 2-1:** Crystalline hydrate structure (Sloan, 1998)

## 2.1 Structural Characteristics of Natural Gas Hydrates

Natural gas hydrate resembles appearance of snow and is usually of white color. Its crystals have a lattice structure which is compactly arranged. Crystals of natural gas hydrate have a structure very similar to ice. Water molecules are the host molecules in such ice-like crystals and they form a spatial polyhedral framework lattice structure with cavities. Diameter of cavities ranges from  $4.8 \times 10^{-10}$ -  $6.9 \times 10^{-10}$  m and they are the place where gas molecules (guest molecules) are located (Hu *et al.*, 2000). No stoichiometric relationship exists between the gas and water.



The latticed water molecules are attached by solid hydrogen bonds at low temperatures and high pressures (Ye and Liu, 2013). The gas and water molecules are tightly bonded by van der Waals force on the other hand. Gas hydrate has a structure that is very similar to that of crystalline compound, or compound inclusion. In a thermodynamic essence, an ideal crystalline model means that hydrate is formed through cavities in the hydrate framework. This hydrate framework can be described as follows: “loose” ice “adsorbs” gas molecules (Ye and Liu, 2013).

There are generally three types of structure of gas hydrates: structure I (sI), structure II (sII), and structure H (sH). The existence of any kind of structure is dependent on crystal lattice parameters, van der Waals force, and free diameters of cavities. Pentagonal dodecahedrons and tetrakaidecahedrons constitute the sI clathrate, while sII includes pentagonal dodecahedrons and hexadecahedrons. sH is different from sI and sII and it is a binary hydrate, that is to say, two kinds of guest molecules in cavities of three various sizes in the stable crystal cells of sH must be present (Ye and Liu, 2013). Six large size cages (L-cage) with 12 pentagonal and 2 hexagonal faces ( $5^{12}6^2$ ) and two small-size cages (S-cage) with 12 pentagonal faces ( $5^{12}$ ) are included in sI unit cell (Sloan, 1998). In some other literature large size cages are denoted by medium size cages (M-cages) (Komatsu *et al.*, 2013). In sII type structure there are 4 hexagonal faces instead of two ( $5^{12}6^4$ ). In the case of sH structure type, in addition to  $5^{12}$  cavities there are  $4^35^66^3$  and  $5^{12}6^8$  cavities as well (Sloan, 1998).

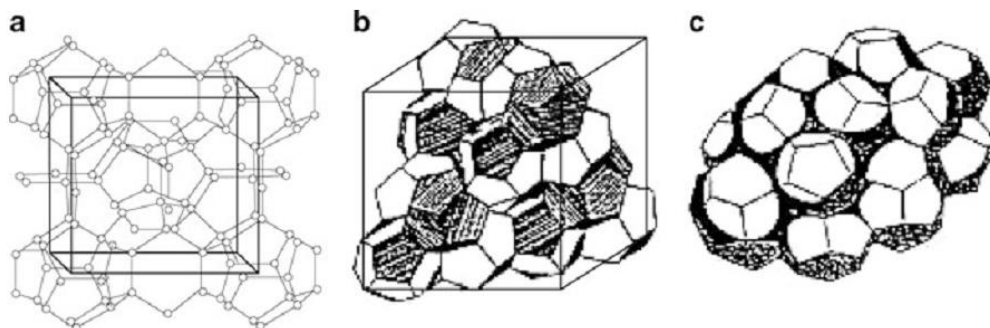


**Figure 2-2:** Unit structures of hydrate crystal (Sloan, 1998): (a) sI (b) sII, and (c)

sH

Gas hydrate crystal structures are linked to their formation. Cubic structure of sI clathrate can only hold small size hydrocarbon molecules such as methane and ethane. It may also hold non-hydrocarbon molecules such as CO<sub>2</sub> and H<sub>2</sub>S. Structure sI is the most widely distributed structure in nature. The structure of sII clathrate is rhombic and it can accommodate both small hydrocarbon molecules such as C<sub>1</sub> and C<sub>2</sub> but also propane (C<sub>3</sub>) and isobutene (i-C<sub>4</sub>). On the other hand, the sH clathrate is hexagonal, and the large “cage” of it can even hold molecules with diameters greater than those of isobutene (i-C<sub>4</sub>), such as i-C<sub>5</sub> and others whose diameters are ranging between  $7.5 \times 10^{-10}$ - $8.6 \times 10^{-10}$  m (Ye and Liu, 2013). In early investigations it was assumed that sH structure existed at laboratory conditions. Today, it is concluded that structures I, II, and H may coexist in several locations. As an example, one of such locations is the continental slope of the Gulf of Mexico (particularly, the Green Canyon area) (Ye and Liu, 2013). Lu *et al.* (2007) confirmed that sH hydrate exists in the natural environment through the analysis of gas hydrate samples recovered from Cascadia. In general, structures II and H are more stable than structure I (Ye and Liu, 2013). The crystal parameters of these three structures are shown in Table 2-1.

**Table 2-1:** Comparison of crystal structure of gas hydrate (Ye and Liu, 2013)

Crystal structure of gas hydrate	sI		sII		sH		
	Small	Big	Small	Big	Small	Medium	Big
Cavity							
Crystal lattice	5 <sup>12</sup>	5 <sup>12</sup> 6 <sup>2</sup>	5 <sup>12</sup>	5 <sup>12</sup> 6 <sup>4</sup>	5 <sup>12</sup>	4 <sup>3</sup> 5 <sup>6</sup> 6 <sup>3</sup>	5 <sup>12</sup> 6 <sup>8</sup>
Number of cavities	2	6	16	8	3	2	1
Average cavity radius, × 10 <sup>-10</sup> m	3.91	4.33	3.902	4.683	3.91	4.06	5.71
Varying rate of radius, %	3.4	14.4	5.5	1.73	-	-	-
Cavity coordinate number	20	24	20	28	20	20	36

Chemical nature, size and shape of the guest molecule play significant role in cavity stability of hydrates (Sloan, 1998). The size of the guest molecule is directly related to the hydration number, in most cases, to its nonstoichiometric value, while shape factor of guest molecule plays minor role for sI and sII in terms of cage occupancy. Another important parameter to be considered is the size ratio of guest molecules to host cavities. Table 2-2 adapted from Sloan (1998) shows size ratios of guest diameter to cavity diameter for different molecules. Ratios denoted with the superscript “ $\zeta$ ” are those occupied by the simple hydrate formers. As an example, methane occupies both the small and large cages of structure I in methane hydrate (Sloan, 1998). On the other hand, propane occupies only the large cages of structure II in propane hydrate (Sloan, 1998). The values in Table 2-2 suggest a size ratio lower bound of approximately 0.76, below which molecular attractive forces contribute less to cavity stability, and above the upper bound ratio of approximately 1.0, it is impossible for the guest molecule to fit into a cavity without distortion (Sloan, 1998). Simple hydrate species, which can occupy the  $5^{12}$  cavity of either structures will also enter the large cavity of that structure.

**Table 2-2:** Ratio of molecular diameters to cavity diameters for Natural Gas Hydrate formers and a few others (Sloan, 1998)

Gas hydrate former		Molecular diameter/cavity diameter for cavity type			
		Structure I		Structure II	
Molecule	Diameter (Å)	5 <sup>12</sup>	5 <sup>12</sup> 6 <sup>2</sup>	5 <sup>12</sup>	5 <sup>12</sup> 6 <sup>4</sup>
<i>He</i>	2.28	0.447	0.389	0.454 <sup>ζ</sup>	0.342 <sup>ζ</sup>
<i>H<sub>2</sub></i>	2.72	0.533	0.464	0.542 <sup>ζ</sup>	0.408 <sup>ζ</sup>
<i>Ne</i>	2.97	0.582	0.507	0.592 <sup>ζ</sup>	0.446 <sup>ζ</sup>
<i>Ar</i>	3.8	0.745	0.648	0.757 <sup>ζ</sup>	0.571 <sup>ζ</sup>
<i>Kr</i>	4.0	0.784	0.683	0.797 <sup>ζ</sup>	0.601 <sup>ζ</sup>
<i>N<sub>2</sub></i>	4.1	0.804	0.700	0.817 <sup>ζ</sup>	0.616 <sup>ζ</sup>
<i>O<sub>2</sub></i>	4.2	0.824	0.717	0.837 <sup>ζ</sup>	0.631 <sup>ζ</sup>
<i>CH<sub>4</sub></i>	4.36	0.855 <sup>ζ</sup>	0.744 <sup>ζ</sup>	0.868	0.655
<i>Xe</i>	4.58	0.898 <sup>ζ</sup>	0.782 <sup>ζ</sup>	0.912	0.687
<i>H<sub>2</sub>S</i>	4.58	0.898 <sup>ζ</sup>	0.782 <sup>ζ</sup>	0.912	0.687
<i>CO<sub>2</sub></i>	5.12	1.00 <sup>ζ</sup>	0.834 <sup>ζ</sup>	1.02	0.769
<i>C<sub>2</sub>H<sub>6</sub></i>	5.5	1.08	0.939 <sup>ζ</sup>	1.10	0.826
<i>c-C<sub>3</sub>H<sub>6</sub></i>	5.8	1.14	0.990	1.16	0.871 <sup>ζ</sup>
<i>(CH<sub>2</sub>)<sub>3</sub>O</i>	6.1	1.20	1.04 <sup>ζ</sup>	1.22	0.916 <sup>ζ</sup>
<i>C<sub>3</sub>H<sub>8</sub></i>	6.28	1.23	1.07	1.25	0.943 <sup>ζ</sup>
<i>i-C<sub>4</sub>H<sub>10</sub></i>	6.5	1.27	1.11	1.29	0.976 <sup>ζ</sup>
<i>n-C<sub>4</sub>H<sub>10</sub></i>	7.1	1.39	1.21	1.41	1.07

## 2.2 Chemical and Physical Properties of Natural Gas hydrates

Natural gas hydrate can be considered as porous and it has lower hardness and shear modulus of elasticity than ice. It resembles ice in density. However, it has a lower value for thermal conductivity and electrical resistivity. Table 2-3 summarizes physical properties of methane hydrate.

**Table 2-3:** Comparison of properties of methane hydrate and ice (Ye and Liu, 2013)

Property	Methane hydrate	Gas hydrate in sandy sediment from sea bottom	Ice
<i>Hardness, Mohs</i>	2-4	7	4
<i>Shear strength, MPa</i>	-	12.2	7
<i>Shear modulus, GPa</i>	2.4	-	3.9
<i>Density, g·cm<sup>-3</sup></i>	0.91	>1	0.917
<i>Acoustic velocity, m·s<sup>-1</sup></i>	3300	3800	3500
<i>Thermal capacity, kJ·cm<sup>-3</sup></i>	2.3	≈2	2.3
<i>Thermal conductivity, W·K<sup>-1</sup> m<sup>-1</sup></i>	0.5	0.5	2.23
<i>Resistivity, kΩ·m</i>	5	100	500

Also, there are some other significant similarities between natural gas hydrates and ice and between hydrate and ice layers. Firstly, both ice and hydrate have similar state changes from fluid to solid. Secondly, both ice and hydrate dissociation is an endothermic process. As a result of these processes a significant heat effect is generated. For example, to melt a gram of ice at 0°C heat of 0.335 kJ value is needed. On the other hand, 0.5-0.6 kJ of heat is needed for a gram of gas hydrate to be dissociated for the temperature ranges of 0-20°C (Ye and Liu, 2013). Lastly, both ice and hydrate undergo volume expansion, 9% for ice and 26-32% for hydrate, respectively (Ye and Liu, 2013). Only fresh water can be transformed into ice or hydrate. Ice- and hydrate-bearing layers have lower conductivity and density values than aquifers. However, they have greater elastic wave propagation velocity than aquifers.

Tens of times lower equilibrium pressure than other condensed phase gases (such as liquefied gas) is shown by hydrate (Ye and Liu, 2013). Upon reaching its critical temperature, hydrate can still form – even during conditions that do not support gas liquefaction. Gas can be accumulated in hydrate in a very huge amount at low equilibrium pressure. As an example, 200 Scm<sup>3</sup> of methane can be contained in 1 g of water (Li, 2000).

### **2.3 Formation of Marine Natural Gas Hydrates**

Continental slopes, island slopes, oceanic rises and inland deep-water zones and marginal seas are the main points for marine gas hydrate deposition.

There is a high possibility for gas hydrates to accumulate when relevant conditions prevail. The basic conditions are: suitable temperatures and pressures, available hydrocarbon gas and also relevant pH which plays significant role in organic matter decomposition, as microorganisms need appropriate pH conditions to sustain their activity of utilizing organic matter for methane gas to be produced (Ye and Liu, 2013).

#### **2.3.1 Gas Origin**

The main hydrocarbon which is found in submarine gas hydrates in nature is methane, with concentrations nearly 100 times higher than other hydrocarbon gases. Natural gas hydrates data from global sea areas were analyzed by Kvenvolden (1995) and he showed that methane was the origin for over 99% of hydrate. Four sources of this methane are present in theory, which can be listed as follows:

- methane dissolved in seawater (from organic matter dissolved or suspended in seawater and methane moved from the atmosphere or seafloor to seawater)
- methane which is deposited and generated by organic matter within a submarine hydrate layer
- methane originating from organic matter in sediments and in sedimentary rock beneath a hydrate layer
- methane of non-biological source (inorganic methane) from deep in the Earth

Methane, which originates from organic matter, is the key contributor to submarine hydrates, as shown by researches (Xia *et al.*, 2001). Methane dissolved in seawater is not concentrated enough to form hydrate. Gas from deep in the Earth is mainly composed of carbon dioxide rather than methane, and methane formed by organic matter within the hydrate layer itself is not rich enough to bear significant hydrate accumulation on its own (Ye and Liu, 2013). The shallower regions of a sedimentary basin contain submarine hydrates as in the case of conventional hydrocarbons. The sedimentary basin is linked to a hydrocarbon source-rock layer system with a sufficiently high abundance of organic matter. Usually, thin sedimentary layer or depositional spaces are a cause for no gas source to form methane hydrate in most oceanic regions. Therefore, submarine methane hydrates are generally distributed at the edges of continents where the gas supply is sufficient (Kvenvolden, 1995). Bacteria or heat reduces the organic matter in sediments or sedimentary rocks beneath a submarine hydrate zone to form methane gas, so there is a possibility for free methane gas layer to underlie a hydrate layer, likely enhanced by conventional natural gas that has migrated there (Froelich *et al.*, 1995). After the thorough consumption of oxygen and carbonate in an aerobic and sulfate-reducing zone, methane starts to form in the sediments.

Organic matter fermentation and CO<sub>2</sub> reduction forms methane gas. It is shown by the isotopic composition of the hydrogen in the hydrate that CO<sub>2</sub> reduction is the main way for methane formation in a sulfate reduction zone in a marine environment. The reactions for methane production are described below (Uchido, 1997; Wright *et al.*, 1999):



As it can be inferred from the reaction, carbon and oxygen are consumed at their atomic ratio of 1:2. Organic matter is the main origin for the carbon required for bacterial synthesis in marine sediments. Therefore, for the potential formation of gas hydrate total organic carbon (TOC) in marine sediments has very important role (Kvenvolden, 1993; Waseda, 1998).

The main controls on the thickness and longevity of a methane synthesis zone in sedimentary environments are represented by the geothermal gradient and the rate of burial. In the case of low geothermal gradient, usable organic carbon is aerobically oxidized or consumed at the sulfate reduction zone before being able to move in the methane synthesis region. This will be the case if sediments are buried too slowly. When opposite occurs, i.e. in the case of high geothermal gradient and rapid burial of sediments, the microorganisms which are capable for synthesizing methane have a hard time surviving because the sediment temperature rises too quickly (Clayton, 1992).

### **2.3.2 Effect of Temperature and Pressure on Hydrate Stability**

Hydrostatic pressure exerted by the water column overlying marine sediments can be high enough to form and stabilize natural gas hydrates. Sufficient high pressure is required to form gas hydrate; so, generally, it is limited to sediment beneath at least 300-600 m of water. Also, the upper 300-1000 m of sediment is generally a limitation for the hydrate itself. The dissociation of hydrate will take place at deeper sediments because of high temperature. The presence of the temperature and pressure at which natural gas hydrates preferable form generally is in shallow sediments in continental slopes and rises and in the shallow sediment of deep-sea plains (Zhang, 1990).

Factors such as sedimentary environment, lithogenesis, subsurface fluids, the degree of mineralization, and the geothermal gradient have significant impact on the formation of natural gas hydrate. Other factors which can influence the stability of hydrates are environmental temperature, pressure, and gas composition. Gas hydrates are always in a balanced state that is sensitive to changes in temperature and pressure together with environmental conditions, because gas hydrates have various compositions. Based on the data taken from many regions, phase diagrams and temperature-pressure equilibrium curves for gas hydrates were prepared. Field surveys, sample analysis, and experimental research investigated various factors which may have influence on diagrams and equilibrium conditions. For example, the stabilization conditions for pure methane hydrate start at about 5°C and 5 MPa (equivalent to 500 m of water depth).



In the presence of other gases, especially, when there is hydrogen sulfide gas inside the hydrate composition, the range of stability will widen considerably.

If, for example, 20% hydrogen sulfide is added to a mixed hydrate of methane and carbon dioxide, the pressure can decrease by 1 MPa approximately at a constant temperature, or the temperature can increase by 2°C at constant pressure (Zhao, 2002; Su, 2000).

Seafloor region that corresponds to the temperature and pressure extents under which stable conditions prevail for natural gas hydrate is called the hydrate stability zone (HSZ). Dissociation of hydrate will take place if it is moved out of the zone. The formation of gas hydrate corresponds to sedimentation period. Because of continuous temporal changes in the isotherm, with ongoing sedimentation, hydrate at the bottom of the stability zone dissociates. Free gas can be produced by saturated water in pores and it can move up into the hydrate stability zone and re-form as hydrate there (Ye and Liu, 2013).

## **2.4 Characteristics of Hydrate Distribution and Reserves**

### **2.4.1 Characteristics of Distribution**

Temperature, pressure, and gas-water contents are the factors on which the stability of natural gas hydrate depends in nature. Also these factors limit hydrate occurrences to the shallow part of lithosphere, that is, not deeper than approximately 2000 m from the surface of the Earth (Ye and Liu, 2013). Approximately 30 important areas of natural gas hydrate have been identified in the seas. These areas have been well investigated and they represent the most attractive prospects and the most concern. They are controlled by geographical patterns and are mainly allocated globally in propitious zones beneath water depths exceeding 300-500 m in seaward continental margins (Figure 2-3).

The continental margin of the Pacific Ocean (e.g., the west coast of Oregon, the Cascadia margin, the south neritic zone of Mexico, the neritic zone and trough of Central America, the neritic zone of Guatemala, the continental margin of Peru, and the Peru-Chile trough), the offshore area of Japan (e.g., the Nankai trench and the

eastern margin of the Sea of Japan), the continental margins along gulf coasts (e.g., the Orco sea basin and the Gulf of Mexico), and the continental margin of the Atlantic (e.g., the Blake Ridge, and offshore zone in the southeast of the USA) are the internationally recognized and studied examples of hydrate areas. Hydrate samples were also collected from the South China Sea and the permafrost layers of Qilian Mountain by China (Ye and Liu, 2013).

The result of marine drilling operations in continental slopes showed that natural gas hydrates have been found to only partially fill the pore spaces of strata. Their distribution is in the form of pieces, bands, discontinuous layers, and massive bodies, which are mainly controlled by lithological characteristics. Layered, massive, or dispersed gas hydrate strata are encountered in available core samples. Layered form is mainly seen in volcanic ash, tuffaceous muds, and turbidities, therefore it usually has small burial depths and high porosity.

Hydrate inside core samples taken from several sites in the Central America has a burial depth of 140.96-141.12 m, porosity of 46% as an example for layered form. In 2002, 45 wellbores at nine sites on Hydrate Ridge of Oregon were drilled (Ye and Liu, 2013). Gas hydrate from these sites occurred mainly in the form of cement. The analysis of hydrate core from one of the boreholes revealed that dispersive distributed hydrate in the form of cement accounted for 75% of total hydrate, while massively dispersed hydrate accounted for only 25% (Figure 2-4) (Ye and Liu, 2013).

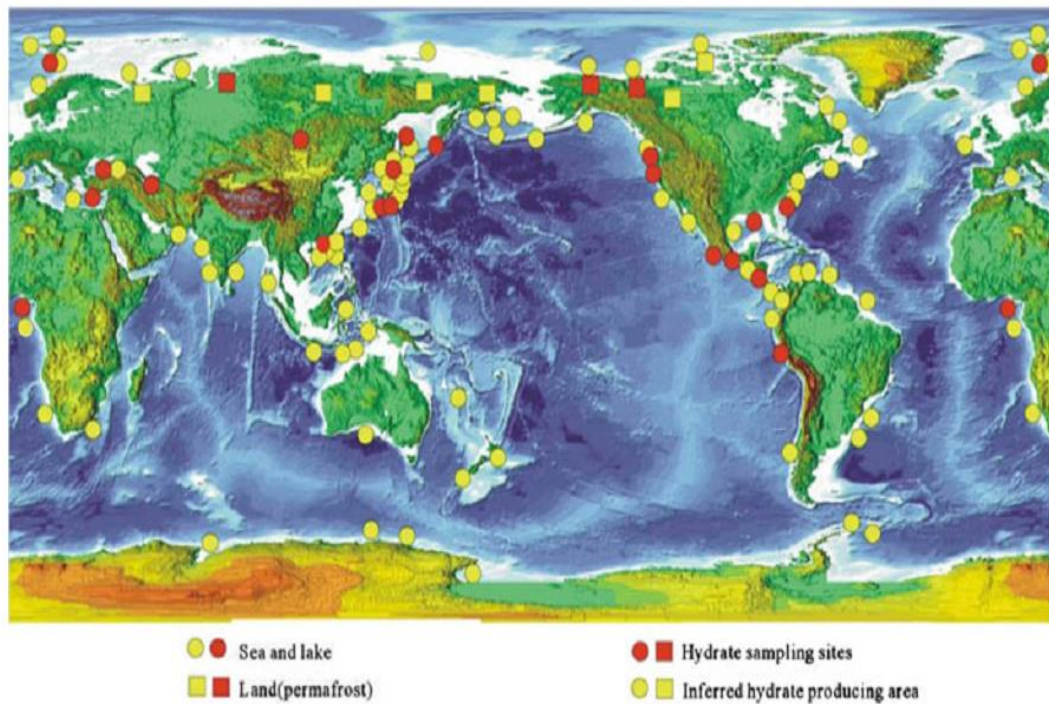


**Figure 2-3:** Global distribution of natural gas hydrates (Ye and Liu, 2013)

Silty mud and muddy siltstone is the formation environment for massive hydrate. Massive hydrate usually has a tremendous burial depth and low porosity, with the prominent exception of Hydrate Ridge where the special geologic structure lets gas hydrate outcrop out of the shallow surface layer. High saturation is common to such hydrate and it results in a high seismic velocity. However, due to free gas, the underlying layers usually have a lower seismic velocity, which results in amplitude anomalies in seismic profiles (Ye and Liu, 2013).

The cracks and cavities of mudstone and sandy dolomite are the possible environments for dispersive hydrate to occur. In fact, the distribution of dispersive hydrate is mostly controlled by these cracks and cavities. Hydrates, which are low in porosity and saturation, have distributions that vary greatly in strata. However, it is possible to find dispersive hydrate in fine-grained sediments rich in fossil organisms also. For example, foraminifera-rich sediments of the South China Sea contain highly saturated dispersive hydrate (Chen *et al.*, 2007).

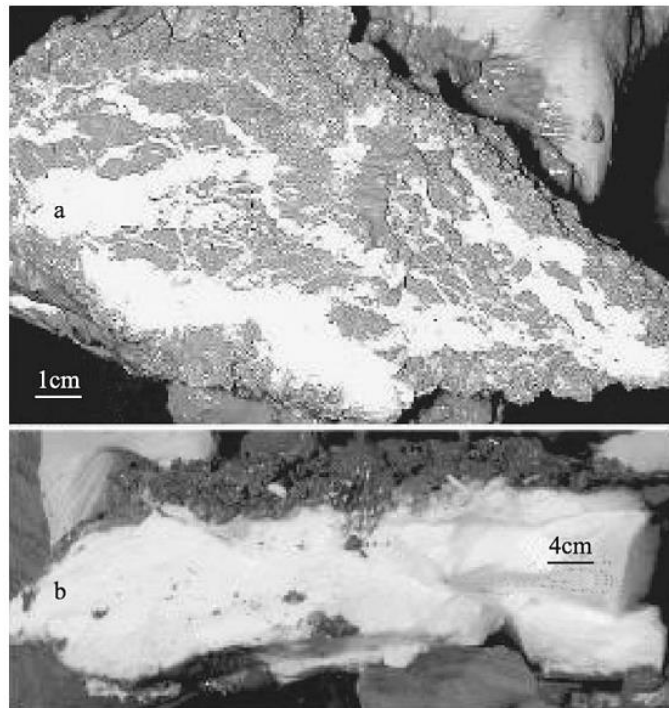


**Figure 2-4:** Gas hydrate samples from sediments of Hydrate Ridge. (a) Layered distribution. (b) Massive distribution (Ye and Liu, 2013)

Multiple factors, such as sedimentary characteristics and structures influence hydrate distributions in sediments. Considering gas sources, biogenetic methane hydrate can be formed easily by sediments with high organic carbon because of the capacity of the rock to generate hydrocarbon, whereas faulted or diapiric structures may carry thermogenic methane gas from deeper regions up into the hydrate stability zone to form hydrate.

With regard to geological volumes there are several possibilities (Ye and Liu, 2013):

- passageways can be provided by a faulted structure for fluid to migrate and also a space can be provided for hydrate growth, so faulted structures can be considered favorable to hydrate formation;

- sedimentary basins with high sedimentation rates are generally under-compacted and can also provide pore space for hydrate formation, but such sediments, usually with low sandy mud content at the depocenter (location of the thickest deposition in a basin), may form blockages to fluid passage and prevent hydrate from growing;
- methane gas and water can be accommodated in coarse sediments with high porosity to form hydrate;
- abundant space can also be possessed by fine-grained sediments rich in fossil organisms for the formation of highly saturated hydrate.

These factors and possibilities can be encountered in a single geological formation as well.

#### **2.4.2 Resource Reserves Prediction**

Without doubt, a huge hydrocarbon resource is represented by allocation of marine gas hydrates, dispersed extensively. However, it is a quite complicated issue to correctly evaluate and quantify this amount. The area, thickness, and porosity of hydrate bearing sediment layer are controlling factors in estimation of hydrate resource reserves. Parameters such as hydrate saturation and hydration number have importance too. A range of environments, defined by numerous varying parameters can host gas hydrates under natural conditions. For example, some environments may differ in sediment compositions, organic matter abundances, geologic structures, geothermal fields, geothermal gradients, temperature and pressure changes with depths, gas sources and compositions, degrees of mineralization of surrounding seawater or fluid, and even different paleo-geothermal fields and paleo-climatic changes which may influence hydrate estimations greatly.

Also, optimization of evaluation methods for the resource reserves has not been carried out. A series of assumptions are the basis for all estimated hydrate reserves; most estimation usually depends on derivations, and resource value predictions are subjective.

It is very hard to quantify current global hydrate reserves. There have been done several studies in which researchers tried to figure out approximate values.

Researchers from the Russian Academy of Sciences calculated methane mineral reserves on average concentrations of  $117\text{-}138.4 \times 10^8 \text{ m}^3/\text{km}^2$  (Ye and Liu, 2013). At least  $1 \times 10^{13}$  t of hydrocarbon reserves (Ye and Liu, 2013) contained in natural gas hydrates is an approximate estimate. This is about twice the hydrocarbon contents from all proven fossil fuels (including coal, petroleum, and natural gas) (Ye and Liu, 2013). Gas hydrates can often act as a seal for underlying free natural gas, because of their impermeability characteristics. Therefore, estimations will go even higher if the free gas under the hydrate-bearing layer is taken into account (Ye and Liu, 2013). Natural gas hydrates will be a key and vast energy source for the future if these evaluations prove to be correct.

## **2.5 Prospecting Techniques**

Despite the fact that natural gas hydrates are on track to being an important supply of alternative energy, numerous problems are of concern. Several technical methods are used in identification of marine gas hydrates, including seismic prospecting, geologic sampling and drilling, well logging, and geochemical detection. However, the most widely used technique is the identification of a bottom simulating reflection (BSR) in seismic data.

### **2.5.1 Seismic Technique**

The propagation velocity of seismic waves increases in the layer due to the presence of gas hydrate in the pores of a sedimentary layer. A low-velocity sedimentary layer is the result of free gas presence in the sediments underlying the hydrate-bearing zone. A high-amplitude reflection is produced at the interface between upper and lower sedimentary layers with strong contrasting velocities and densities by seismic waves. This reflection is called the bottom simulating reflection (BSR) (Holbrook *et al.*, 1996). This reflection is approximately parallel to the sea bottom but different from submarine multiple wave. It roughly follows the same shape as the seafloor, often cutting across reflections coming from geological strata. Waves pass through

sea-bottom beds and propagate downward in seismic method. The stratigraphic compaction with increasing depth causes wave velocity to rise.

In locations where natural gas hydrate occurs in sediments, the seismic wave first passes through the high-velocity hydrate-bearing layer and then through the low-velocity layer containing free gas.

Interval velocities of layers again rise with depth in a normal pattern below this. Therefore, the seismic profile can show an interval-velocity anomaly (i.e., a location where a higher velocity upper layer overlies a low-velocity lower layer) and BSR is the result of this, a possible indicator of gas hydrate (Ye and Liu, 2013). In addition, hydrate-bearing sedimentary layers have nearly homogenous densities, which result in a decrease in the strength of reflected waves through such sediments. Therefore, a “blank zone” above the BSR is being formed that is parallel or oblique to reflected wave through normal sediments. This can be considered as another possible indicator of gas hydrates. The existence of hydrates can be inferred by a BSR or amplitude blank zone. However, a uniform and compact lithology can be a cause for a blank zone also. Free gas may not be contained in a low-velocity layer below the BSR. Instead a mudstone of low interval velocity or loose sandstone of high permeability may be contained. Therefore, other methods should be considered in parallel for efficient identification of gas hydrates. Example techniques are wave impedance section and amplitude versus offset (AVO) techniques.

AVO is one of the seismic prospecting techniques used to identify physical properties and lithological characters using P- and S-wave characteristics and reflection amplitude changes that occur with increasing offset between the source and receiver (Zheng, 1992; Wu, 2002). The AVO technique is widely used for gas hydrate research because hydrate sediments have specific P- and S- wave characteristics. First of all the technique involves designing geological models to show different occurrences of gas hydrate. On this basis, the AVO response characteristics of a single reflector are forward calculated according to the elastic parameters such as P- and S-wave velocities, density and Poisson's ratio. To

constrain the BSR origin, thickness of free gas, and thickness and saturation of hydrate, the modeled characteristics are compared with actual AVO responses thereafter (Wu *et al.*, 2004). Thus, the AVO method can be considered as a theoretical model-based analysis technique.

Verification of the parameters that went into construction of AVO method should be done together with the accuracy and suitability of the theoretical model. This verification can be done by further acoustic studies of hydrate sediments.

### **2.5.2 Drilling to Get Cores**

The most effective method to recover and identify natural gas hydrate is drilling. However, it is always used along with seismic and other methods to constrain where the core is taken. Because of the fact that all or most of gas hydrate contained in the core will dissociate due its physical properties when the drill core is lifted to the surface of sea at normal temperature and pressure, pressure-retaining cores have been developed in order to maintain the core at its original pressure. The European Union's Institute of Marine Science and Technology succeeded in developing a new and improved pressure-retaining corer to recover gas hydrate in 1997 (Ye and Liu, 2013).

### **2.5.3 Logging Methods**

Logging is another effective method for gas hydrate exploration in addition to seismic characterization and drilling. Gas hydrates can cement sediments, making the porosity and permeability of the media to decrease. Also, gas hydrates can compact the porous media. Therefore, the sediments not only have a remarkable response on the seismic profile but also have anomalous indications in well log curves. Four conditions must be satisfied when logging methods are used to identify a layer bearing gas hydrate (Ye and Liu, 2013):

1. high resistivity
2. short acoustic wave propagation time
3. remarkable gas expansion during drilling
4. anomaly in a drilling area with two or more holes



Also, a low anomaly in the natural electric field during well logging by gamma ( $\gamma$ ) ray is observed.

A lower natural potential difference is observed in hydrate-bearing layer, compared with gas- and water-saturated layers, because hydrate plugs up pores and consequently decreases diffusion and infiltration. Hydrate dissociation causes a remarkable change in the slumping of the well wall when a hydrate-bearing layer is hit during drilling. Caliper well log curve shows this readily. A greater well diameter is observed than adjacent layers. The hydrate-bearing layer can have relatively low porosity, so it is generally easy to identify in logging curves.

#### **2.5.4 Geochemical Exploration**

Geochemical methods used for gas hydrate exploration mainly include determinations of hydrocarbon gas contents, ion-concentration anomalies of pore water, isotope geochemical anomalies, and indicator minerals. Geochemical parameter changes in hydrate-bearing layers are determined by using these methods. For example, chlorine concentration anomalies in pore water samples from hydrate sediments were first discovered by Hesse and Harrison (1981). Characterization of  $\text{Cl}^-$  concentrations as well as increasing and decreasing trends in C, Cl, H, and O isotope geochemical anomalies were done in the Blake Ridge area (Paull and Ryo, 2000; Watanabe *et al.*, 2000, Lu *et al.*, 2000; Hesse *et al.*, 2000; Oba *et al.*, 2000). Authigenic minerals are found in nearly all places where there is a development of gas hydrates, indicating that such minerals are closely related to hydrate formation. Bitumen, natural aluminum, amorphous sulfur, and pyrite are other indicator minerals. Pyrite is regarded as an indicator of the violent activity of submarine hydrocarbon gas (Ye and Liu, 2013).



## CHAPTER 3

### A REVIEW ON RESEARCH ON CH<sub>4</sub> REPLACEMENT BY CO<sub>2</sub> IN NATURAL GAS HYDRATES

Practical recovery of methane in the clathrate hydrates can be accomplished with CO<sub>2</sub>. High-pressure CO<sub>2</sub> is injected below sea beds in this method. Difference of thermodynamic stability between methane and CO<sub>2</sub> hydrates is supposed to be the driving force for the replacement reaction to occur (Komatsu *et al.*, 2013). This method is defined by CH<sub>4</sub>-CO<sub>2</sub> swap, and it allows a possibility for both methane utilization and permanent storage of CO<sub>2</sub>. Several studies have been done recently which were investigating properties, kinetics and numerical models of replacement process of methane in the clathrate hydrates by carbon dioxide. This chapter focuses on research summary behind methane replacement in natural gas hydrates by injection of CO<sub>2</sub>.

#### 3.1 Thermodynamics and Fundamentals

Phase equilibria of the gas-solid mixtures and the thermal properties of the clathrate compounds relate thermodynamics of CH<sub>4</sub>-CO<sub>2</sub> replacement reactions. In other words, the difference of the phase equilibria for methane hydrates and CO<sub>2</sub> hydrates can derive the possibility of replacement reactions (Komatsu *et al.*, 2013). Figure 3-1 shows the equilibrium diagram of CH<sub>4</sub>-CO<sub>2</sub>-H<sub>2</sub>O system. In this diagram, areas A and B are located above the equilibrium curve of H<sub>2</sub>O-hydrate-CO<sub>2</sub> and below H<sub>2</sub>O-hydrate-CH<sub>4</sub> curve.

Therefore, in theory, gaseous CH<sub>4</sub> and CO<sub>2</sub> hydrate can coexist in these areas, and it can be concluded that CO<sub>2</sub> hydrate is more stable than CH<sub>4</sub> hydrate under certain condition (Zhao *et al.*, 2012). Also, for example, at 280 K, CO<sub>2</sub> can exist as hydrate at 2 MPa; however it is not possible for methane to exist as hydrate under this condition. Consideration of replacement reactions for which methane in clathrate compound is replaced by CO<sub>2</sub> is possible by using the concept of differences in phase behavior (Komatsu *et al.*, 2013).

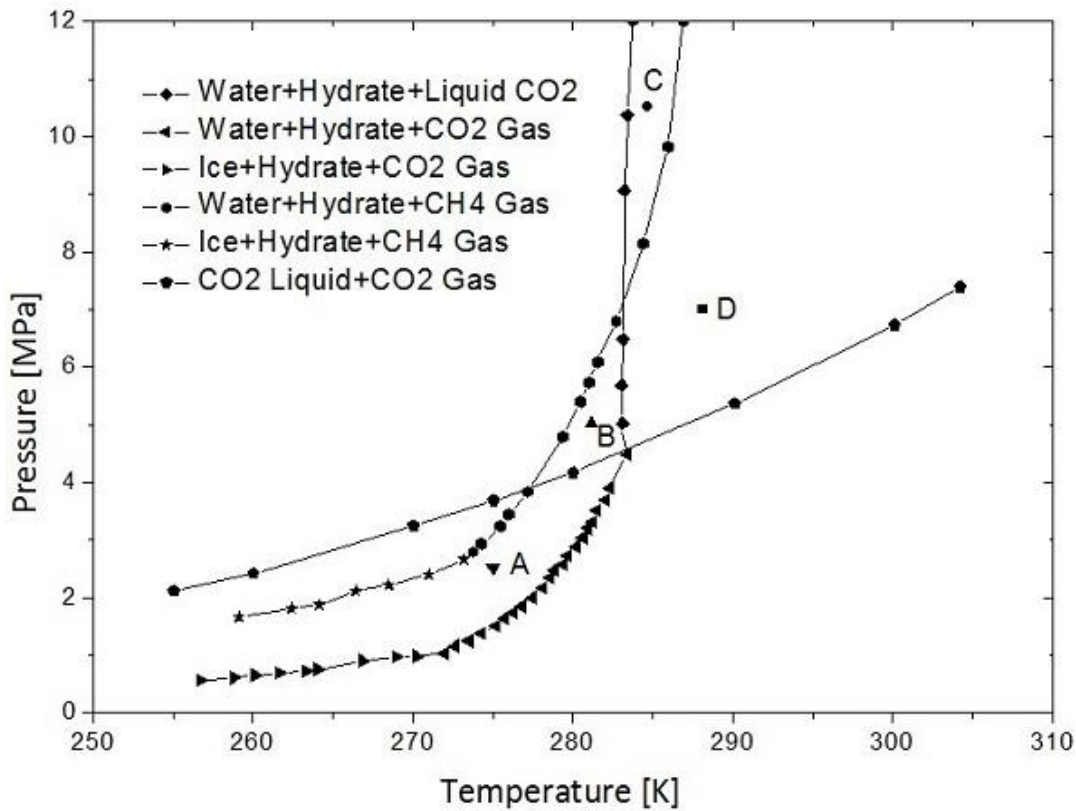


**Figure 3-1:** CH<sub>4</sub>-CO<sub>2</sub>-H<sub>2</sub>O phase equilibrium diagram (Zhao *et al.*, 2012)

For the development of hydrate processing technologies, it is necessary to predict the phase equilibrium data. Therefore, thermodynamic models are used to implement this step. Statistical thermodynamic models which were derived by van der Waals and Platteeuw are the base for developed thermodynamics models (Komatsu *et al.*, 2013).

A simple model is used similar to that of Langmuir for gas adsorption (Komatsu *et al.*, 2013).

As an example, the difference between the chemical potential of H<sub>2</sub>O in the empty hydrate lattice ( $\mu_{H_2O}^\beta$ ) and the chemical potential of water in the filled hydrate lattice ( $\mu_{H_2O}^H$ ), is

$$\Delta\mu_{H_2O}^H = \mu_{H_2O}^\beta - \mu_{H_2O}^H = -RT \sum_m \vartheta_m * \ln(1 - \sum_i \theta_{mj}) \quad (3-1)$$

where  $\vartheta_m$  is the number of cavities of type  $m$  per water molecule in the lattice. The fraction of type  $m$  cavities occupied by gas component  $l$  is

$$\theta_{ml} = \frac{C_{ml}f_l}{(1+\sum_j C_{mj}f_j)} \quad (3-2)$$

where  $C_{ml}$  is the Langmuir constant of gas component  $l$  in cavities of type  $m$ , and  $f_l$  is the fugacity of gas component  $l$  (Komatsu *et al.*, 2013).

The usefulness of a thermodynamic model is dependent on its ability to correlate the  $P$ - $T$  diagrams together with provision of estimations of the fluid and hydrate phases and possibly the occupancy of the guest molecule within the hydrate structures.

Also, the possibility for CH<sub>4</sub>-CO<sub>2</sub> replacement in the hydrate thermodynamically was proven by experimental measurements and theoretical calculations. Gas chromatography and Raman spectroscopy were used by Uchida *et al.* (2005) to analyze several formation and decomposition processes of CH<sub>4</sub>-CO<sub>2</sub> mixed gas hydrates. It was shown by the experimental results and theoretical calculation that, when the temperature is below 283 K, the equilibrium pressures of methane hydrate are higher than those of carbon dioxide hydrate at the same temperature. Phase equilibrium conditions of CH<sub>4</sub>-CO<sub>2</sub>-H<sub>2</sub>O system in porous media were studied by Anderson *et al.* (2003). Results of Uchida *et al.* (2005) were obtained and supported by their experimental data. Stabilities of CH<sub>4</sub> hydrate, CO<sub>2</sub> hydrate, and CH<sub>4</sub>-CO<sub>2</sub> mixed hydrate were studied by Geng *et al.* (2009) with the use of molecular

dynamics (MD) simulations. A temperature range of 260-280 K and a pressure of 5 MPa was chosen in these simulations.

It was inferred from the simulation that the CH<sub>4</sub>-CO<sub>2</sub> mixed hydrate is the most stable among the three hydrates discussed, so in theory, after CO<sub>2</sub> is injected into the CH<sub>4</sub> hydrate under suitable conditions, transformation of CH<sub>4</sub> hydrate into the more stable CH<sub>4</sub>-CO<sub>2</sub> mixed hydrate will be accomplished, while production of CH<sub>4</sub> gas will be achieved.

### 3.2 Kinetics of Replacement Mechanism

Uchida *et al.* (2000) were the first investigators by who it was proved that the replacement reaction occurs on the contact surface between CH<sub>4</sub> hydrate and CO<sub>2</sub> gas by using Raman spectroscopy. It was suggested that the rate of replacement is very slow and the induction time can take several days. The composition ratio of CH<sub>4</sub> and CO<sub>2</sub> in the vapor phase ( $X_{CH_4}/X_{CO_2}$ ) was measured by Uchida *et al.* (2005) at various times during the formation process of CH<sub>4</sub>-CO<sub>2</sub> mixed gas hydrates. They found that the ratio varied with the formation progressing and obtained the following logarithmic formulation to fit the data:

$$X_{CH_4}/X_{CO_2} = (X_{CH_4}/X_{CO_2})_0 + \alpha \cdot \log t \quad (3-3)$$

where  $t$  is the time,  $(X_{CH_4}/X_{CO_2})_0$  is the initial composition ratio, and  $\alpha$  is a fitting parameter related to condensation rate of CH<sub>4</sub> molecules from the vapor phase. Other conclusions made by Uchida *et al.* (2005) were: more CO<sub>2</sub> than CH<sub>4</sub> as a whole was consumed during the hydrate formation and more CH<sub>4</sub> was consumed in the early stages. This phenomenon can be attributed to the structure of hydrate and the sizes of CH<sub>4</sub> and CO<sub>2</sub> molecules. Crystal structure types of CO<sub>2</sub> and CH<sub>4</sub> hydrate are both type sI. Six medium cages (M-cage) and two small cages (S-cage) form sI hydrate's unit cell. The molecular dimension of CO<sub>2</sub> is a bit larger than the CH<sub>4</sub> molecular dimension. Also, the molecular size of CO<sub>2</sub> is between that of the M-cage and S-cage of sI hydrate. Therefore, molecules of CO<sub>2</sub> occupy the M-cages mainly. CH<sub>4</sub> molecules were able to occupy both S-cages and M-cages during early stages while M-cages were occupied by CO<sub>2</sub> only, leading to more CH<sub>4</sub> gas consumption.

Then, during further stages, a replacement reaction was achieved, and M-cages which held CH<sub>4</sub> molecules were occupied by CO<sub>2</sub> molecules. CH<sub>4</sub> gas was released, consequently the ratio of CH<sub>4</sub> in the vapor phase increased.

Two phases were denoted by Uchida *et al.* (2005) to represent the replacement reaction: (1) decomposition of some CH<sub>4</sub> molecule and the transfer of generated gaseous CH<sub>4</sub> into the vapor phase; (2) occupation of the M-cages by CO<sub>2</sub> molecules and re-occupation of the S-cages by CH<sub>4</sub> molecules because of the memory effect. A schematic diagram showing the exchange process of the guest molecule in the M-cages and the CH<sub>4</sub> re-occupation in the S-cages is shown in Figure 3-2.

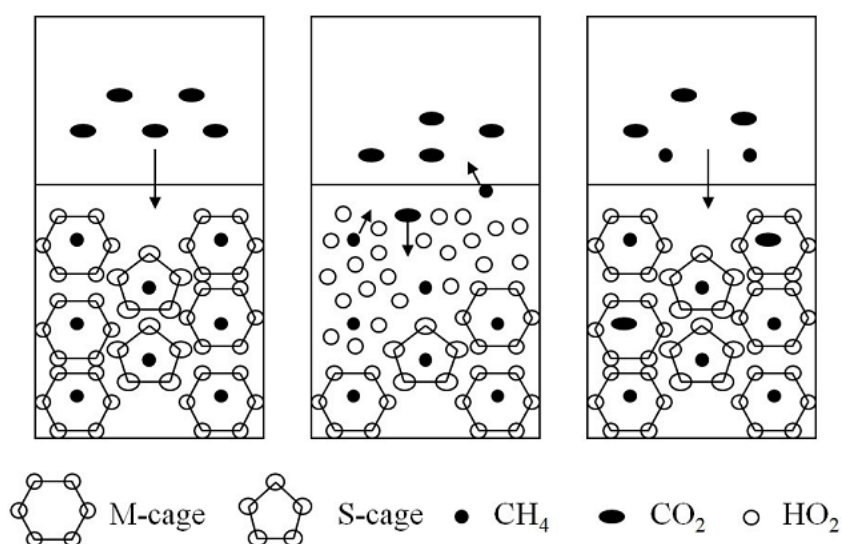


**Figure 3-2:** Schematic diagram of replacement of the guest molecule in the M-cage and the re-occupation of S-cage by CH<sub>4</sub> (Zhao *et al.*, 2012)

It is necessary to consider thermodynamic stability of methane - CO<sub>2</sub> mixed hydrates and distribution of guest molecules between bulk fluid and hydrate phases for estimating the CH<sub>4</sub>-CO<sub>2</sub> replacement reaction. Distribution coefficient of methane and CO<sub>2</sub> between gas and hydrate phases was measured by Ohgaki *et al.* (1996). They also showed that CO<sub>2</sub> is favored in the hydrate phase over that of the gas phase compared to methane. Negligible changes in the hydrate structures occurred in that case because compositions in both fluid and hydrate phases changed under different feed compositions continuously.

So, there is a possibility to initiate replacement reactions when the balance of chemical potential (in some sources, fugacity) of each molecule between bulk fluid and hydrate phases is altered or changed by external forces. Negative Gibbs energy is also observed through replacement reactions due to this difference in distribution of the guest molecules (Yezdimer *et al.*, 2002). In this case, negative Gibbs energy implies feasibility of the replacement reactions.

In another study held by Hirohama *et al.* (1996) it was suggested that the driving force for CH<sub>4</sub>-CO<sub>2</sub> replacement in the hydrate was the fugacity difference between different phases. Models for decomposition of CH<sub>4</sub> hydrate and formation of CO<sub>2</sub> hydrate during the replacement process were built by Ota *et al.* (2005), where it was assumed that the driving force for CH<sub>4</sub>-CO<sub>2</sub> replacement in the hydrate was proportional to the fugacity difference between the gas and the hydrate phase. The model formulation for the methane hydrate decomposition is (Ota *et al.*, 2005):

$$\frac{dn_{CH_4.H}}{dt} = -k_{Dec}A(f_{CH_4.H} - f_{CH_4.G}) \quad (3-4)$$

$$\frac{1}{k_{Dec}} = \frac{1}{k_{Dec.R}} + \frac{1}{k_{Dec.D}} \quad (3-5)$$

where  $n_{CH_4.H}$  is the remaining amount of CH<sub>4</sub> in the hydrate phase,  $t$  is the reaction time,  $f$  is the fugacity, and  $k_{Dec}$  is the overall rate constant of the decomposition.  $k_{Dec}$  includes  $k_{Dec.R}$ , which is the reaction rate constant of decomposition and  $k_{Dec.D}$ , which is the rate of mass transfer in the hydrate phase.  $A$  is the surface area between the gas and the hydrate phase, and H and G refer to the hydrate phase and the gas phase respectively. It is possible to establish a model of CO<sub>2</sub> hydrate formation during replacement similarly (Ota *et al.*, 2005):

$$\frac{dn_{CO_2.H}}{dt} = k_{Form}A(f_{CO_2.G} - f_{CO_2.H}) \quad (3-6)$$

$$\frac{1}{k_{Form}} = \frac{1}{k_{Form.R}} + \frac{1}{k_{Form.D}} \quad (3-7)$$

where  $n_{CO_2.H}$  is the amount of CO<sub>2</sub> in the hydrate phase and  $k_{Form}$  includes  $k_{Form.R}$  and  $k_{Form.D}$  rate constants.



Calculation of the fugacity from the model including the van der Waals-Platteeuw theory and the Soave-Redlich-Kwong equation of state (SRK-EOS) was used by Ota *et al.* (2005). Experimental parameters (T, P) were constant in the SRK-EOS equation for the calculation of fugacity and the resulting compositions were measured by Raman spectroscopy. Constant surface area between the gas and the hydrate phase was assumed in the study. Activation energies for CH<sub>4</sub> hydrate decomposition and CO<sub>2</sub> formation were calculated with the usage of slope of the Arrhenius plot. It was pointed by Ota *et al.* (2005) that the rate constant of decomposition seemed to dominate the CH<sub>4</sub> hydrate decomposition. Also, it was supposed that the mass transfer likely dominated CO<sub>2</sub> hydrate formation during the replacement process.

Nagayev *et al.* (1979) and Rueff *et al.* (1988) reported experimental data for CO<sub>2</sub> and CH<sub>4</sub> hydrate formation respectively, from which the activation energy for CO<sub>2</sub> hydrate formation is 57.98 kJ/mol and that for CH<sub>4</sub> hydrate decomposition is 54.49 kJ/mol. However, Ota *et al.* (2005) reported that the activation energy for CO<sub>2</sub> hydrate formation is 73.3 kJ/mol and that for CH<sub>4</sub> hydrate decomposition is 14.5 kJ/mol from these models. Experimental data from work of Li *et al.* (2007) show that the activation energies are 68.4 kJ/mol and 28.8 kJ/mol respectively. Interaction between formation of CO<sub>2</sub> hydrate and decomposition of CH<sub>4</sub> hydrate during the replacement reaction process may be the cause for these differences in activation energies. It can be deduced that the formation of CO<sub>2</sub> hydrate can supply sufficient heat for the decomposition of CH<sub>4</sub> hydrate, if an analysis and comparison of the activation energy during the replacement process is carried out. Together with this, CH<sub>4</sub> hydrate's self-protection can be prevented by the extra heat and promotion of decomposition of CH<sub>4</sub> hydrate further can be achieved (Zhao *et al.*, 2012).

### **3.3 Accomplished Experimental Studies on Replacement Reaction**

Numerous experimental studies have been carried out recently for the purpose of investigation of methane hydrate replacement by carbon dioxide.

Researchers used gaseous CO<sub>2</sub>, liquid CO<sub>2</sub>, CO<sub>2</sub> emulsions, CO<sub>2</sub>/N<sub>2</sub> mixtures and etc. This section summarizes the experimental studies made by selected researchers.

### 3.3.1 Replacement of CH<sub>4</sub> Hydrate by Gaseous CO<sub>2</sub>

Replacement experiments by use of gaseous CO<sub>2</sub> under different conditions have been done by researchers extensively. Most widely used schematic diagram of the experimental apparatus for replacement with CO<sub>2</sub> is illustrated in Figure 3-3.

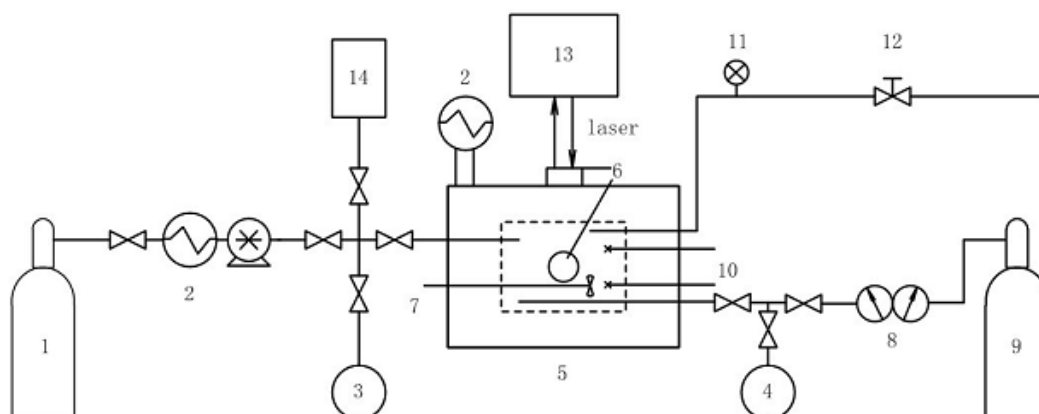


**Figure 3-3:** Schematic diagram of the experimental apparatus (Zhao *et al.*, 2012)

Experimental set-up consists of high pressure cell with a magnetic agitator inside, cooling system for maintaining constant temperature, data acquisition system, and a laser Raman spectrometer or a gas chromatograph for gas phase composition analysis (Zhao *et al.*, 2012). Experimental procedure involves the following steps (Zhao *et al.*, 2012): (1) the cell is filled with desired amount of distilled water, when required pressure value is reached, the magnetic agitator is started to promote the CH<sub>4</sub> hydrate formation; (2) when the experimental measurements remain unchanged, CH<sub>4</sub> hydrate formation is considered to be completed. The cell is exposed to high pressure CO<sub>2</sub> gas, confirmation of which is observed by Raman spectrometer or the gas chromatograph; (3) the system is controlled at the required pressure and temperature - the replacement reaction starts at this instant. Gas sample is taken out after the start of reaction to be analyzed at required intervals; (4) the hydrate mixtures are decomposed by heating, and the compositions are evaluated.

Variation of amount of the decomposed CH<sub>4</sub> hydrate ( $Q_{CH_4,Dec}$ ) and formed CO<sub>2</sub> hydrate ( $Q_{CO_2,Form}$ ) with time are shown in Figures 3-4 and 3-5 respectively, which were taken from the studies of Ota *et al.* (2005), who performed experiments in bulk media. Three main conclusions can be made based on the experimental data: (1) promotion of CH<sub>4</sub> hydrate decomposition and CO<sub>2</sub> hydrate formation is achieved to increase the temperature correspondingly at the same pressure; (2) CH<sub>4</sub> hydrate amount which is decomposed is almost concordant with the amount of formed CO<sub>2</sub> hydrate. By this phenomenon it is proved that the core of the replacement reaction is the process of occupation of CH<sub>4</sub> molecules' cages with CO<sub>2</sub> molecules; (3) the rate of the reaction is quite fast during the early stages (approximately 10 h), but it starts to slow afterwards.

The results reported by Ota *et al.* (2005) were re-obtained by Wang *et al.* (2007) and Li *et al.* (2008) who also performed experiments in bulk media. The data reported by them indicated the same tendency for variation of the decomposed CH<sub>4</sub> hydrate and formed CO<sub>2</sub> hydrate with time during the replacement process. After the first 2 hours, the rate of CH<sub>4</sub> hydrate decomposition and CO<sub>2</sub> hydrate formation retards in Wang's (2007) experiment. In Li's (2008) experiment, it took 10 hours to sustain the high replacement rate. However, in their experiments the amount of CO<sub>2</sub> hydrate formed is much more than that of decomposed CH<sub>4</sub> hydrate. This difference can be related to the free water amount. There is no free water at the start of the replacement reaction in Ota's experiment; therefore, the amount of decomposed CH<sub>4</sub> hydrate is consistent with that of formed CO<sub>2</sub> hydrate. Free water exists in the hydrate system in the experiment of Wang (2007) and Li (2008). The amount of CO<sub>2</sub> gas dissolved in the free water and formed CO<sub>2</sub> hydrate with the free water is much more than that used for replacing CH<sub>4</sub> from the hydrate. So, it is very important to consider the free water saturation in the NGH (Natural Gas Hydrate) stratum when the actual exploitation of natural gas with CO<sub>2</sub> is projected.

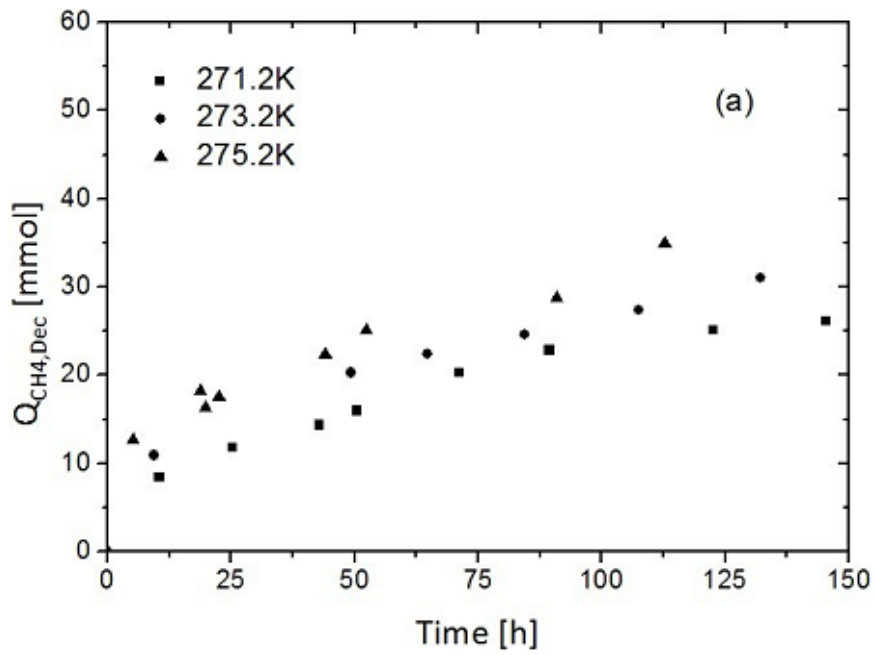


**Figure 3-4:** Amount of the decomposed CH<sub>4</sub> hydrate ( $Q_{CH_4, Dec}$ ) versus time (Ota *et al.*, 2005)

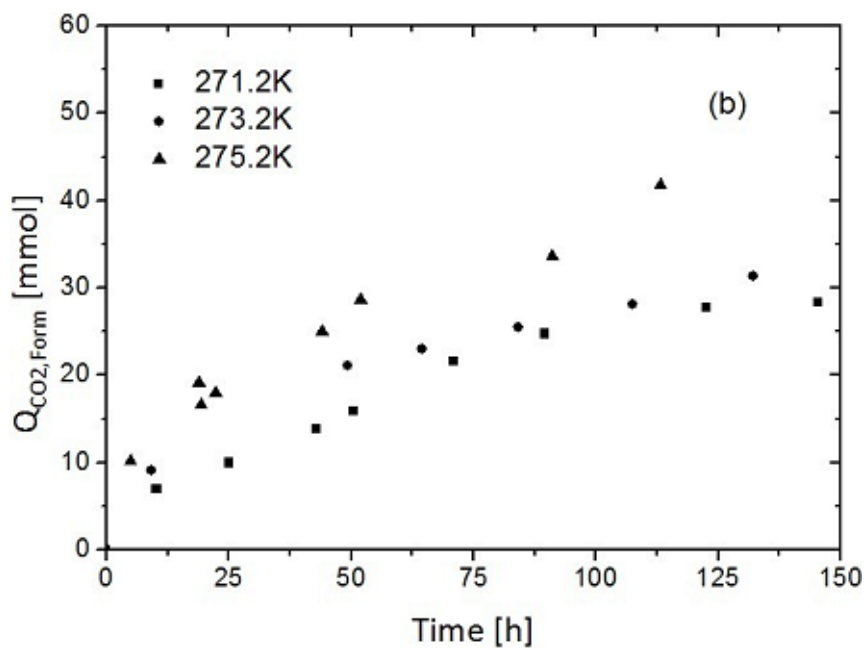


**Figure 3-5:** Amount of the formed CO<sub>2</sub> hydrate ( $Q_{CO_2, Form}$ ) versus time (Ota *et al.*, 2005)

Extensive research related with CH<sub>4</sub> replacement by gaseous CO<sub>2</sub> has been done by Ors (2012). Pure methane hydrate was formed in a porous media (sandstone with particle size of 0.25-0.5 mm) and was subject to CO<sub>2</sub> injection afterwards. Cyclic behavior at pressure gauges were observed after CO<sub>2</sub> injection, reason of which was related to CH<sub>4</sub>-CO<sub>2</sub> swap. It took approximately 6 hours to observe CH<sub>4</sub>-CO<sub>2</sub> swap and corresponding increase in pressure. Gas chromatography analysis which were performed at the instant of CO<sub>2</sub> injection and after the CH<sub>4</sub>-CO<sub>2</sub> swap indicated the following results: mole fractions of CH<sub>4</sub> and CO<sub>2</sub> at the instant of CO<sub>2</sub> injection were determined as 50.4% and 49.6% respectively, while after CH<sub>4</sub>-CO<sub>2</sub> swap mole fractions of CH<sub>4</sub> and CO<sub>2</sub> were determined as 92.31% and 7.69% respectively.

In summary, the feasibility of CH<sub>4</sub> replacement by use of gaseous CO<sub>2</sub> is proven based on the experimental results reported by different researchers. However, it was found that the replacement rate becomes extremely slow after the early stages of reaction. Together with this, the replacement efficiency cannot satisfy the requirements of commercial production of NGH. The need for developing more efficient methods of exploiting natural gas from the hydrate with CO<sub>2</sub> is emerging.

### **3.3.2 Replacement of CH<sub>4</sub> Hydrate by Liquid CO<sub>2</sub>**

Several experiments were conducted to perform replacement process with the use of liquid CO<sub>2</sub>. Such studies have been done by Ota *et al.* (2005) and Zhou *et al.* (2008) extensively. In their experiments the initial temperature was 273.2 K and the initial pressure is 3.25 MPa, and the experiments are performed in bulk media. In addition to the experimental set-up used for replacement by gaseous CO<sub>2</sub>, a liquefying apparatus is added to perform liquefaction of CO<sub>2</sub>. The procedure involves the following steps: (1) CH<sub>4</sub> hydrate is formed in a high pressure cell; (2) the cell is purged with high pressure CO<sub>2</sub> and is constantly pressurized to the required value by keeping introducing CO<sub>2</sub>; (3) to replace CH<sub>4</sub> from the hydrate, saturated liquid CO<sub>2</sub> is introduced into the cell at the instant when the temperature of the system is controlled at the required value; (4) Raman spectroscopy is used to observe the replacement process. The remaining hydrate mixture is resolved and analyzed after a given amount of time, when CO<sub>2</sub> remaining in the cell is released.

Ota *et al.* (2005) reported data which shows the time profile of the mole fractions of CH<sub>4</sub> and CO<sub>2</sub> in the hydrate phase during experiment. The data is presented in Figure 3-6. It can be deduced that the molar fraction of CH<sub>4</sub> hydrate decomposition is consistent with that of CO<sub>2</sub> hydrate formation. This phenomenon approves the feasibility of methane replacement by using liquid CO<sub>2</sub> as well. It also proves that the replacement reaction's essence is the further CH<sub>4</sub> molecules' cages occupation by CO<sub>2</sub> molecules.

In their study accomplished by Zhou *et al.* (2008), the replacement of CH<sub>4</sub> by use of liquid CO<sub>2</sub> was performed by using the same conditions as in Ota's (2005) experiment. CH<sub>4</sub> ratios replaced from the hydrate of the two experiments are shown in Figure 3-7 redrawn from Zhou *et al.* (2008). It can be observed that the results match roughly in less than 100 h.

Another similar study conducted by Li *et al.* (2011) included several changes in experimental conditions. The initial temperature and pressure were set to 282.2 K and 6 MPa respectively. Also the experiment was conducted in porous sediment. According to his research, CH<sub>4</sub> recovery ratio can reach approximately 45% after 288 hours. In Ota's (2005) experiment the recovery ratio reaches a value of 37% after 307 hours and the recovery ratio is 18.6% after 96 hours in Zhou's (2008) work.

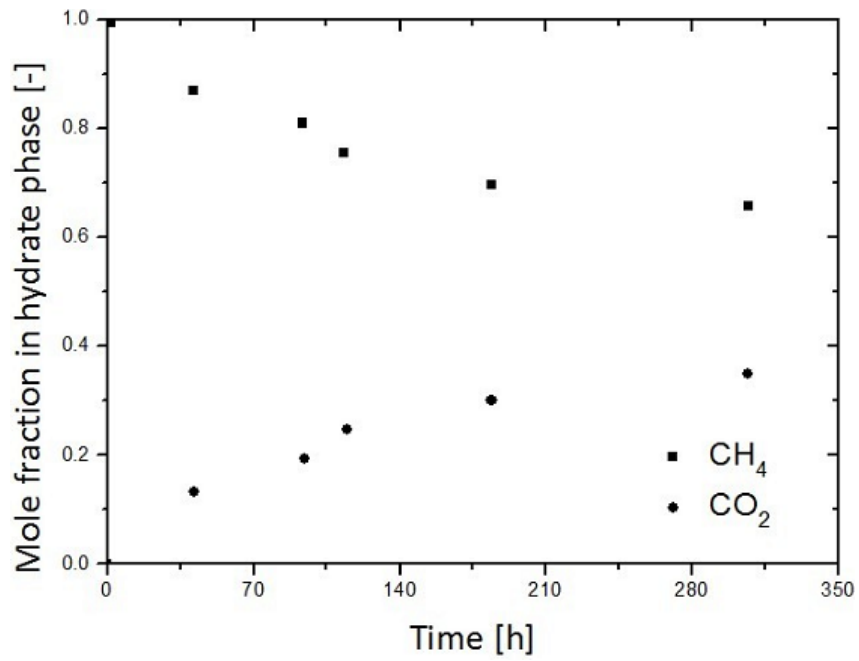


**Figure 3-6:** Mole fraction of CH<sub>4</sub> and CO<sub>2</sub> in the hydrate phase as a function of time (Ota *et al.*, 2005)

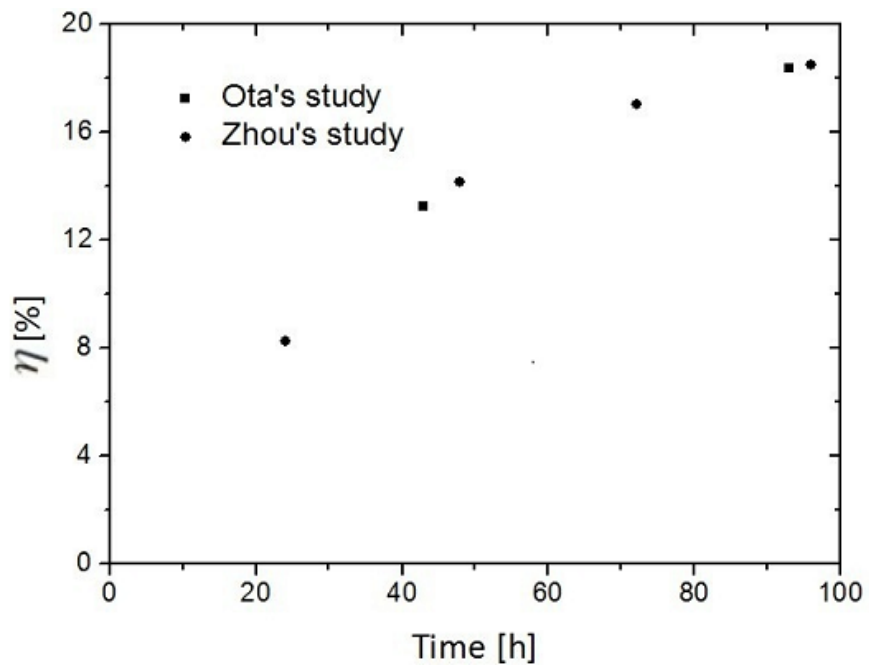


**Figure 3-7:** CH<sub>4</sub> ratios replaced from the hydrate of the two different experiments (Zhou *et al.*, 2008)

The guest molecules' transformation in the different cages and hydrate during the replacement process were observed by Ota *et al.* (2005) with Raman spectroscopy. CH<sub>4</sub> remaining in each cage and hydrate with time is shown in Figure 3-8 taken from Ota *et al.* (2005).

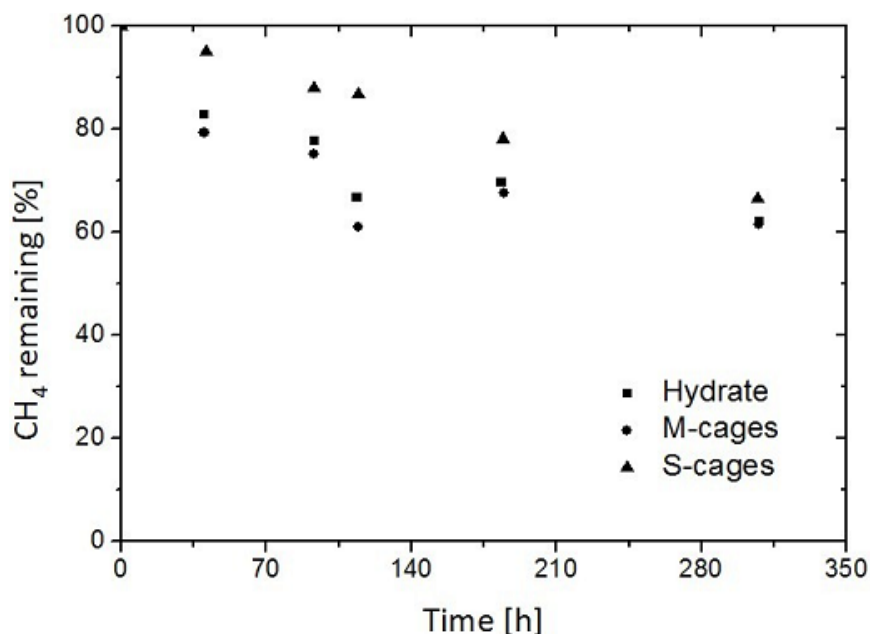


**Figure 3-8:** Evolution of CH<sub>4</sub> in the M-cages, S-cages and hydrate with time (Ota *et al.*, 2005)

From the graph it can be observed that the CH<sub>4</sub> remaining in both the M-cages and S-cages decreased with time, however decline in the S-cages is much gradual than that in the M-cages. Also there is a consistency between the ratio of CH<sub>4</sub> in the M-cages and CH<sub>4</sub> in the hydrate. This proves that the replacement reaction mainly advances in the M-cages (Zhao *et al.*, 2012).

In summary, in order to prove the feasibility of replacing CH<sub>4</sub> from the hydrate with liquid CO<sub>2</sub>, researchers have applied numerous experimental methods. An improvement in replacement rate, efficiency and reaction time in experiments done with liquid CO<sub>2</sub> was achieved compared with the replacement experiments with gaseous CO<sub>2</sub>. Investigators inferred that usage of liquid CO<sub>2</sub> is much more preferable than gaseous CO<sub>2</sub>.



### 3.3.3 Replacement of CH<sub>4</sub> Hydrate by CO<sub>2</sub> Emulsion

Researchers have started to investigate the reason of slow replacement rate after early stages of reaction. Yoon *et al.* (2004) were one of the investigators in this area and according to their experimental study, during early stages, the contact area between CO<sub>2</sub> molecules and CH<sub>4</sub> hydrate is large, therefore, the reaction rate is rapid. With progression in reaction, the crust layer of CH<sub>4</sub> hydrate is covered with CO<sub>2</sub> hydrate, and a shielding effect is provided by the CO<sub>2</sub> hydrate. So, CH<sub>4</sub> hydrate decomposition is hindered and consequently rate decreases and the reaction finally ceases.

McGrail *et al.* (2004) proposed the method of enhanced gas hydrate recovery (EGHR) with the aim to improve the replacement reaction rate. An emulsion in which water is continuous phase and CO<sub>2</sub> is the dispersed phase is prepared in this method. Emulsion is substituted for gaseous and liquid CO<sub>2</sub> to replace CH<sub>4</sub> gas from the hydrate. This method is a combination of the advantages of controlled multiphase flow, heat, and mass transport processes in hydrate-bearing porous media according to McGrail's (2004) opinion. It makes a full use of the thermodynamic and physical properties of mixtures in the H<sub>2</sub>O-CO<sub>2</sub> system. Thus, the contact area between CO<sub>2</sub> molecules and CH<sub>4</sub> hydrate is increased, creating enhancement of the replacement reaction.

Along with this study, numerical simulations were implemented by White and McGrail (2009) to analyze the replacement process of CH<sub>4</sub> from the hydrate stratum by using gaseous CO<sub>2</sub>, liquid CO<sub>2</sub> and CO<sub>2</sub> emulsion. His simulation results indicate that the replacement rate with CO<sub>2</sub> emulsion is the highest among these three methods.

If three forms of carbon dioxide are compared, CO<sub>2</sub> emulsion is considered as the best solution for the replacement reaction; however, the technique for preparing CO<sub>2</sub> emulsion is still undeveloped. A new kind of emulsifier, TMN-6 (octa(ethylene glycol)-2,6,8-trimethyl-4-nonyl ether) was used by DhanuKa *et al.* (2006) for CO<sub>2</sub> emulsion preparation. The stability of the emulsion increases with pressure at a temperature below 318 K according to DhanuKa's (2006) experiment.

In another study performed by Zhou *et al.* (2008) CO<sub>2</sub> emulsion was used to replace CH<sub>4</sub> in the hydrate in porous media. Similar apparatus used for liquid CO<sub>2</sub> injection was used in his study. The only difference is that CO<sub>2</sub> emulsion was used instead of liquid CO<sub>2</sub>. Three groups of replacement experiments were performed by Zhou *et al.* (2008). The experimental initial pressure and temperature were the same, CO<sub>2</sub>-in-water (C/W) emulsions with ratios of 90:10, 70:30, and 50:50 (W<sub>CO<sub>2</sub></sub>:W<sub>H<sub>2</sub>O</sub>) were used to replace CH<sub>4</sub> from its hydrate. Calculation of CH<sub>4</sub> ratios replaced from the hydrate of the three groups of experiments by use of CO<sub>2</sub> emulsion and one group of experiment by use of liquid CO<sub>2</sub> at fixed intervals is done in this study. Figure 3-9 taken from Zhou *et al.* (2008) shows the summary of these calculations.

Replacement rates of CH<sub>4</sub> versus time in different experiments are shown in Figure 3-10, redrawn from Zhou *et al.* (2008). From this figure it can be concluded that the ratios of CH<sub>4</sub> replacement with emulsions are higher than that with liquid CO<sub>2</sub>. It is also evident that with increasing mass ratio of liquid CO<sub>2</sub> in the emulsion replacement efficiency increases as well. So, it can be presumed that CO<sub>2</sub> emulsion is more efficient than liquid CO<sub>2</sub> in replacing CH<sub>4</sub> from the hydrate.

Together with this, a comparison of the replacement ratio of CH<sub>4</sub> by use of CO<sub>2</sub> emulsion and gaseous CO<sub>2</sub> was done by Zhou *et al.* (2008) in order to prove the superiority of CO<sub>2</sub> emulsion in replacing CH<sub>4</sub> from the hydrate. Three groups of distinct experiments were performed by Zhou (2008) under different conditions. Figures 3-11 and 3-12 taken from the work of Zhou *et al.* (2008) show the different molar quantities of CH<sub>4</sub> gas replaced by gaseous CO<sub>2</sub> and CO<sub>2</sub> emulsion versus time respectively.

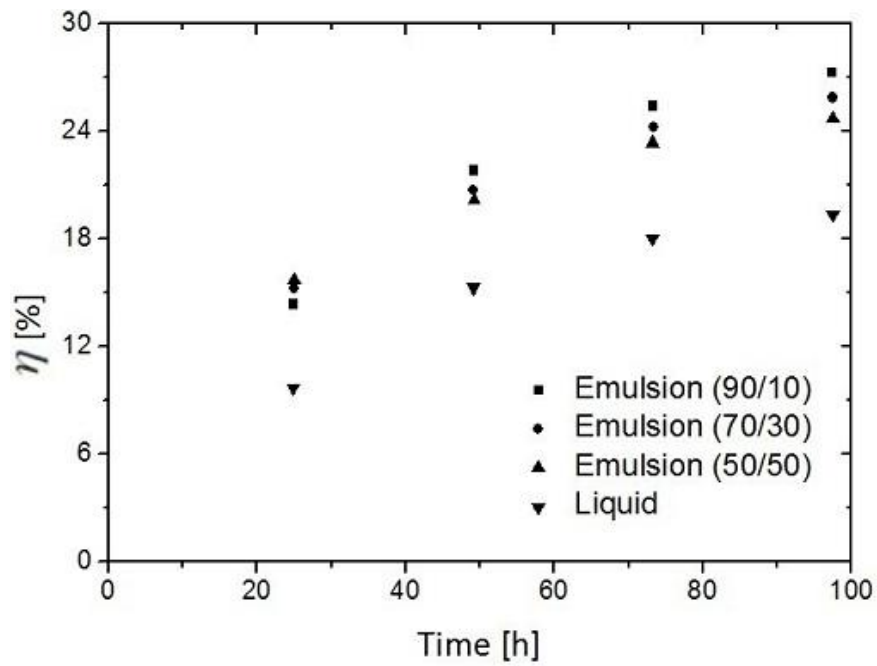


**Figure 3-9:** Ratios of CH<sub>4</sub> replaced from the hydrate with different forms of CO<sub>2</sub> (Zhou *et al.*, 2008)

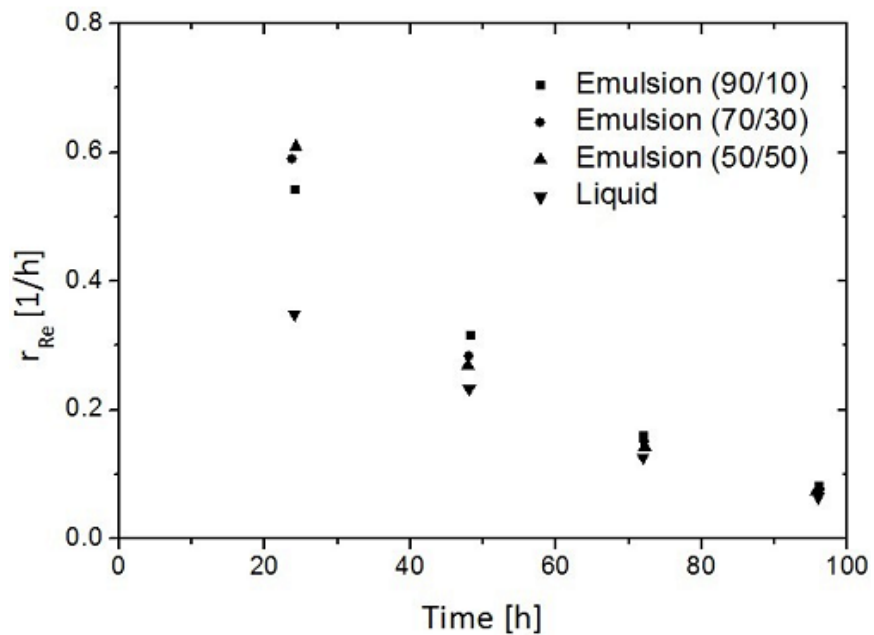


**Figure 3-10:** CH<sub>4</sub> replacement rates with different forms of CO<sub>2</sub> (Zhou *et al.*, 2008)

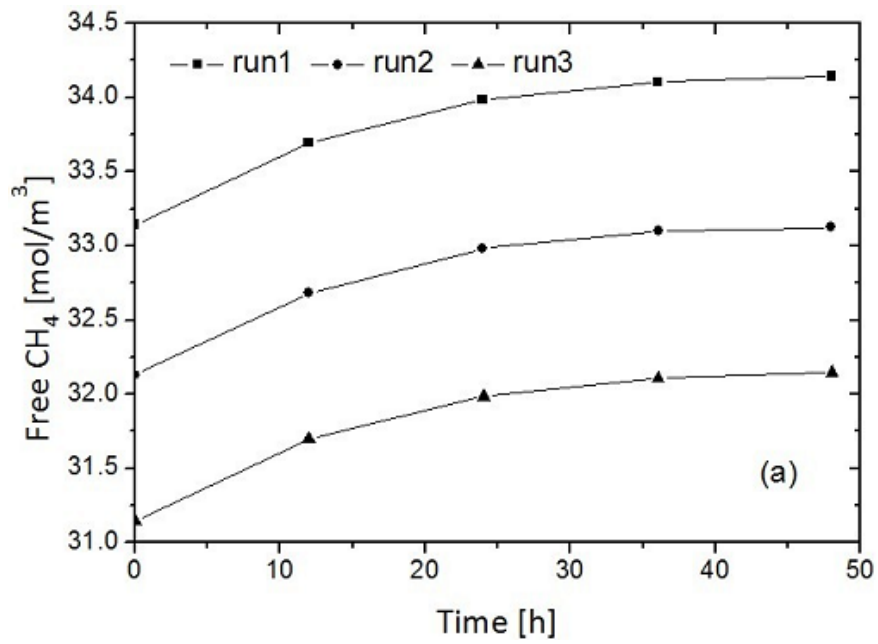


**Figure 3-11:** Amount of the replaced CH<sub>4</sub> gas by gaseous CO<sub>2</sub> against time (Zhou *et al.*, 2008)

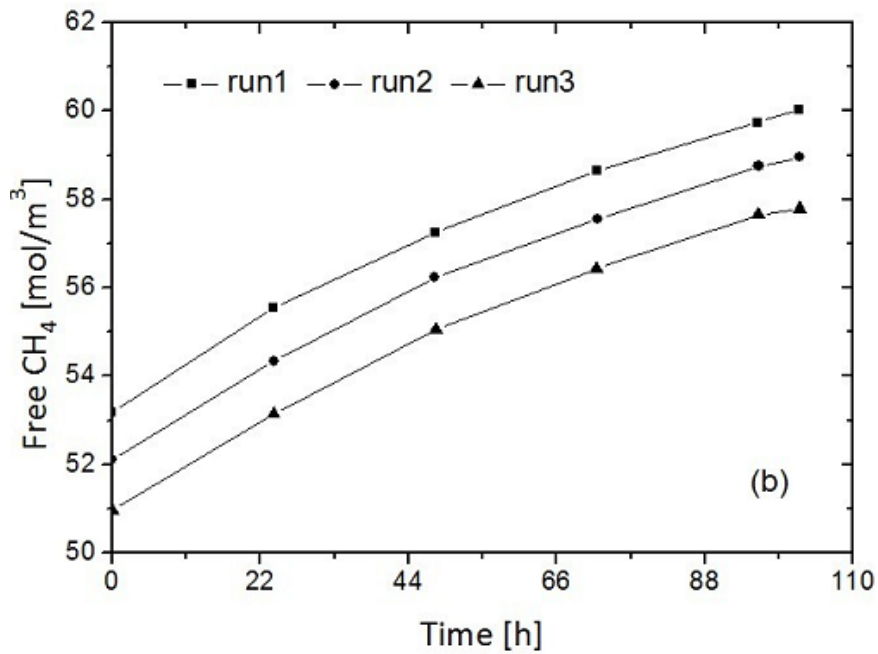


**Figure 3-12:** Amount of the replaced CH<sub>4</sub> gas by CO<sub>2</sub> emulsion against time (Zhou *et al.*, 2008)

Two conclusions can be reached from Figures 3-11 and 3-12: (1) CO<sub>2</sub> emulsion is more applicable and efficient than gaseous CO<sub>2</sub> in replacing CH<sub>4</sub> from hydrate; (2) the replacement rate with gaseous CO<sub>2</sub> starts to slow down after reaction for approximately 10 hours, in about 50 hours reaction stops. The rate of reaction in case of CO<sub>2</sub> emulsion is higher, and the reaction time can take more than 100 hours. As explained by Zhou *et al.* (2008) the reason for such results is due to the higher reaction temperature and the better conductivity and diffusivity of the CO<sub>2</sub> emulsion. CH<sub>4</sub> hydrate decomposition is promoted by the heat given by emulsion and the replacement rate is increased. Larger reaction area between CO<sub>2</sub> molecules and CH<sub>4</sub> hydrate is achieved due to better diffusivity of the CO<sub>2</sub> emulsion and the reaction time outspreads.

As stated by Zhang *et al.* (2009), further research should be done on such subjects as the kinetics of CH<sub>4</sub> replacement by CO<sub>2</sub> emulsion, the varieties and contents of emulsifier, the ratio of water and liquid CO<sub>2</sub>, the influence on replacement rate of dispersed phase in the emulsion. When it comes to the process of actual exploitation from the porous media, distribution characteristics of CH<sub>4</sub> hydrate in the stratum and the pumping of CO<sub>2</sub> emulsion need to be considered.

To sum up, it is proved in the literature that CO<sub>2</sub> emulsion is more efficient in replacing CH<sub>4</sub> from the hydrate when compared with gaseous CO<sub>2</sub> and liquid CO<sub>2</sub>. However, preparation techniques of CO<sub>2</sub> emulsion is still immature. The experimental studies on the replacement with CO<sub>2</sub> emulsion are limited; therefore, factors which influence reaction are not quite clear. There is a need to study technique of CO<sub>2</sub> emulsion preparation and the optimum conditions for replacement with CO<sub>2</sub> emulsion in the future.



## CHAPTER 4

### STATEMENT OF THE PROBLEM

Natural gas hydrates remain stable as long as they are in mechanical, thermal and chemical equilibrium with their environment. To distort the system and produce gas from hydrates, several techniques were proposed and simulated both numerically and experimentally.

Of these, CO<sub>2</sub> injection into methane bearing sediments was proposed as a method both to sequester carbon dioxide gas and produce hydrocarbons from hydrates. CH<sub>4</sub>-CO<sub>2</sub> swap as a result of exposure of hydrates to the injected carbon dioxide gas has been studied extensively by several institutions and researchers. The majority of works was done by firstly forming pure methane hydrate at laboratory conditions and thereafter injecting CO<sub>2</sub>. However, natural gas hydrates are not present in deep ocean sediments of purely methane gas. Along with methane gas, hydrates may be composed of other hydrocarbon gases together with non-hydrocarbon gases, including H<sub>2</sub>S and CO<sub>2</sub>.

The purpose of this research is to form natural gas hydrate by using a mixture of CH<sub>4</sub> (95%), C<sub>3</sub>H<sub>8</sub> (3%), CO<sub>2</sub> (2%) gases. Formation characteristics and property changes of the natural gas hydrate formed from mixture of gases are to be investigated. Upon formation of hydrate it is aimed to inject CO<sub>2</sub> into hydrate media. The objective is to figure out, whether CH<sub>4</sub>-CO<sub>2</sub> swap phenomenon prevails if the experiments are performed with mixture of gases.





## CHAPTER 5

### EXPERIMENTAL SET-UP AND PROCEDURE

To reach the established aim, various tests were performed. These include formation of pure CH<sub>4</sub> hydrate, formation of hydrate from the gas mixture, and injection of CO<sub>2</sub> into the hydrate media. The following experimental set-up and procedure were used to form hydrate and investigate the CH<sub>4</sub>-CO<sub>2</sub> swap process.

#### 5.1 Experimental Equipment

A high pressure cell (Figure 5-1) made from stainless steel was used to form the hydrate. The cell is resistant to pressure values up to 5000 psi-g. Volume of the cell is equal to 600 cm<sup>3</sup>.

Coarse grained sandstone is used as an environment for hydrate growth. Sand particles are screened by using sieves of ASTM numbers of 35 and 60. This corresponds to particle diameters between 0.25 and 0.5 mm.

The cell is placed inside a constant temperature water bath. To decrease the temperature of the water inside the bath refrigerated circulator is used. Refrigerated circulator is operated without interruption during the formation period of hydrates.

Pressure and temperature inside the cell are recorded by two pressure transducers and by a thermocouple respectively, which are connected directly to the cell. At some stage, third pressure transducer was connected to cell from bottom to measure pressure of injected carbon dioxide. Another thermocouple is used to measure the temperature of the constant temperature water bath. Calibration of the

thermocouples was done according to the refrigerated water circulator, which is company calibrated. “Beamex MC5 Multifunction Calibrator” is used to calibrate pressure transducers.

Two pumps are used during the experiments, high pressure syringe pump and vacuum pump. High pressure syringe pump is used to inject water and saturate sediments inside the cell. Tap water is used throughout experiments and no analysis of water properties was done. Also, it is used to inject pressurized air for the calculation of porosity. Vacuum pump is used to evacuate the cell and its connections.

Schematic diagram of the experimental set-up is given in Figure 5-2. Also, Figures 5-3 and 5-4 show photos of the experimental set-up.



**Figure 5-1:** High pressure cell used in experiments

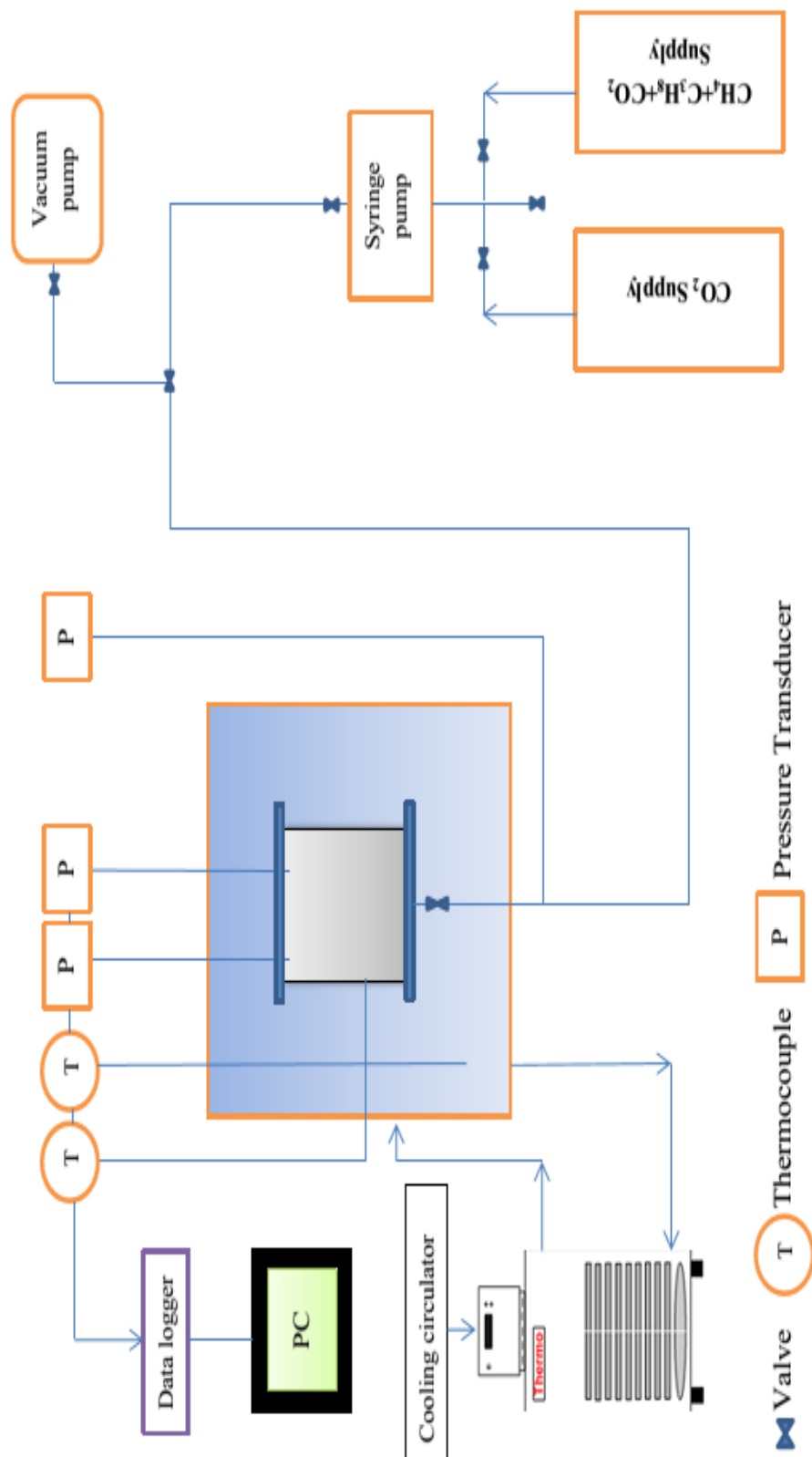


Figure 5-2: Schematic representation of the experimental set-up

Table 5-1 shows the properties of the apparatus used in the experimental studies.

**Table 5-1:** Specification of the apparatus used in experimental studies

<b>Constant Temperature Water Bath</b>	
Trademark	WiseCircu WCL Ultra Low Temperature Refrigerated Circulator
Model	WCL-P12
Capacity	12 lt
Refrigerator	368 W
Temperature range	-40 °C to 100 °C
Temperature accuracy	± 0.1 °C
Temperature uniformity	± 0.2 °C at -20 °C

**Table 5-1:** Specification of the apparatus used in experimental studies (Cont.)

<b>Pressure Transducers</b>	
Trademark	Keller Sensors
Pressure Range	0 – 250 bar G
Output	4 - 20 mA
Supply	12 to 35 V
Precision	± 1 psig
<b>Thermocouples</b>	
Trademark	Elimko
Model	PT - 100
Temperature Range	-30 to +40 °C
Precision	± 0.2 °C
<b>Data Logger and Controller</b>	
Trademark	Elimko
Model	E-680-08-2-0-16-1-0
Voltage	220 V
Data Transfer	RS485 Mod Bus
Data Analysis	A package program of Elimko, Turkey
<b>High Pressure Syringe Pump</b>	
Trademark	Teledyne Isco
Model	500D Pump Module
Capacity	507 ml
Flow Range	0. 001 – 204 ml/min
Flow Accuracy	0.5% of setpoint
<b>Vacuum Pump</b>	
Trademark	Javac, England
Model	DS40
Voltage	220 V/ 50 Hz
Type	Single Stage High Vacuum

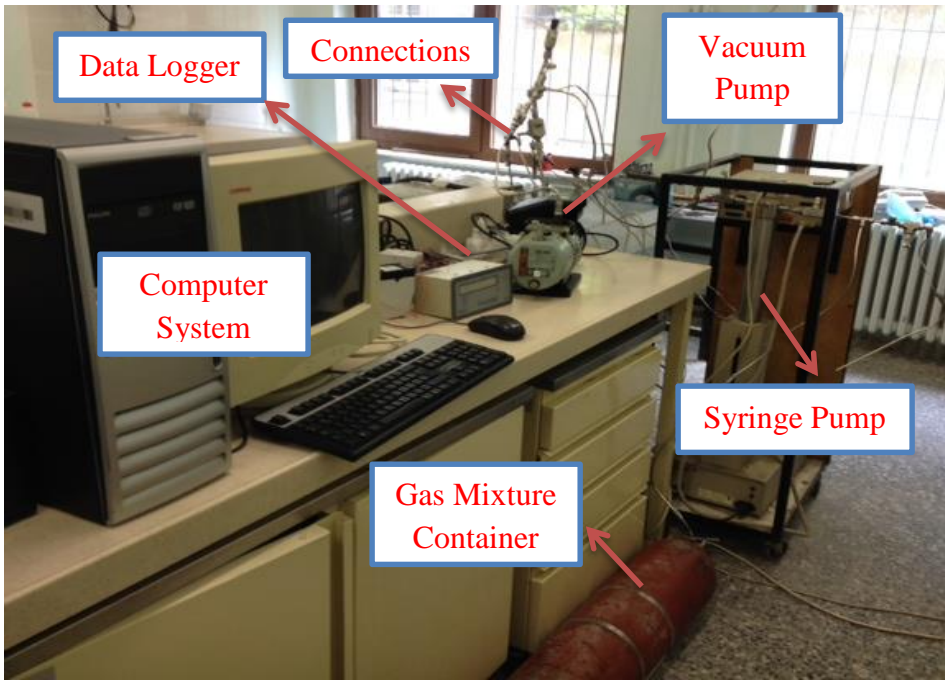


**Figure 5-3:** Experimental set-up (profile view)

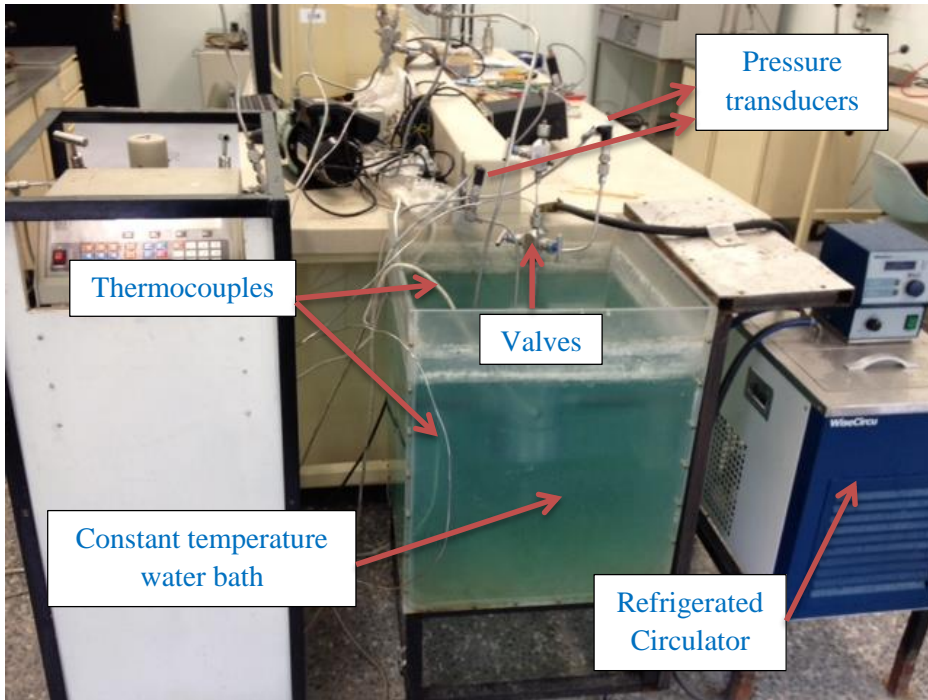


**Figure 5-4:** Experimental set-up (front view)

## 5.2 Experimental Procedures

As it was mentioned earlier, several steps were followed while carrying out experiments.

Experimental procedures can be listed as follows:

- I. Grained sandstone is screened in sieves. ASTM numbers of the sieves are selected as 35 and 60 in order to achieve particle diameters between 0.25 and 0.5 mm providing medium size grained particles. The same sandstone sample was used for different experiments, which was dried in an oven at 105°C for one day after each run.
- II. Top and bottom lids of the cell are screened with a filter with openings less than 0.25 mm in size to achieve no sand intrusion. Then the cell is filled with screened sand particles either completely or partially. The cell was filled completely with sand particles during Run#1, Run#2, Run#3, Run#4 and Run#5. It was filled partially with sand particles during Run#6 and Run#7.
- III. The cell is placed inside the water bath and leakage test is performed. To accomplish leakage test, the cell pressure is increased up to 1500 psi-g by air. Then it is let to stabilize at constant room temperature for several tens of hours.
- IV. Being sure that there is no leakage problem in the cell, the pressure is released, then, the cell together with connections is evacuated by vacuum pump.
- V. Two methods are used to determine pore volume. By injection of air and using Boyle's law of gas expansion initial estimate is made. Then, definite amount of water is injected into the system both to saturate sediments and determine pore volume. Water is injected into the cell by the help of syringe pump at atmospheric conditions. Injection of water is stopped when syringe pump indicated an increase of pressure up to level 200 psi-g. Volume of the injected water is recorded by syringe pump as well. Because water has very low compressibility value, we can take the value at the instant of increase in pressure as pore volume.

- VI. After determining amount of pore volume, part of the water is drained back to achieve required percent saturation of water inside the void volume. During experiments water constituted 50-60% of the void volume. To achieve homogenous distribution of water saturation inside sediments, the system was let to stabilize for several hours.
- VII. Mixture of gases (target composition of which is CH<sub>4</sub> (95%), C<sub>3</sub>H<sub>8</sub> (3%), CO<sub>2</sub> (2%)), real composition is illustrated in Table 6-4) is injected into the system at a pressure, greater than hydrate equilibrium pressure at a temperature of 16°C - to sustain this condition, the initial value of the injected gas pressure was kept as 1300 psi-g approximately (the preparation method of the gas mixture with this composition is illustrated in Chapter 6). Then the cooling process is initiated. Depending upon room temperature conditions, initial temperature was changing, however it was set to reach 4°C by the cooling circulator.
- VIII. The system is let to stabilize until the equilibrium conditions are reached. Pressure and temperature variations are recorded every 10 seconds. Upon stabilization of pressure, gas mixture is injected again up to a predetermined level, depending on the conditions, to consume the water, left in the pore spaces. The procedure is repeated until whole water volume is consumed.
- IX. After depleting all of the water for hydrate formation, CO<sub>2</sub> is injected into the system. The injection of carbon dioxide is accomplished by constantly applying pressure of approximately 770 psi-g from the CO<sub>2</sub> cylinder.
- X. Samples for gas chromatography analyses are taken when mixture inside pressure supply is prepared, during each hydrate formation, after constant injection of carbon dioxide gas from the constant pressure supply, and during and after replacement processes explained in Chapter 6. Samples for gas chromatography are taken by using sampling syringe by connecting syringe to the valves located at the top of the high-pressure cell (Figure 5-4) and subsequent gradual opening of the valves. During each sampling process, pressure together with temperature are carefully monitored, because it is not acceptable to interfere with the system.



XI. Therefore, this sampling operation must be carried out very carefully, to avoid any Joule-Thompson effect (temperature change of a gas/liquid when it is forced through a valve) and also to avoid subsequent pressure drop in the system.



## CHAPTER 6

### EXPERIMENTAL RESULTS AND DISCUSSION

In this study two main experiments were conducted to investigate the formation properties of CH<sub>4</sub>-C<sub>3</sub>H<sub>8</sub>-CO<sub>2</sub> mixture hydrates together with investigation of CH<sub>4</sub>-CO<sub>2</sub> swap in case of this mixture.

The first part of this research was carried out only with methane. Hydrates were formed in a cell in sediments, saturated with water, by using methane gas only with a specified initial pressure and temperature. Unconsolidated porous media (sandstone) was used as an environment for hydrate growth. The aim of the first experiment was to determine the formation properties and to observe hydrate growth by using methane only.

The second part of this research involved formation of hydrate in porous media in the case of mixture of gases whose main components were: CH<sub>4</sub> (95 %), C<sub>3</sub>H<sub>8</sub> (3 %) and CO<sub>2</sub> (2 %). The composition of the mixture was selected based on the results of the investigations accomplished by “The Institute of Marine Sciences and Technology” of Dokuz Eylul University regarding the hydrate depositions in the Black Sea region (Kucuk *et al.*, 2013). Then, carbon dioxide was injected into already formed hydrate and CH<sub>4</sub>-CO<sub>2</sub> swap was investigated. Samples for gas chromatography analysis were taken in each experiment during the procedure of hydrate formation and during CH<sub>4</sub>-CO<sub>2</sub> swapping process.

In all experiments formation of hydrates was carried out in sandstone environment with particle size between 0.25 and 0.5 mm. This range for particle size was

selected in order to achieve medium grained sand. Also, this particle range was selected in order to prevent intrusion of sand particles into the connections and also to achieve size distribution in which hydrates will be easily formed.

In the second case the target composition of the mixture of gases is: CH<sub>4</sub> (95%), C<sub>3</sub>H<sub>8</sub> (3%) and CO<sub>2</sub> (2%). To prepare this mixture with specified composition, a computer program (MATLAB) developed by Merey (2013) was used. This code uses Peng-Robinson equation of state for calculating compressibility factors. The volume of the pressure supply and temperature conditions are entered together with target pressure value. With the usage of real gas law, total number of moles are calculated. Then, by using the molar fraction of each component, partial pressure of each component is calculated. Afterwards, the constant pressure supply is filled with each component step by step in increasing order of partial pressure values.

In all graphs presented in this work, P1 and P2 represent pressure values inside the cell, obtained from pressure transducers attached to the top of the cell.

Complete list of the experiments which were performed is shown in Table 6-1.

**Table 6-1:** List of the experiments performed throughout this study

<b>Run#</b>	<b>Explanation</b>
1	Pure Methane Hydrate Formation
2	“Memory Effect” of Pure Methane Hydrate
3	CH <sub>4</sub> -C <sub>3</sub> H <sub>8</sub> -CO <sub>2</sub> Mixture Hydrate Formation
4	“Memory Effect” of CH <sub>4</sub> -C <sub>3</sub> H <sub>8</sub> -CO <sub>2</sub> Mixture Hydrates
5	CO <sub>2</sub> Injection from Constant Pressure Supply
6	Replacement of Free Gas with CO <sub>2</sub>
7	Repeatability of Replacement of Free Gas with CO <sub>2</sub> Experiment

### 6.1 Pure Methane Hydrate Formation (Run #1)

At the beginning of the experiment, parameters such as void volume, water volume and water saturation were obtained. The values of those parameters are shown in Table 6-2.

**Table 6-2:** Experimental parameters for Run #1

Void volume calculated by air injection,  cm <sup>3</sup>	Void volume calculated by water injection,  cm <sup>3</sup>	Water volume,  cm <sup>3</sup>	Water saturation,  %
<b>384.4</b>	<b>381</b>	<b>190</b>	<b>49.4</b>

Initial pressure,  $P_i$ , was set to 1255 psia, and initial temperature,  $T_i$ , was set to 16 °C. The temperature of the water bath was cooled down to 4 °C by continuously operating the cooler. After waiting for approximately 50 hours, the equilibrium pressure of 621 psia was achieved. Then the pressure inside the cell was again increased up to 1255 psia in order to consume water inside the sediments for hydrate formation. This procedure was carried out until the point, when no more pressure decrease is observed, meaning that no free water exists inside sediments for hydrate formation. Figure 6-1 shows the behavior of the system after the first 118 hours of the experiment. During several intervals both pressure transducers were plugged, as it can be readily seen from Figure 6-1. For example, pressure transducer P2 showed constant pressure value between 55 and 60 hours. At the end of 60 hours, however, it was unplugged and showed the same value as pressure transducer P1. Pressure transducer P1 was also plugged between 76 and 80 hours and between 92 and 119 hours as it showed constant pressure values during that intervals.

Because the formation of hydrate is an exothermic reaction, during the points of hydrate formation there is significant increase in temperature inside the high-pressure cell. If the process is investigated at more detailed plot, this fact can be

readily seen. Figure 6-2 shows the section, when the increase in temperature at the point of formation of hydrate is observed.

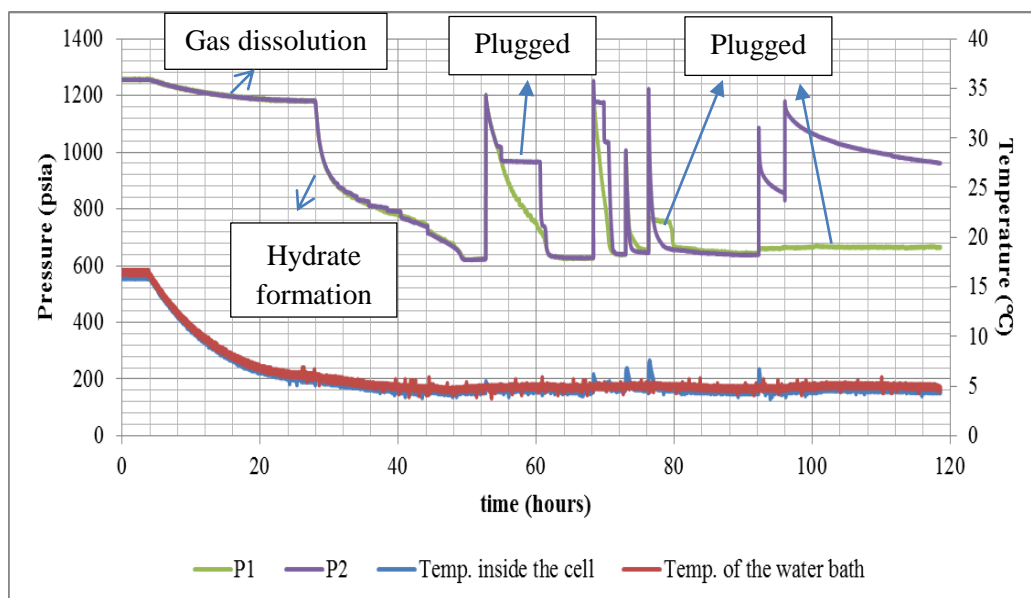


**Figure 6-1:** Response of the system after first 118 hours

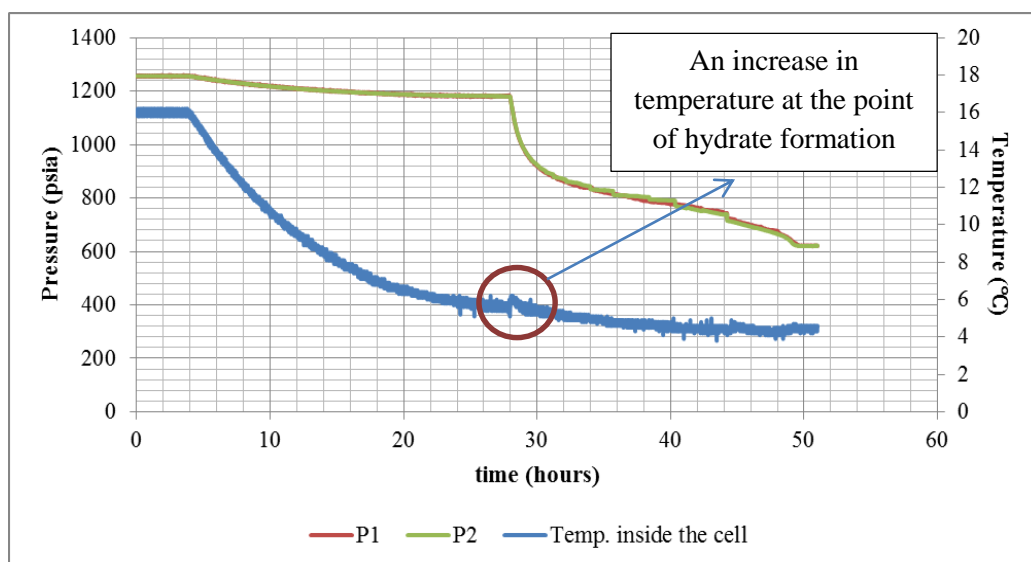


**Figure 6-2:** Segment of the increase in temperature at the point of hydrate formation

## 6.2 “Memory Effect” of Pure Methane Hydrate (Run #2)

After the consumption of all of the water in the system and forming hydrate for the first time the system was brought to initial conditions. This was accomplished in order to form hydrate again and to observe so called “memory effect”. The second process is illustrated in Figure 6-3. The system was brought to its initial conditions ( $T_i = 16^\circ\text{C}$ ,  $P_i = 1255$  psia) and the experiment was initiated thereafter. It should be noted that after hydrate formation it was dissociated until initial conditions of formation were obtained (Figure 6-3).

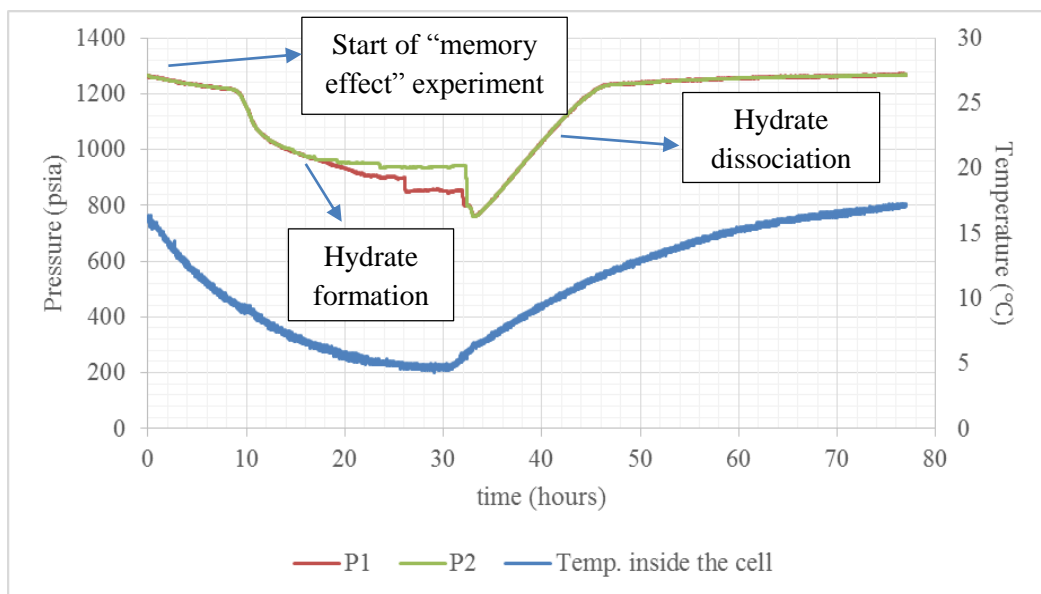


**Figure 6-3:** Investigation of “memory effect”

The first experiment is denoted by “Case 1” and the second experiment, that is, the experiment where “memory effect” was investigated is denoted by “Case 2”. It has been verified that it took less time for the formation of hydrate and an increase in temperature in “Case 2” was observed earlier than in “Case 1”. This fact is shown in Figures 6-4 and 6-5. From Figures 6-4 and 6-5 it is evident that it took approximately 24 hours to observe first hydrate formation in “Case 1” and 10 hours in “Case 2”.

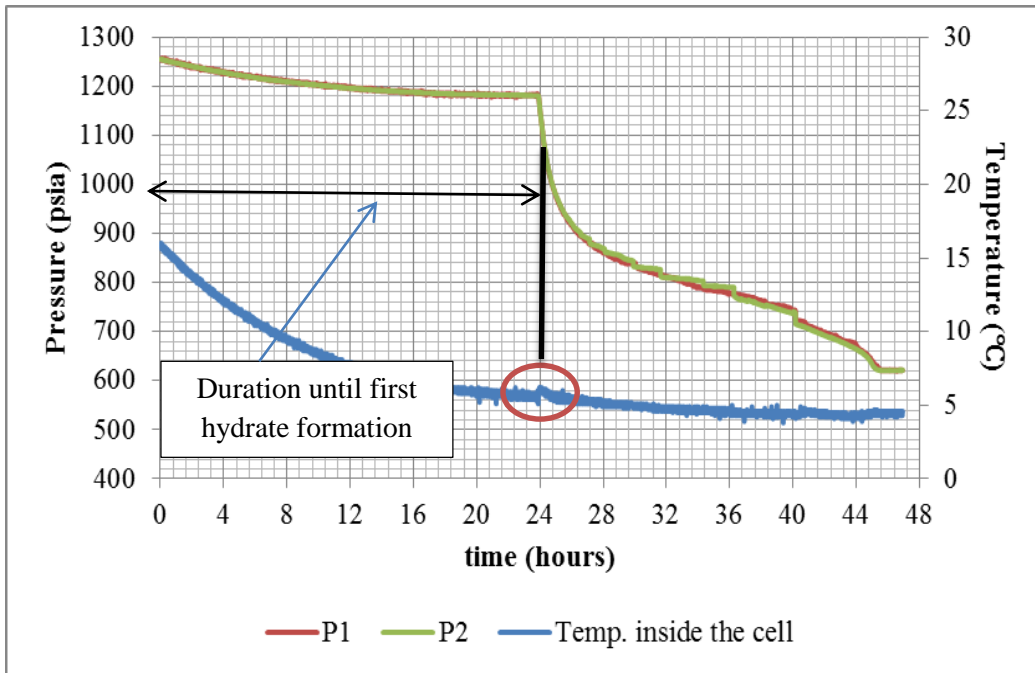


**Figure 6-4:** Illustration of hydrate formation for “Case 1”

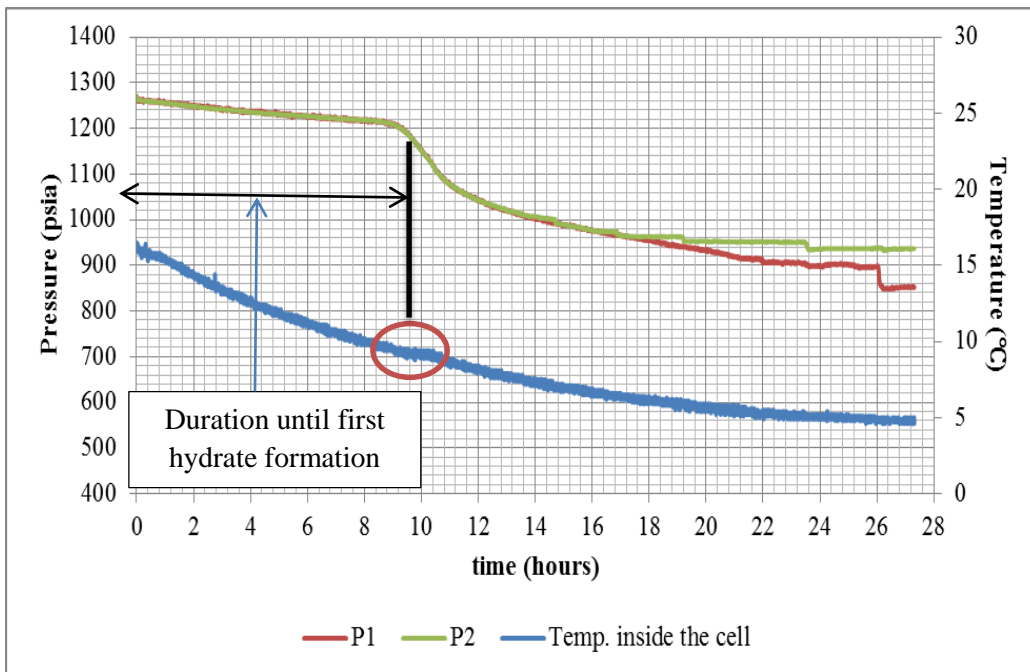


**Figure 6-5:** Illustration of hydrate formation for “Case 2”



Also, the temperature and pressure at which first hydrate formation was observed in “Case 2” was relatively higher than in “Case 1” ( $P \approx 1180 \text{ psia}$  and  $T \approx 5.8^\circ\text{C}$  during “Case 1” and  $P \approx 1200 \text{ psia}$  and  $T \approx 9.4^\circ\text{C}$  for “Case 2”). It should be noted that pure methane hydrate formation temperatures at 1180 psia and 1200 psia are  $11.5^\circ\text{C}$  and  $11.7^\circ\text{C}$  respectively, obtained from “CSMHYD” program which predicts the thermodynamics of stable hydrate structures at given pressure, temperature and composition conditions (Center For Hydrate Research, 2010).

Pressure versus temperature diagram ( $P$ - $T$  diagram) can give valuable information regarding formation properties of hydrates. Figure 6-6 shows combination of pressure versus temperature responses for two cases. Figure 6-6 was drawn based on the data of “Case 1” and “Case 2”. Pressure and temperature values between 24 and 45 hours of pure methane hydrate formation test (Figure 6-1) were used to construct  $P$ - $T$  diagram for “Case 1”, pressure and temperature values between 10 and 45 hours of pure methane hydrate formation for “memory effect” experiment (Figure 6-3) were used to construct  $P$ - $T$  diagram for “Case 2”.

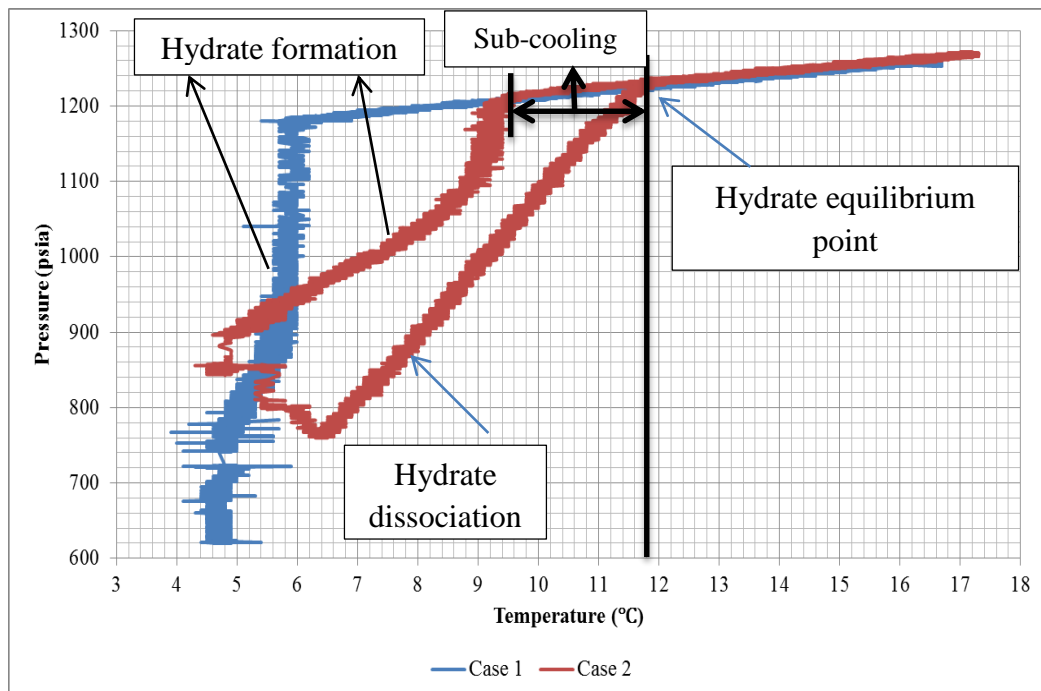


**Figure 6-6:**  $P$ - $T$  diagram for two cases

Several important conclusions can be obtained from the analysis of the Figure 6-6. Temperature spans of sub-cooling process for two cases differ significantly. The temperature interval of sub-cooling for “Case 2” is considerably lower than that of “Case 1”. At hydrate equilibrium point, pressure is equal to 1230 psia and temperature is equal to 11.8°C. It should be noted that at a pressure of 1230 psia hydrate equilibrium temperature obtained from “CSMHYD” program (Center For Hydrate Research, 2010) is equal to 11.9°C. For “Case 1” no dissociation was carried out, because of the fact that pressure was increased for free water consumption.

Formation of hydrate and observation of an increase in temperature corresponds to sharp decrease in slope in pressure. The first point when this decrease in slope starts is the initial point for comparison. In Figure 6-7 number of moles of free gas versus time is illustrated instead of pressure versus time. A computer program (FORTRAN) developed by Parlaktuna and Dogan (2002) was used in calculation of free gas mole numbers. In this program, calculation of the number of free gas moles is done by using the real gas law defined in Equation 6-1 (Bulbul, 2007). The program calculates compressibility factor ( $z$ ) at first stage according to pressure and temperature conditions (Bulbul, 2007). Volume of the free gas inside the cell is taken to be 190 cm<sup>3</sup> by ignoring expansion of volume created by hydrate formation. The expansion of the volume by hydrate formation is ignored based on the fact that water inside the sediments was partially consumed for hydrate formation in both cases.

$$P * V = z * n * R * T \quad (6-1)$$

where;

P: pressure inside the cell (psia)

V: volume of the free gas occupied (ft<sup>3</sup>)

z: gas compressibility factor

n: number of free gas moles inside the cell, moles

T: temperature inside the cell ( $^{\circ}R$ )

R: universal gas constant ( $10.73 \frac{psia \cdot ft^3}{mole \cdot ^{\circ}R}$ )

As it can be seen from the plot, the behavior of number of free gas moles in the system is close to polynomial for “Case 1”, but rather it is close to linear behavior in “Case 2”. The linearity in behavior can be linked to the fact that “memory effect” of water plays significant role in forming or hosting new gas molecules for hydrate formation, as water molecules were already exposed to hydrate formation, and during repetition hydrate formation tends to exhibit linear behavior.

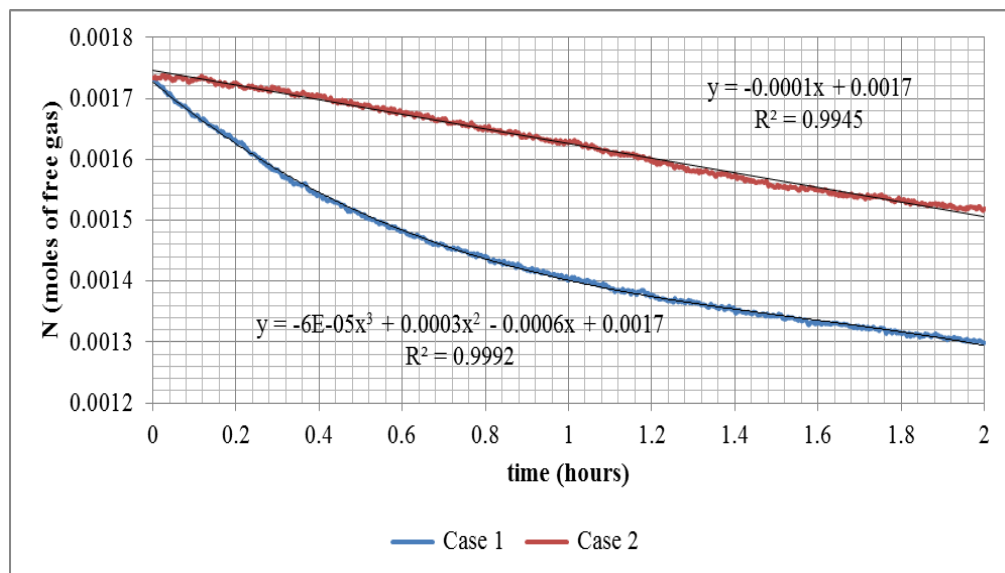


**Figure 6-7:** Combination of responses for two cases after first 2 hours from the start of sharp decrease in slope in pressure, *i.e.*, observation of formation of first hydrate

### 6.3 CH<sub>4</sub>-C<sub>3</sub>H<sub>8</sub>-CO<sub>2</sub> Mixture Hydrate Formation (Run #3)

The next experiment was conducted with a mixture of gases, fractional composition of which is given in the Table 6-4. As it was mentioned at the beginning of Chapter 6, the preparation of gas mixture was carried out with the usage of MATLAB program, developed by Merey (2013). After the preparation of the gas mixture, sample for GC analysis was taken in order to determine the accuracy of the program and also to check the values. Table 6-4 illustrates the results of this analysis, and the achieved values are quite reliable and are very close to target values.

Sand sediments, dried at 105 °C for one day after the experiment with pure methane, were used in order to pack the cell. For this case, experimental parameters are shown in Table 6-3.

**Table 6-3:** Experimental parameters of Run #3

Void volume calculated by air injection,  cm <sup>3</sup>	Void volume calculated by water injection,  cm <sup>3</sup>	Water volume,  cm <sup>3</sup>	Water saturation,  %
<b>311</b>	<b>304</b>	<b>156</b>	<b>50.2</b>

**Table 6-4:** Composition of the prepared gas mixture

<b>Component</b>	<b>Mole percent (%)</b>
<i>CH<sub>4</sub></i>	95.095
<i>C<sub>2</sub>H<sub>6</sub></i>	0.019
<i>C<sub>3</sub>H<sub>8</sub></i>	2.965
<i>CO<sub>2</sub></i>	1.810
<i>i-butane</i>	0.054
<i>n-butane</i>	0.056

From the Table 6-4 it is evident that some impurities such as ethane, i-butane and n-butane are present in the prepared gas mixture. Their occurrence can be attributed to the fact that propane that was used in preparing gas mixture was present not in pure form – several other hydrocarbons existed as well.

Initial temperature was set to 16°C and initial pressure was set to 1291 psia. Initial conditions were set similar to the previous experiment with pure methane. After waiting for 12 hours and being sure that no leakage is present, cooler was started in

order to cool the system down to 4°C. The illustration of the behavior of the system is expressed in Figure 6-8. Pure methane hydrate formation graph is also plotted in order to observe the differences between these two conditions. As it can be observed, formation of hydrate from mixture of hydrates is accomplished earlier than formation of pure methane hydrate. This observation is quite reasonable, because of the fact that the equilibrium pressure at 16 °C for the mixture of gases with specified composition is equal to 828.5 psia (Center for Hydrate Research, 2010). The start of the experiment corresponds to the pressure value of 1290 psia approximately for the mixture of gases, therefore, conditions are above equilibrium pressure, and hydrate formation directly starts. In pure methane case, at 16 °C hydrate equilibrium pressure is equal to 1923 psia (Center for Hydrate Research, 2010) and initial condition for pressure value (1300 psia approximately) is less than equilibrium pressure. Therefore, formation of hydrate will not be accomplished until the pressure inside the cell will reach a value above hydrate equilibrium pressure. During that interval, methane will dissolve inside water, and also nucleation of hydrate will take place continuously, but the system will not be able to form hydrates.

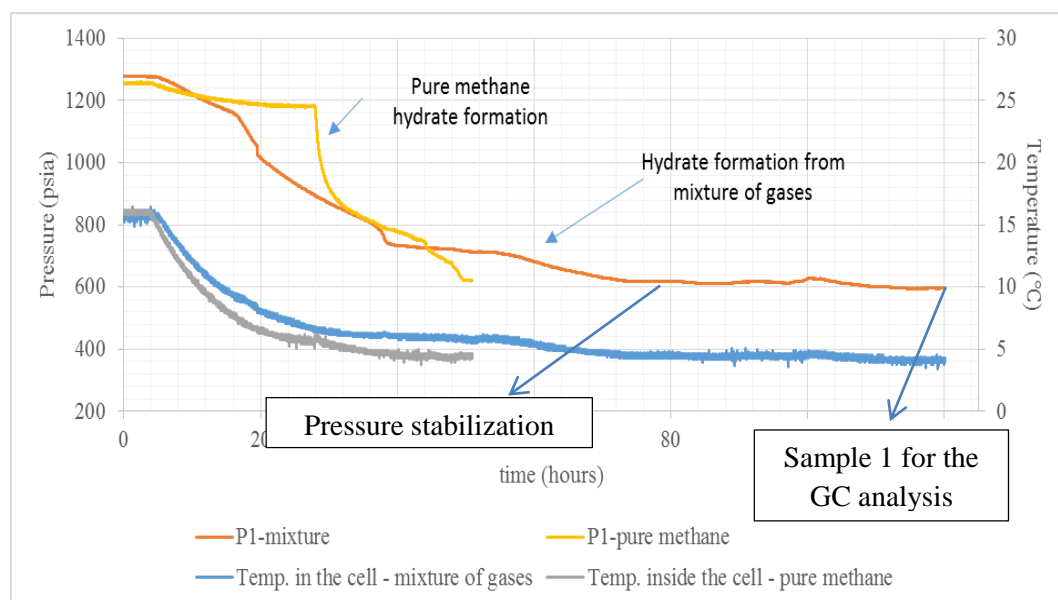


**Figure 6-8:** Behavior of the system for the first 120 hours

It should be noted that during natural gas hydrate formation from the mixture of gases, composition changed continuously until pressure stabilization was achieved. At the end of pressure stabilization a sample for gas chromatography was taken. Results of the analysis are illustrated in Table 6-5.

**Table 6-5:** Sample 1 results

<b>Component</b>	<b>Mole percent (%)</b>
<i>CH<sub>4</sub></i>	98.671
<i>C<sub>2</sub>H<sub>6</sub></i>	0.007
<i>C<sub>3</sub>H<sub>8</sub></i>	0.357
<i>CO<sub>2</sub></i>	0.931
<i>i-butane</i>	0.006
<i>n-butane</i>	0.027

The results from the analysis indicate that the amounts of propane and carbon dioxide drastically decreased as compared to that of methane, fraction of which increased in the mixture. To explain this observation, comprehensive analysis of hydrate stability theory explained in Section 2-1 should be visited, especially Table 2-2 should be carefully analyzed.

Table 2-2 is of great importance in interpreting consumption of moles of gases in the mixture. It can be inferred that propane stabilizes large  $5^{12}6^4$  cavity of sII structure only. Methane with diameter ratio of 0.655 is not able to stabilize the large cavity of sII and carbon dioxide (0.769) cannot easily compete with propane (0.943) in stabilizing  $5^{12}6^4$  cavity of sII.

Therefore, mole percent of  $C_3H_8$  drastically decreased in the free gas composition. It can be noted that consumption of methane will be lower than consumption of carbon dioxide when diameter ratios are considered.  $CO_2$  having 1.00 and 1.02

guest diameter/cavity diameter ratio respectively for  $5^{12}$  cavities of sI and sII will be more easily able to form hydrate structure, as compared to  $\text{CH}_4$ , which has 0.86 and 0.87 ratios. So, the fraction of methane in gas phase increased significantly.

Figures 6-9 and 6-10 show pictures of the hydrate formed in sand sediments in case of mixture of gases.



**Figure 6-9:** Clear picture of formed hydrate in sand sediments



**Figure 6-10:** Inflammation of hydrate formed in sand sediments

#### **6.4 “Memory Effect” of CH<sub>4</sub>-C<sub>3</sub>H<sub>8</sub>-CO<sub>2</sub> Mixture Hydrates (Run #4)**

In this experiment, the remaining pressure in the cell was released and was let to stabilize for approximately one day. Also the cooler was set to 16.1°C to sustain initial conditions. When temperature reached required value, the pressure was again increased up to 1291 psia. This was accomplished in order to investigate the “memory effect” when applying the same initial conditions. Response of the system is expressed in Figure 6-11.



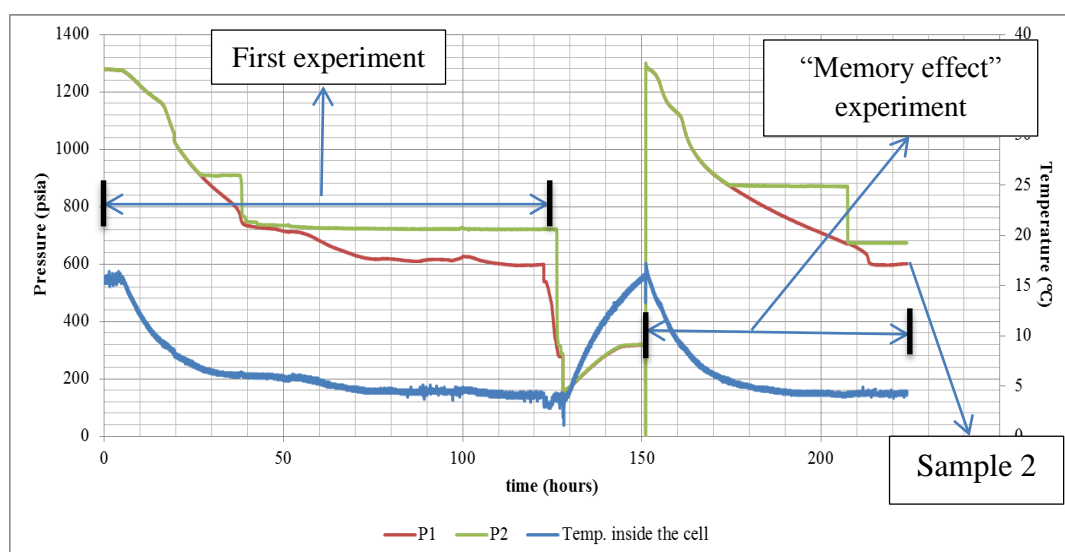


**Figure 6-11:** Illustration of the system response until the end of “memory effect”

Results of the analyses from the gas chromatography after the “memory effect” are shown in Table 6-6.

**Table 6-6:** Sample 2 results

Component	Mole percent (%)
$CH_4$	98.767
$C_2H_6$	0.007
$C_3H_8$	0.148
$CO_2$	1.043
<i>i-butane</i>	0.003
<i>n-butane</i>	0.031

From Tables 6-5 and 6-6 it can be inferred that there is no significant difference between the two measurements, therefore experiments were successfully performed.

As in the case of pure methane, number of moles in gas phase versus time were prepared, which are shown in Figures 6-12 and 6-13. However, no clear equation

can be established in this case. From the Figure 6-13 it can be seen that after approximately 3.5 hours there is drastic decrease in number of free gas moles versus time for “Case 2”.

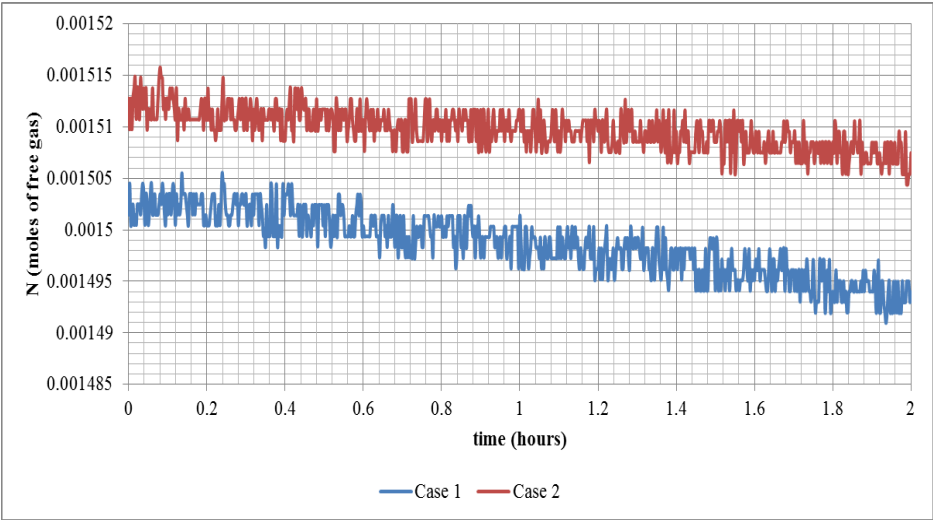


**Figure 6-12:** Combination of responses for two cases after first 2 hours from the start of sharp decrease in slope of pressure, i.e., observation of formation of first hydrate

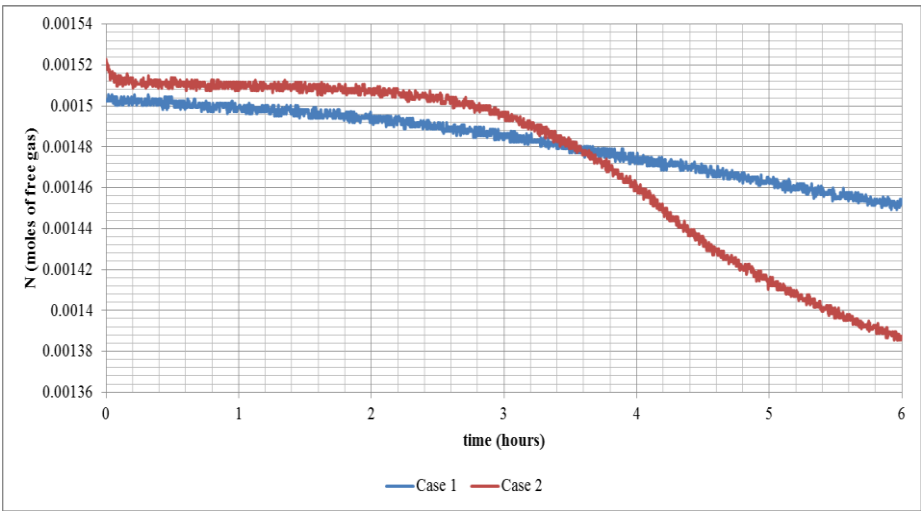


**Figure 6-13:** Combination of responses for two cases after first 6 hours from the start of sharp decrease in slope of pressure, i.e., observation of formation of first hydrate

### 6.5 CO<sub>2</sub> Injection from Constant Pressure Supply (Run #5)

In this experiment formation of hydrate was accomplished and afterwards injection of CO<sub>2</sub> from constant pressure source into the system was initiated. The illustration of the behavior of the system for complete hydrate formation and consumption of all the water inside sediments is given in Figure 6-14. Experimental parameters are given in Table 6-7.

**Table 6-7:** Experimental data for Run #5

Void volume calculated by air injection, cm <sup>3</sup>	Void volume calculated by water injection, cm <sup>3</sup>	Water volume, cm <sup>3</sup>	Water saturation, %
<b>325</b>	<b>315</b>	<b>172</b>	<b>53.1</b>

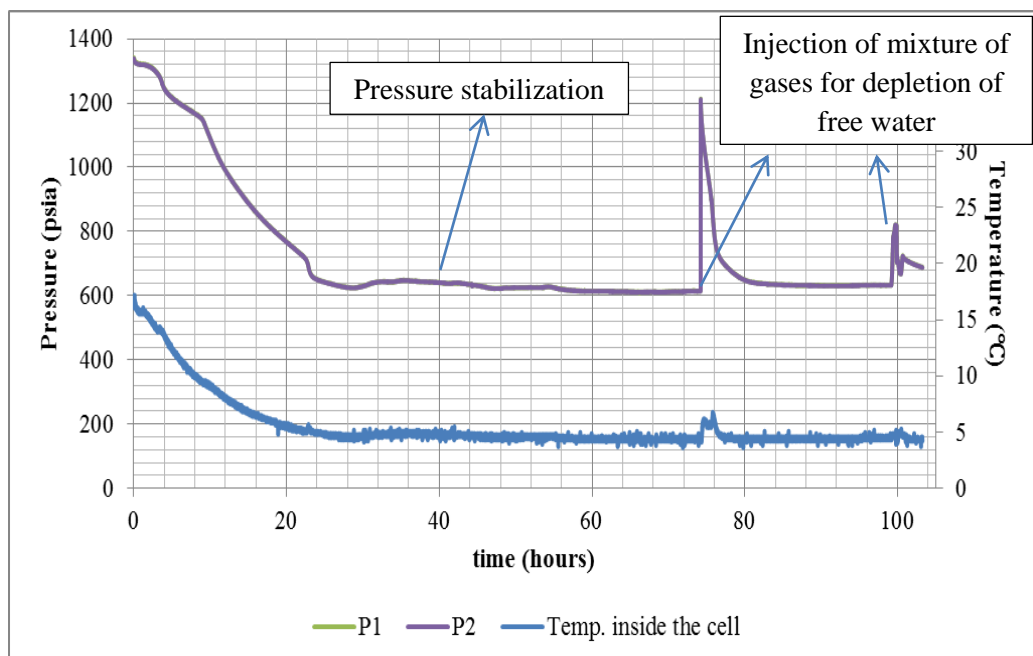


**Figure 6-14:** Illustration of hydrate formation for the first 104 hours

At the end of this experiment a sample was taken and sent for gas chromatography analysis again and the results are given in Table 6-8.

**Table 6-8:** Composition of the gas mixture at the end of hydrate formation

<b>Component</b>	<b>Mole percent (%)</b>
<i>CH<sub>4</sub></i>	98.666
<i>C<sub>2</sub>H<sub>6</sub></i>	0.003
<i>C<sub>3</sub>H<sub>8</sub></i>	0.125
<i>CO<sub>2</sub></i>	1.184
<i>i-butane</i>	0.002
<i>n-butane</i>	0.019

At the end of the experiment of formation of hydrate the start of constant CO<sub>2</sub> injection from the constant pressure source cylinder is implemented. CO<sub>2</sub> is injected from the bottom of the cell and its pressure is recorded by pressure transducer P3, located in the tubing connecting the constant pressure cylinder and the bottom part of the high-pressure cell (Figure 6-15). Therefore, the pressure inside the high-pressure cell, and the pressure of the CO<sub>2</sub> injected is known. The pressure inside CO<sub>2</sub> cylinder is approximately equal to 772 psia, but it can change according to the room temperature conditions. The illustration of the behavior of the system for the first 112 hours is given in Figure 6-16.

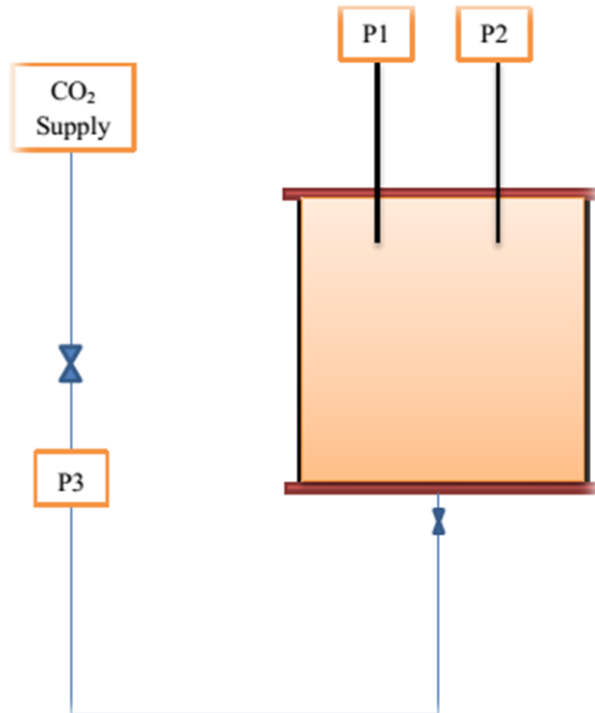


**Figure 6-15:** Schematic representation of constant carbon dioxide injection process

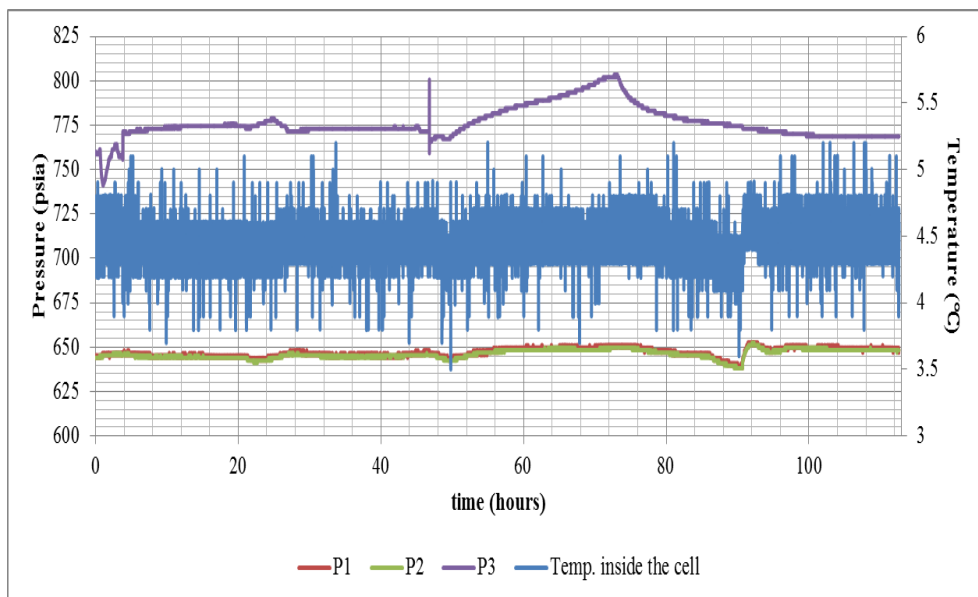


**Figure 6-16:** Response of the system from the start of CO<sub>2</sub> injection for 112 hours

As it can be seen from the Figure 6-16, no significant change in the system was observed from the beginning up to the first 112 hours of the experiment. Actually, while completely depleting water for the formation of hydrate, significant reduction in permeability was observed. This observation is based on the fact that it was hard to increase the pressure in order to reduce the amount of water inside the cell. For example, to increase the pressure up to a value of 1200 psia inside a cell, syringe pump applied a pressure of 2500 psia for approximately 10 minutes. With each decrease of amount of water for formation of hydrate even higher pressure was required to apply on the cell. Also, because of the fact that gravity pulls water down, higher hydrate saturations in the lower layered sediments is a fact. Therefore, it is very hard to break up the solid bonds of hydrate by injecting CO<sub>2</sub> at the given pressure (772 psia approximately). The injection of carbon dioxide was continued for another 146 hours approximately and the behavior of the system during this time period is given in Figure 6-17.

The continuation of injection of CO<sub>2</sub> from the constant pressure cylinder did not have any effect on the pressure distribution inside the cell, nor did it have any CH<sub>4</sub> replacing effect as well, because CO<sub>2</sub> was not able to penetrate through the impermeable barrier throughout the sediments in the bottom part of the cell.

Therefore, after waiting for approximately 250 hours, and observing no change in pressure distribution, it can be proposed that the injection of CO<sub>2</sub> at 772 psia pressure was not be able to replace CH<sub>4</sub> in sediments, nor it was even able to flow through sediments.

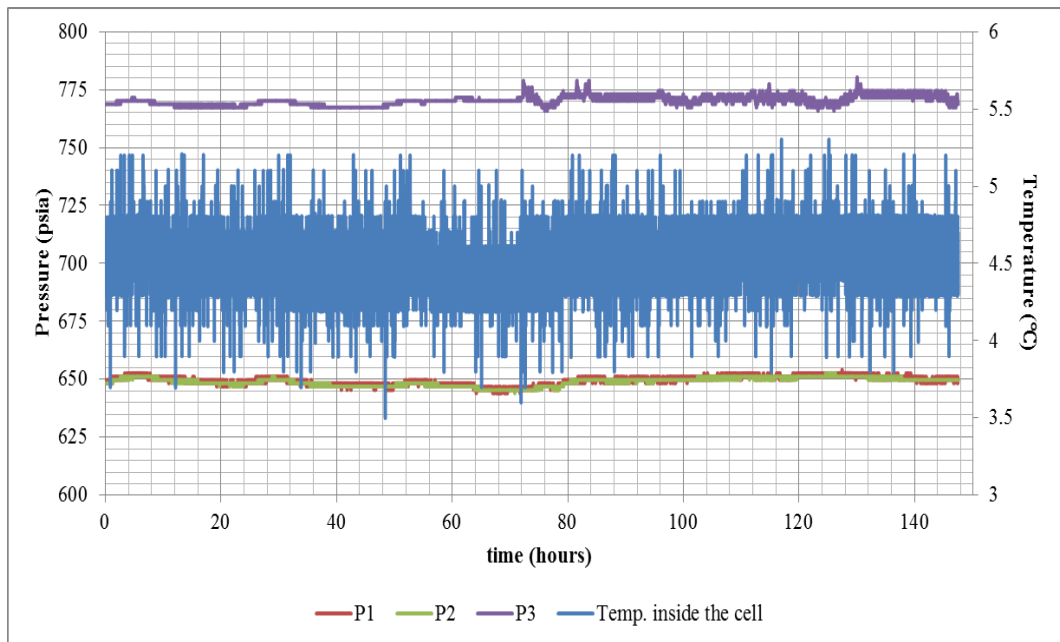


**Figure 6-17:** Response of the system after another 145 hours

It is possible that the distribution of hydrate saturation is not the same inside the cell and higher saturation in the bottom part of the cell and relatively low saturation in the upper parts are expected. This is attributed to gravitational force as it was mentioned earlier. Therefore, it was decided to inject CO<sub>2</sub> from the upper part of the high-pressure cell. The illustration of the behavior of the system after injection of CO<sub>2</sub> from the upper part of the cell is given in Figure 6-18. As it can be seen from the Figure 6-18, upon injection the pressure inside the cell increases to that of almost injection pressure value. But, after waiting for approximately 50 hours, no significant change in pressure and temperature is observed. Injected carbon dioxide was not able to replace methane and subsequent increase in free gas pressure was not observed. Subsequent rise in pressure results from the fact that methane will be replaced from the hydrate phase and will exert significant pressure inside the system. It is supposed that in this case also, injected CO<sub>2</sub> was not able to penetrate through the impermeable hydrate layers from upwards.

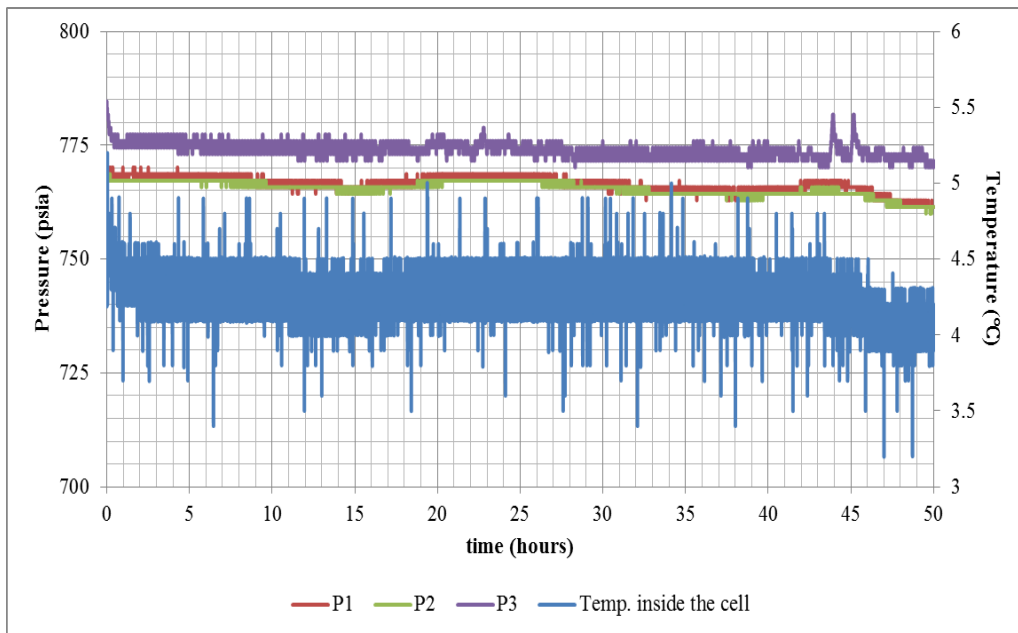


**Figure 6-18:** Response of the system upon injection of CO<sub>2</sub> from the top part of the cell after 50 hours

At the end of 50 hours period the experiment was finished and before releasing the system, sample for gas chromatography analysis was taken. Results are expressed in Table 6-9.

If Tables 6-8 and 6-9 are compared, it can be stated that mole percent of CO<sub>2</sub> together with C<sub>3</sub>H<sub>8</sub> increased. A decrease in CH<sub>4</sub> is observed on the contrary. Because gas composition inside the cell was subject to constant injection of CO<sub>2</sub>, carbon dioxide increase in the mixture together with CH<sub>4</sub> decrease is reasonable. However, an increase in number of moles of C<sub>3</sub>H<sub>8</sub> implies that injection of CO<sub>2</sub> resulted in escape of propane molecules from hydrate media.



**Table 6-9:** Composition of the gas mixture at the end of CO<sub>2</sub> injection

<b>Component</b>	<b>Mole percent (%)</b>
<i>CH<sub>4</sub></i>	92.403
<i>C<sub>2</sub>H<sub>6</sub></i>	0.035
<i>C<sub>3</sub>H<sub>8</sub></i>	1.129
<i>CO<sub>2</sub></i>	6.365
<i>i-butane</i>	0.018
<i>n-butane</i>	0.051

### 6.6 Replacement of Free Gas with CO<sub>2</sub> (Run #6)

In the next experiment which was carried out, different technique was implemented. Instead of applying carbon dioxide into the already formed hydrate from constant pressure source and waiting for some time, it was decided to simultaneously inject CO<sub>2</sub> and withdraw free gas above the formed hydrate in the sediments (Figure 6-19). To do so, the amount of sand pack was reduced and clear zone was left for free gas to evolve. Upon complete consumption of water for hydrate formation, this free gas composition was gradually removed by applying constant CO<sub>2</sub> into the cell. Afterwards, the response of the system to the injected carbon dioxide was investigated. For this case, experiment was carried out by using the parameters shown in Table 6-10.

**Table 6-10:** Experimental parameters for Run #6

Void volume calculated by air injection, cm <sup>3</sup>	Void volume calculated by water injection, cm <sup>3</sup>	Water volume, cm <sup>3</sup>	Water saturation in the cell, %
<b>465</b>	<b>452</b>	<b>245</b>	<b>52.6</b>

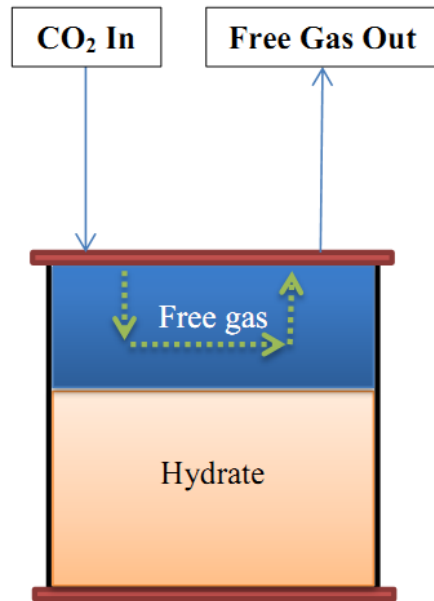


**Figure 6-19:** Schematic representation of replacement process

In this case, because of the fact that less amount of sand pack was used, void volume increases. The same initial conditions were used for hydrate formation in this case. Complete behavior of the system is given in Figure 6-20. The pressure of the CO<sub>2</sub> injected into the cell was approximately equal to 701 psia. When the process of simultaneous CO<sub>2</sub> injection and free gas withdrawal was started, firstly the pressure of the free gas increased to a value of injected CO<sub>2</sub>, 701 psia from an initial constant value of 657 psia. At the instant when the process was completed and the valves of the tubes for both injection and withdrawal were closed, the pressure exerted by free gas started to increase and simultaneous drop in temperature inside the cell was observed. The free gas pressure increased to a value of 753 psia approximately and stayed constant. Detailed illustration of the above mentioned observations is described in Figures 6-21 and 6-22. Also, gas samples for the analysis were taken both during replacement process of free gas and during subsequent stabilization of the system, results of which are given in Table 6-11.

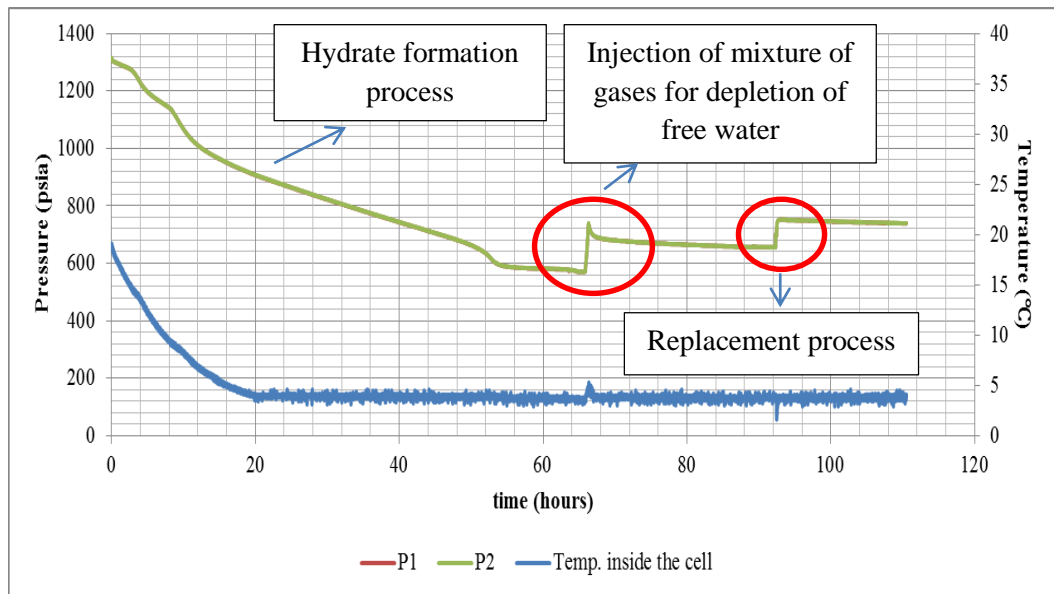


**Figure 6-20:** Total response of the system for the case of simultaneous CO<sub>2</sub> injection and free gas withdrawal

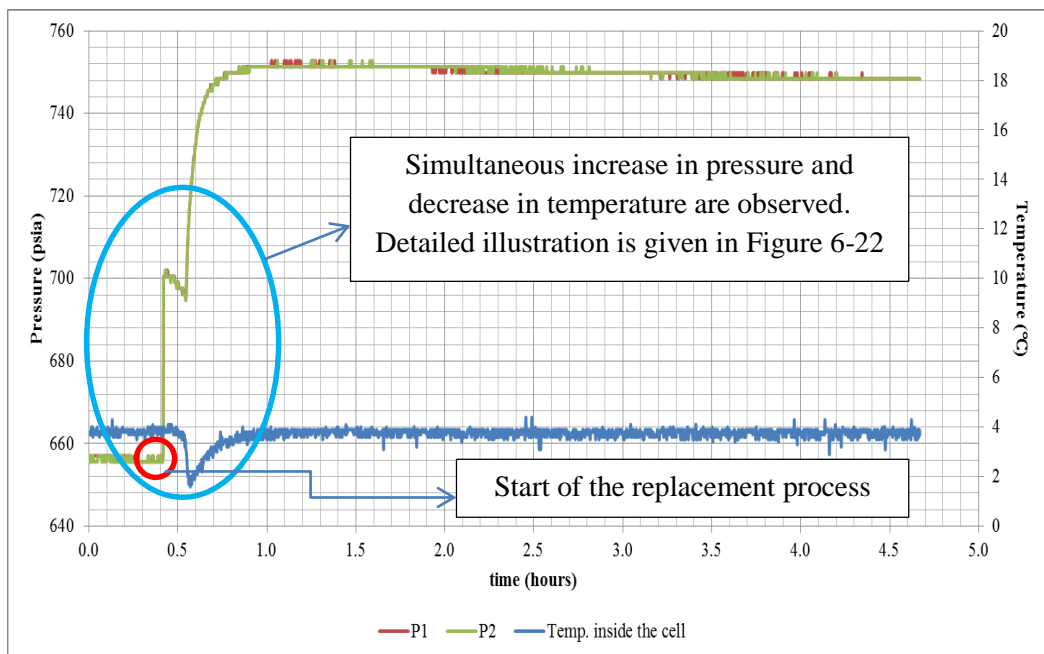


**Figure 6-21:** Response of the system during the first 4 hours from the start of the process of CO<sub>2</sub> injection and free gas removal

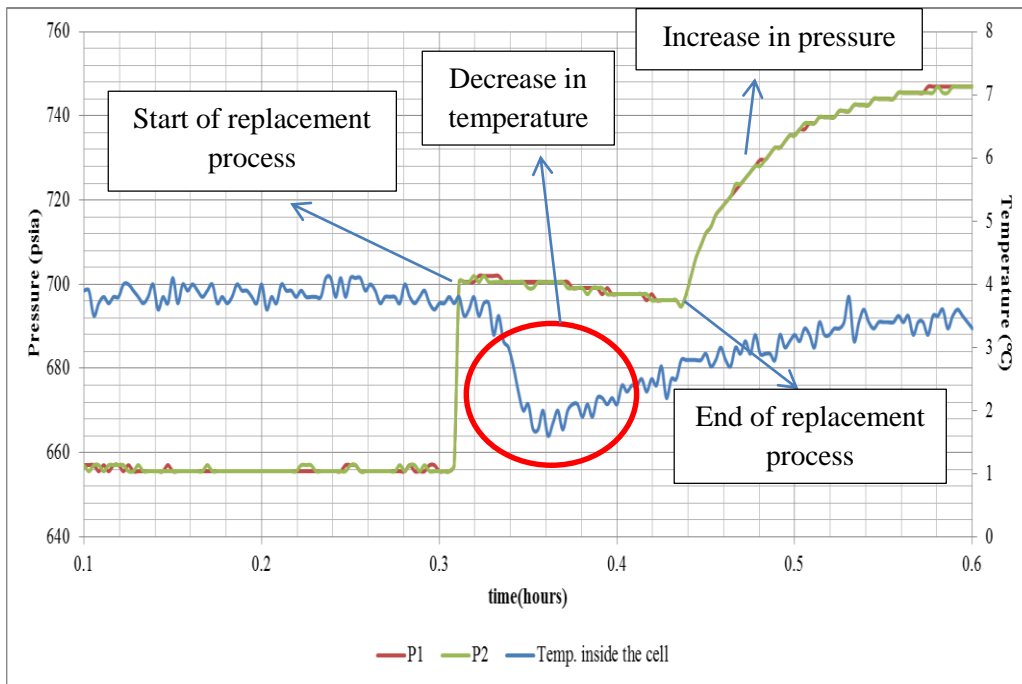


**Figure 6-22:** Detailed illustration of the effects of replacement process on the hydrate media

**Table 6-11:** Composition of the gas mixture during and after free gas replacement

Component	Mole percent during replacement (%)	Mole percent after replacement (%)
$CH_4$	20.139	36.494
$C_2H_6$	-	0.006
$C_3H_8$	0.103	1.120
$CO_2$	79.758	62.360
<i>i-butane</i>	-	0.019
<i>n-butane</i>	0.006	0.025

Gas chromatography analyses support the fact that after the free gas replacement by injected  $CO_2$ , “ $CH_4$ - $CO_2$  swap” took place in the system. At the instant when the valve was closed, sudden decrease in temperature and increase in free gas pressure

suggest that CH<sub>4</sub> trapped inside hydrate was pulled out and hydrate dissociation occurred, which is an endothermic reaction. Also, although both CH<sub>4</sub> and CO<sub>2</sub> form structure I hydrate and most probably CO<sub>2</sub> will displace CH<sub>4</sub> from the system, significant increase (almost 10 fold) in C<sub>3</sub>H<sub>8</sub> fraction is observed despite the fact that C<sub>3</sub>H<sub>8</sub> forms class II hydrate.

It is also necessary to consider phase state of the mixture inside the cell during and after replacement processes. For the compositions during and after replacement processes given in Table 6-11 phase diagram was established, shown in Figures 6-23 and 6-24 using Prode software, which is designed to predict properties of pure fluids and mixtures, multiphase equilibria and process simulation (Prode Properties, 2013). Bubble point and dew point curves are also indicated in these figures, therefore easy comparison and discussion can be made. As it can be observed from the Figures 6-23 and 6-24, experimental conditions, that is pressure and temperature conditions during and after replacement indicate that the mixture is in gaseous state.

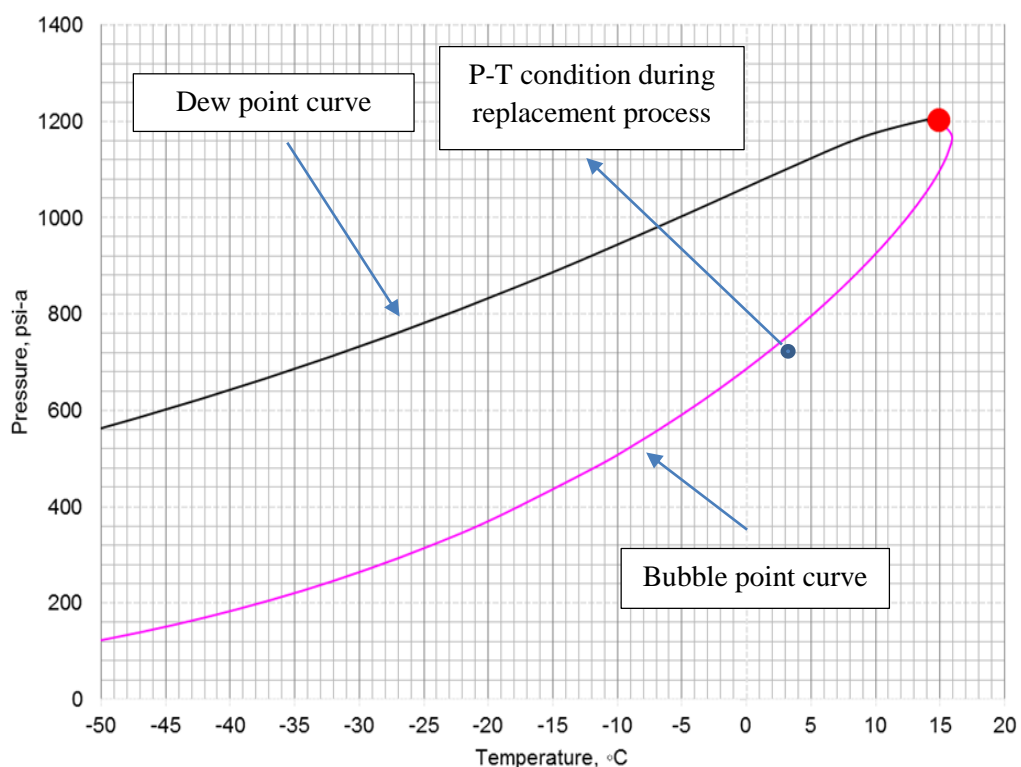


**Figure 6-23:** P-T diagram for mixture of gases during replacement (Run#6)

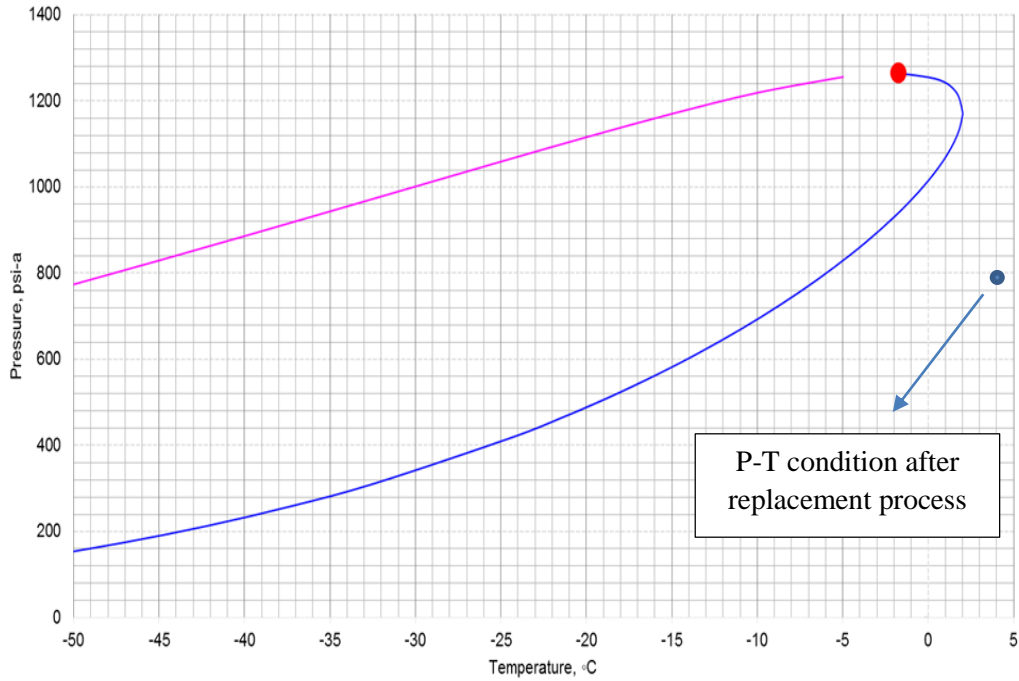


**Figure 6-24:** P-T diagram for mixture of gases after replacement (Run#6)

**6.7 Repeatability of Replacement of Free Gas with CO<sub>2</sub> Experiment (Run #7)**

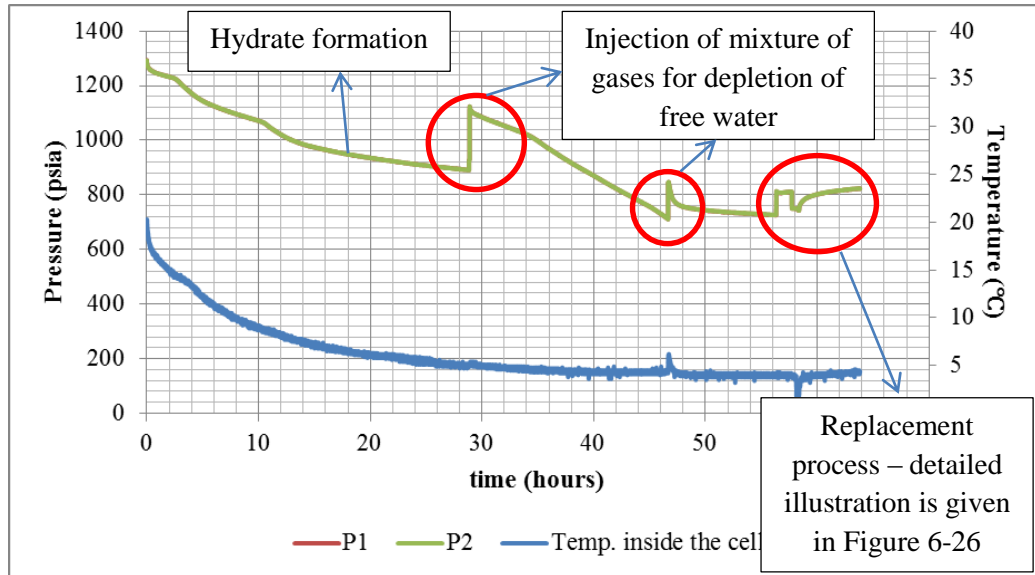
In order to observe the same effect of CO<sub>2</sub> on the formed hydrate, it was decided to repeat Run #6. Experimental parameters are given in Table 6-12.

**Table 6-12:** Experimental parameters for Run #7

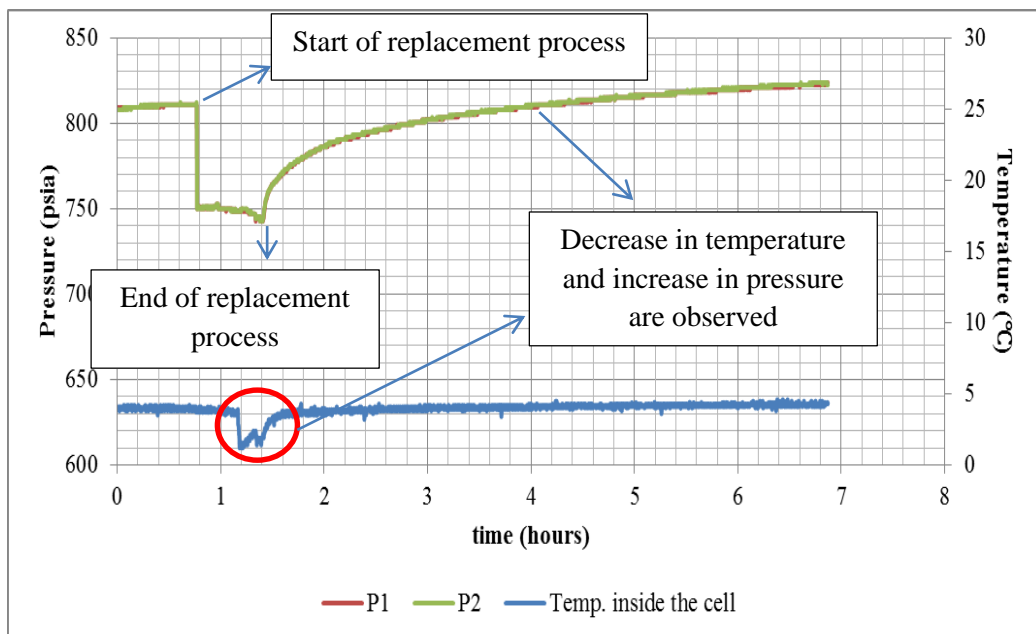
Void volume calculated by air injection, cm <sup>3</sup>	Void volume calculated by water injection, cm <sup>3</sup>	Water volume, cm <sup>3</sup>	Water saturation in the cell, %
<b>455</b>	<b>442</b>	<b>215</b>	<b>47</b>

Illustration of the behavior of the system starting from the beginning is given in Figure 6-25. It can be seen from the Figure 6-25 that at the point of CO<sub>2</sub> injection and free gas replacement decrease in temperature and subsequent increase in pressure are observed. If that portion of the process is investigated in details and

also in a smaller range of time, major changes can be clearly noted. Figure 6-26 illustrates the response of the system in a small range of time period.



**Figure 6-25:** Response of the system during repeatability experiment



**Figure 6-26:** Detailed illustration of the effects of replacement of free gas by CO<sub>2</sub> in the case of repeatability experiment

Samples for gas chromatography analysis were taken in this case as well and the results are described in Table 6-13.

**Table 6-13:** Results for the replacement process of the free gas with CO<sub>2</sub> for “Repeatability Experiment”

<b>Component</b>	<b>Mole percent during replacement (%)</b>	<b>Mole percent after replacement (%)</b>
<i>CH<sub>4</sub></i>	14.236	97.470
<i>C<sub>2</sub>H<sub>6</sub></i>	-	0.004
<i>C<sub>3</sub>H<sub>8</sub></i>	0.0215	0.158
<i>CO<sub>2</sub></i>	85.742	2.336
<i>i-butane</i>	-	0.002
<i>n-butane</i>	-	0.029

Phase diagrams are also constructed in order to discuss phase state of the mixture in case of Run#7. These diagrams are illustrated in Figures 6-27 and 6-28. It can be inferred from Figure 6-27 that prevailing P-T conditions in the cell during replacement process indicate that the system is in two-phase (vapor and liquid) state. This indication is quite reasonable, because the mole fraction of CO<sub>2</sub> inside the gas mixture is very high, and CO<sub>2</sub> tends to be in liquid state at the prevailing P-T conditions. But, if Figure 6-28 is analyzed, it can be inferred that after replacement the system is completely in gas phase, because of the fact that methane has a very high fraction inside the gas mixture in this case, and it is gaseous at the prevailing P-T conditions in the system.



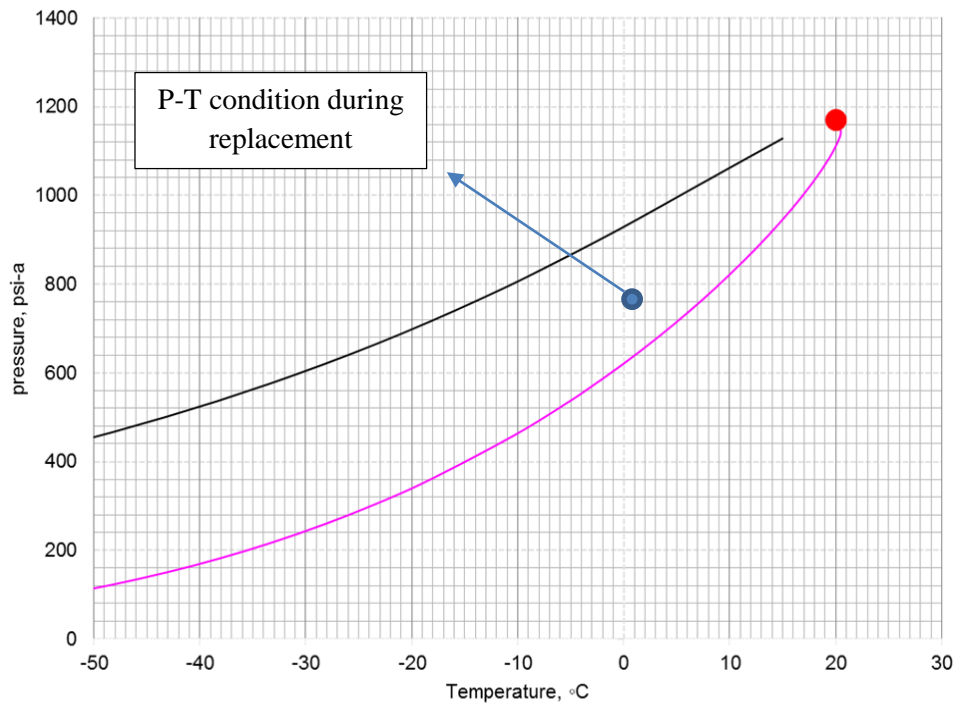


**Figure 6-27:** P-T diagram for mixture of gases during replacement (Run#7)

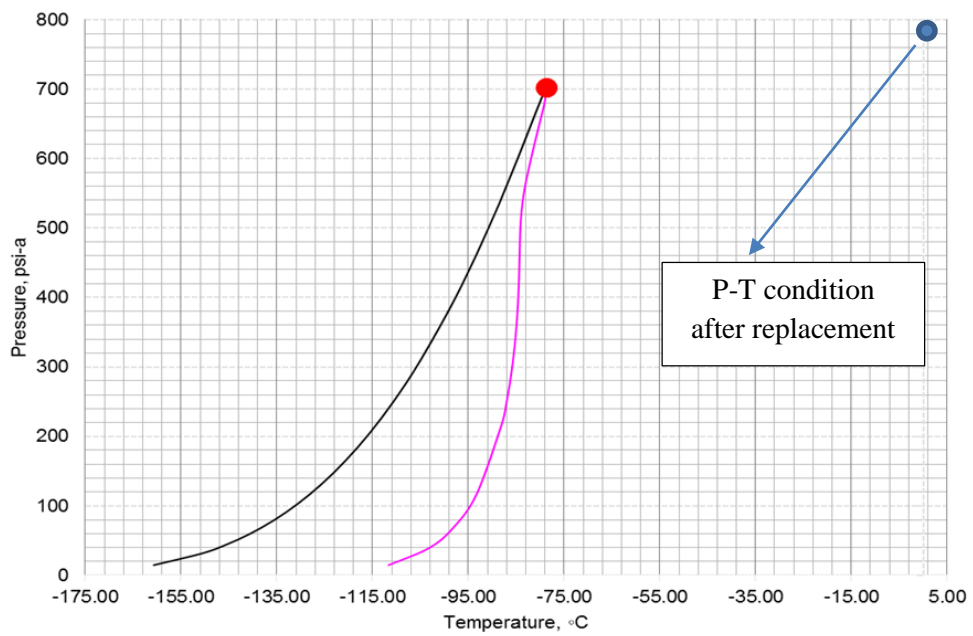


**Figure 6-28:** P-T diagram for mixture of gases after replacement (Run#7)

The experiment of replacement process of the mixture of gases by CO<sub>2</sub> was carried out several times. In total there were 4 experiments carried out. Analyses for gas chromatography were taken in three of them. Results of another test performed are summarized in Table 6-14.

**Table 6-14:** Trial 3 results for the replacement process of the free gas with CO<sub>2</sub>

<b>Component</b>	<b>Mole percent during replacement (%)</b>	<b>Mole percent after replacement (%)</b>
<i>CH<sub>4</sub></i>	3.911	96.746
<i>C<sub>2</sub>H<sub>6</sub></i>	0.037	0.008
<i>C<sub>3</sub>H<sub>8</sub></i>	0.034	0.472
<i>CO<sub>2</sub></i>	95.981	2.704
<i>i-butane</i>	0.0098	0.010
<i>n-butane</i>	0.013	0.055

It can be inferred from Tables 6-11, 6-13, 6-14 that after replacement process fractions of several gases changed drastically. Sharp increase in number of methane and propane moles is observed in free gas mixture. This observation supports the well-known CH<sub>4</sub>-CO<sub>2</sub> swap process. Clear illustration of dissociation process of hydrate was shown in Figures 6-22 and 6-26. In addition, gas chromatography analyses prove this dissociation process. Replacement of free gas by CO<sub>2</sub> resulted in decomposition of hydrate and escape of CH<sub>4</sub> in all three trials.

As it was mentioned previously, injection of carbon dioxide resulted not only in methane, but also in propane release in all three trials. Propane forms structure II hydrate and its release caused by molecule forming structure I hydrate is quite interesting. This increase in fraction is quite high. Therefore, to explain these results, a literature survey was carried out to figure out whether similar results when production of higher hydrocarbon gas was encountered.

Similar results were obtained by Beeskow-Strauch *et al.* (2012). In their study, CO<sub>2</sub> was injected to the CH<sub>4</sub>-C<sub>2</sub>H<sub>6</sub> mixed sII hydrate and a conversion to sI hydrate occurred.

The reason is explained as the larger size of both these newly introduced molecules which makes them preferentially suitable for large cages. Therefore, the aim to maximize number of large cages enforces a structural conversion of sII to sI during the replacement reaction.

As stated by Beeskow-Strauch *et al.* (2012), “offering new guest molecules to existing hydrates might result in an impulse for a structural rearrangement to optimize guest-to-cavity ratios and this restructuring process is attended by a strong molecular disorder which results in a large interface between gas and hydrate phase. In the course of an exchange reaction, it supports an intense molecule exchange between hydrate phase and adjacent gas phase”.

Their study was concluded with the remark that the key driving force for the exchange process is the aim for equilibrium state of the chemical potential between all phases. Structural changes (sI-sII) of the gas hydrates improve the effectiveness of the molecule exchange in hydrates. Thermodynamic stability in terms of *P-T* conditions has only a minor effect with respect to exchange processes and seems to influence particularly the start of the exchange.

In another similar study, made by Schicks *et al.* (2011) the following conclusions were obtained: (1) chemical disequilibrium state between the hydrate phase and environmental gas phase induces the conversion process; (2) decomposition and reformation process, in terms of rearrangement of molecules can describe the conversion process on a molecular level.

The kinetics of the process can be influenced by some other factors such as the surface area of the hydrate phase, the thermodynamic stability of the hydrate phases, the mobility of the guest molecules and the formation kinetics of the resulting hydrate phase (Schicks *et al.*, 2011).

With the experimental data presented in the work of Schicks *et al.* (2011), some new aspects were found in an area of CH<sub>4</sub> recovery from gas hydrates in nature by induction of CO<sub>2</sub>. It was found that structure II CH<sub>4</sub>-C<sub>3</sub>H<sub>8</sub> mixed hydrates, which are supposed to be more stable than simple structure I CO<sub>2</sub> hydrates, also convert into a structure I CO<sub>2</sub>-rich hydrate.

These explanations (Beeskow-Strauch *et al.*, 2012; Schicks *et al.*, 2011) can be crucial in explaining the results obtained in this study. The injection of CO<sub>2</sub> constantly from constant pressure cylinder did not have replacing effect. The surface area of the hydrate phase and the guest-to-cavity ratio in that process played significant role.

The observation of production of heavier hydrocarbons during the second case, replacement of free gas by CO<sub>2</sub> can be clearly supported by the conclusions and remarks made by Beeskow-Strauch *et al.* (2012) and Schicks *et al.* (2011).

## CHAPTER 7

### CONCLUSION

In order to investigate CH<sub>4</sub>-CO<sub>2</sub> swap process, mixture of gases with known composition was used. The mixed structure II CH<sub>4</sub>-C<sub>3</sub>H<sub>8</sub>-CO<sub>2</sub> hydrates were formed and exposed to gaseous CO<sub>2</sub>. Hydrate formation processes were analyzed together with conversion processes by using gas chromatography analysis.

After completing this experimental study, observations and experimental data suggest the following remarks:

- (1) Formation of natural gas hydrates with mixture of gases in porous media, specifically, with addition of CO<sub>2</sub> (2%) and C<sub>3</sub>H<sub>8</sub> (3%) along with CH<sub>4</sub> (95%) to form a hydrate, decreases the permeability of the unconsolidated porous media, based on experimental observations.
- (2) Gaseous CO<sub>2</sub> injected constantly from the pressure cylinder of approximately 772 psia pressure, was not able to penetrate through the cemented sediments and replace CH<sub>4</sub> from the hydrate. Therefore, predicted CH<sub>4</sub>-CO<sub>2</sub> swap process and its properties were not observed.

As it was indicated in Chapter 6, when exposure of formed hydrate to gaseous CO<sub>2</sub> did not give results, another method was implemented. The volume of the unconsolidated material was reduced to establish a space for free gas to evolve.

Then, the free gas was replaced by CO<sub>2</sub> and interaction was observed. Samples for gas chromatography were taken during and after replacement process. During that experiment there were some remarkable points to be indicated:

- (1) Exposure of the hydrate to the gaseous CO<sub>2</sub> in this case resulted in dissociation of hydrate and a decrease in temperature together with subsequent increase in pressure was observed. The decrease in temperature is clear illustration of hydrate dissociation process, as this process is an endothermic process. An increase in pressure again supports this phenomenon as number of moles of CH<sub>4</sub> increases in the system. Under constant volume and temperature assumption, an increase in number of moles results in pressure rise.
- (2) Experimental data verifies that CH<sub>4</sub> can be produced from CH<sub>4</sub>-C<sub>3</sub>H<sub>8</sub>-CO<sub>2</sub> mixture hydrates.
- (3) The results show that not only CH<sub>4</sub> but some other hydrocarbons can be produced by injection of CO<sub>2</sub>. Specifically, in this study, C<sub>3</sub>H<sub>8</sub> was produced from the hydrate as its mole fraction increased by ten-fold after the replacement process. Therefore, the release of hydrocarbon of higher number is also induced by the injection of CO<sub>2</sub>. However, this release continues up to a point when an equilibrium state between a mixed gas phase and mixed hydrate phase is reached.

## CHAPTER 8

### RECOMMENDATION

Based on the observations and conclusions from this experimental study several recommendations can be proposed:

- (1) In the future studies it is highly recommended to continuously monitor gas composition while injecting CO<sub>2</sub> from constant pressure source and also during and after replacement process of free gas mixture above formed hydrate by CO<sub>2</sub>.
- (2) It is also recommended to determine the hydrate saturation profile inside the cell by using CT (Computer Tomography) scan during and after hydrate formation.
- (3) According to the results of this study, the stability of newly formed CO<sub>2</sub> hydrate after replacement process is under question. In a hydrate reservoir, newly formed CO<sub>2</sub> hydrate may be exposed to natural gases released from deeper sources. The flow rate of the natural gas moving upward can vary, therefore the concentration of hydrocarbon in the pore water can also change – this may lead to conversion of CO<sub>2</sub> rich hydrate in a natural environment into hydrocarbon hydrate, thus, releasing CO<sub>2</sub> into the ecosystem. Based on this scenario, in the future studies it is recommended to implement the replacement in reversed order. Firstly, it is necessary to form hydrate from CO<sub>2</sub> or from a mixture of CO<sub>2</sub> with hydrocarbon gases and furthermore expose formed hydrate to hydrocarbon gas/hydrocarbon gas mixture and observe reconversion of formed structure I CO<sub>2</sub>-rich hydrate into structure II

or structure I hydrate depending on the gas which was used during exposure process.



## REFERENCES

- Anderson, R., Llamedo, M., Tohidi, B., Burgass, R.W., “Experimental measurement of methane and carbon dioxide clathrate hydrate equilibria in mesoporous silica”. *J. Phys. Chem. B* 2003, 107, 3507-3514.
- Beeskow-Strauch, B., Schicks, J.M., “The driving forces of guest substitution in gas hydrates – a laser Raman study on CH<sub>4</sub>-CO<sub>2</sub> exchange in the presence of impurities”. *Energies* 2012, 5, 420-437.
- Bulbul, S., “Hydrate Formation Conditions of Methane Hydrogen Sulfide Mixtures”, MSc Thesis, Middle East Technical University, 2007.
- Center for Hydrate Research, CSMHYD software, Chemical Engineering Department, Colorado School of Mines. Retrieved from: <http://www.hydrates.mines.edu> (Accessed on August 7, 2014).
- Chen Z., Yang H., Huang Q., “Characteristics of cold seeps and structures of chemo-auto-synthesis-based communities in seep sediments”. *J. Trop. Oceanogr.* 2007, 26 (6), 73–82.
- Clayton C. “Source volumetrics of biogenic gas generation bacterial gas”. Paris: Technip; 1992. p. 191–204.
- Collett, T.S. “Energy Resource Potential of Natural Gas Hydrates”. *AAPG Bulletin: Tulsa, OK, USA, 2002; Volume 86, pp. 1971–1992.*
- DhanuKa, V.V., DicKson, J.L., Ryoo, W., Johnston, K.P., “High internal phase CO<sub>2</sub>-in-water emulsions stabilized with a branched nonionic hydrocarbon surfactant”. *J. Colloid Interface Sci.* 2006, 298, 406–418.40.

Froelich P., Kvenvolden K., Torres M. “Geochemical evidence for gas hydrate in sediments near the Chile Triple Junction”. In: Proceedings of ODP science results, College Station, TX, 1995, p. 279-86.

Geng, C.Y., Wen, H., Zhou, H., “Molecular simulation of the potential of methane reoccupation during the replacement of methane hydrate by CO<sub>2</sub>”. J. Phys. Chem. A 2009, 113, 5463–5469.

Hesse R., Harrison W., “Gas hydrates (clathrates) causing pore-water free shearing and oxygen isotope fractionation in deep-water sedimentary sections of terrigenous continental margins”. Earth Planet Sci. Lett. 1981, 11, 453–562.

Hesse R., Frappe S., Egeberg P., “Stable Isotope studies (Cl, O and H) of Interstitial waters from Site 997” Blake Ridge gas hydrate field, West Atlantic. Sci Results. 2000, 164, 129–37.

Hirohama, S., Shimoyama, Y., Tatsuta, S., Nishida, N., “Conversion of CH<sub>4</sub> hydrate to CO<sub>2</sub> hydrate in liquid CO<sub>2</sub>”. J. Chem. Eng. Jpn., 1996, 29, 1014–1020.

Holbrook W., Hoskins H., Wood W., “Methane hydrate and free gas on the Blake Ridge from vertical seismic profiling”. Science. 1996, 273, 1840–3.

Hu C., Qiu J., “Structure properties and applications of natural gas hydrates”. Nat. Gas Chem. Ind., 2000, 25(4), 48–52.

Klauda, J.B., Sandler, S.I., “Global distribution of methane hydrate in ocean sediment”. Energy Fuels, 2005, 19, 459–470.

Komatsu H., Ota M., Smith R.L., Inomata H., “Review of CO<sub>2</sub>-CH<sub>4</sub> clathrate hydrate replacement reaction laboratory studies – Properties and kinetics”. Journal of the Taiwan Institute of Chemical Engineers, 2013, 44, 517-537.

Kucuk H.M., Dondurur, D., Ozel, O., Parlaktuna, M., Sinayuc, C., Cifci, G., Meray S., Darilmaz, E., “Gas Hydrate Potential Offshore Amasra-Zonguldak and Possible Reasons for Multiple BSR Reflection Occurrence”. The 20<sup>th</sup> International

Geophysical Congress and Exhibition of Turkey, 25-27 November, 2013, Antalya, Turkey.

Kvamme, B., Graue, A., Buanes, T., Kuznetsova, T., Ersland, G., "Storage of CO<sub>2</sub> in natural gas hydrate reservoirs and the effect of hydrate as an extra sealing in cold aquifers". *Int. J. Greenhouse Gas Control* 2007, 1, 236–246.

Kvenvolden K., "A review of the geochemistry of methane in natural gas hydrate". *Org. Geochem.* 1995, 23, 997–1008.

Kvenvolden K., "Gas hydrates: geological perspective and global change". *Rev. Geophys.* 1993, 31, 173–87.

Lee, H.; Seo, Y.; Seo, Y.-T.; Moudrakovski, I.L.; Ripmeester, J. "Recovering Methane from Solid Methane Hydrate with Carbon Dioxide". *Angew. Chem. Int. Ed.* 2003, 42, 5048–5051.

Li Y., "Technique of stabilizing methane in ice". *Foreign Oilfield Eng.* 2000, 1, 27–9.

Li, Z.Z., Guo, X.Q., Chen, G.J., Wang, J.B., Yang, L.Y., Wang, T., "Experimental and kinetic studies on methane replacement from methane hydrate formed in SDS system by using pressurized CO<sub>2</sub>". *J. Chem. Ind. Eng. (China)* 2007, 58, 1197–1203.

Li, Z.Z., Guo, X.Q., Wang, J.B., Yang, L.Y., "Experiment studies on CH<sub>4</sub> recovery from hydrate using CO<sub>2</sub> in different systems". *Natu. Gas Ind.* 2008, 28, 129–132.

Li, X.S., Zeng, Z.Y., Li, G., Chen, Z.Y., Zhang, Y., Li, Q.P., "Experimental Investigation into Replacement of CH<sub>4</sub> in Hydrate in Porous Sediment with Liquid CO<sub>2</sub> injection" In: *Proceedings of the 7th International Conference on Gas Hydrates (ICGH)*, Edinburgh, UK, 17–21 July 2011.

Lu, H., Seo, Y., Lee, J., Moudrakovski, I.L., Ripmeester, J.A., Chapman, N.R., Coffin, R.B., Gardner, G., Pohlman, J., "Complex gas hydrate from the Cascadia Margin". *Nature* 2007, 445, 303–306.

Lu H., Matsumoto R., Watanabe Y., “Major element geochemistry of the sediments from Site 997, Blake Ridge, Western Atlantic”. *Sci. Results.*, 2000, 164, 147–9.

Max, M.D., Johnson, A.H., Dillon, W.P., “Economic Geology of Natural Gas Hydrate” Springer: Berlin, Germany and Dordrecht, Netherlands, 2006.

McGrail, B.P., Zhu, T., Hunter, R.B., White, M.D., Patil, S.L., Kulkarni A.S., “A New Method for Enhanced Production of Gas Hydrate with CO<sub>2</sub>” In: Proceedings of the AAPG Hedberg Conference on Gas Hydrates: Energy Resource Potential and Associated Geologic Hazards, Vancouver, Canada, 12–16 September 2004.

Merey, S. Computer Program “eos.m”. 25 May 2013.

Milkov, A.V. “Molecular and stable isotope compositions of natural gas hydrates: A revised global dataset and basic interpretation in the context of geological settings”. *Org. Geochem.*, 2005, 36, 681–702.

Nagayev, V.B., Gritsenko, A.I., Murin, V.I. “CO<sub>2</sub> Hydrates and CO<sub>2</sub> Sequestration” In: Proceedings of the All Union Conference on Calorimetry and Chemical Thermodynamics, Ivonovo, Russia, 25–27 September 1979.

Oba T., Shikama A., Okada H. “Oxygen isotopic record of the last 0.8 m.y. at the Blake Ridge, Site 994C”. *Sci. Results.*, 2000, 164, 173–5.

Ohgaki, K., Takano, K., Sangawa, H., Matsubara, T., Nakano, S. “Methane exploitation by carbon dioxide from gas hydrates-phase equilibria for CO<sub>2</sub>-CH<sub>4</sub> mixed hydrate system”. *J. Chem. Eng. Jpn.* 1996, 29, 478-483.

Ors, O., “Investigation of the interaction of the CO<sub>2</sub> and CH<sub>4</sub> Hydrate for the Determination of Feasibility of CO<sub>2</sub> Storage in the Black Sea Sediments”. MSc Thesis, Middle East Technical University, 2012.

Ota, M., Abe, Y., Watanabe, M., Smith, R.L., Inomata, H. “Methane recovery from methane hydrate using pressurized CO<sub>2</sub>”. *Fluid Phase Equilib.* 2005, 228, 553–559.

Park, Y., Kim, D.-Y., Lee, J.-W., Huh, D.-G., Park, K.-P., Lee, J., Lee, H. "Sequestering carbon dioxide into complex structures of naturally occurring gas hydrates". *Proc. Natl. Acad. Sci.* 2006, 103, 12690-12694.

Parlaktuna, M. and Dogan A. H., Computer Program "A\_Rate.For". 2 February 2002.

Paull C., Ryo M., "LEG 164 overview" In: *Proceedings of the ocean drilling program, scientific results, College Station, TX, vol 164; 2000, p. 3-10.*

Prode Properties, Multiphase equilibria in Excel, Retrieved from: <http://www.prode.com> (Accessed on August 24, 2014).

Radler, M. "World crude and natural gas reserves rebound in 2000". *Oil Gas J.* 2000, 98, 121–123.

Rueff, R.M., Sloan, E.D., Yesavage, V.F., "Heat-capacity and heat of dissociation of methane hydrates". *AIChE J.* 1988, 34, 1468–1476.

Sassen, R., Joye, S., Sweet, S.T., DeFreitas, D.A., Milkov, A.V., MacDonald, I.R., "Thermogenic gas hydrates and hydrocarbon gases in complex chemosynthetic communities, Gulf of Mexico continental slope". *Org. Geochem.* 1999, 30, 485–497.

Schicks, J.M., Luzi, M., Beeskow-Strauch, B. "The conversion process of hydrocarbon hydrates into CO<sub>2</sub> hydrates and vice versa: Thermodynamic considerations". *J. Phys. Chem. A* 2011, 115, 13324–13331.

Sloan ED. "Clathrate hydrates of natural gases". 2nd ed. New York: Marcel Dekke, 1998.

Soloviev, V.A. "Global estimation of gas content in submarine gas hydrate accumulations". *Russ. Geol. Geophys.* 2002, 43, 609–624.

Su X. "Some advances in marine gas hydrates from the Blake Ridge and the Hydrate Ridge". *Earth Sci. Front.* 2000, 7(3), 257–65.

Uchido T. “Methane hydrates in deep marine sediments-X-ray CT and NMR studies of ODP Leg 164 hydrates”. *Geol. News Geol. Surv. Jpn.*, 1997, 510, 36–42.

Uchida, T., Ikeda, I.Y., Takeya, S., Kamata, Y., Ohmura, R., Nagao, J., Zatsepina, O.Y., Buffett, B.A. “Kinetics and stability of CH<sub>4</sub>-CO<sub>2</sub> mixed gas hydrates during formation and long-term storage”. *Chem. Phys. Chem.* 2005, 6, 646–654.

Uchida, T., Takeya, S., Ebinuma, T. “Replacing Methane with CO<sub>2</sub> in Clathrate Hydrate: Observation Using Raman Spectroscopy”. In *Proceedings of the 5th International Conference on Greenhouse Gas Control Technologies*, Cairns, Australia, 13–16 September 2000.

Wang, J.B., Guo, X.Q., Chen, G.J., Li, Z.Z., Yang, L.Y. “Experimental research on methane recovery from natural gas hydrate by carbon dioxide replacement”. *J. Chem. Eng. Chin. Univ.* 2007, 21, 715–719.

Waseda A. “Organic carbon content, bacterial methanogenesis, and accumulation processes of gas hydrates in marine sediments”. *Geochem. J.* 1998, 32, 142–57.

Watanabe Y., Matsumoto R., Lu H., “Trace element geochemistry of the Blake Ridge sediments at Site 997”. *Sci. Results*, 2000, 164, 151–63.

White, M., McGrail, P. “Designing a Pilot-Scale Experiment for the production of natural gas hydrates and sequestration of CO<sub>2</sub> in class 1 hydrate accumulations”. *Energy Procedia*, 2009, 1, 3099–3106.

Whiticar M., Faber E., Schoell M. “Biogenic methane formation in marine and freshwater environments: CO<sub>2</sub> reduction vs. acetate fermentation –isotope evidence”. *Geochim. Cosmochim. Acta.* 1986, 50, 693–709.

Wright J., Dallimore S., Nixon F., “Influences of grain size and salinity on pressure temperature thresholds for methane hydrate stability in JAPEx/JNOC/GSC Mallik 2L-38 gas hydrate research-well sediments”. *GSC Bull.* 1999, 544, 229–39.

Wu Z. “Some problems when carrying out hydrate investigation and assessment by using AVO technique”. *Mar. Geol. Lett.* 2002, 18(6), 28–32.

Wu Z., Chen J., Gong J., “Application of AVO technique to the hydrate exploration”. *Mar. Geol. Lett.* 2004, 20(6), 31–5.

Xia X., Dai J., Song Y. “Resource evaluation and gas sources of submarine natural gas hydrate”. *Nat. Gas Geosci.* 2001, 12(1–2), 11–5.

Ye Y., Liu C., “Natural Gas Hydrates, Experimental Techniques”, 2013, Springer Geophysics.

Yezdimer, E.M., Cummings, P.T., Chialvo, A.A. “Determination of the gibbs free energy of gas replacement in SI clathrate hydrates by molecular simulation”. *J. Phys. Chem. A.* 2002, 106, 7982–7987.

Yoon, J.H., Kawamura, T., Yamamoto, Y., Komai. T. “Transformation of methane hydrate to carbon dioxide hydrate: in situ Raman spectroscopic observations”. *J. Phys. Chem. A* 2004, 108, 5057–5059.

Zhang Z. “Geologic control and potential resource reserve of natural gas hydrate in shallow sea”. *Nat. Gas Geosci.* 1990, 1, 25–31.

Zhang, W., Wang, Z., Li, W.Q., Li, W.Y., He, D.W. “Research progress in the enhanced replacing methane out of gas hydrate by carbon dioxide emulsion”. *Nat. Gas Chem. Eng.* 2009, 34, 59–63.

Zhao S. “Research actuality and Chinese countermeasures of natural gas hydrate”. *Adv. Earth Sci.* 2002, 17(3), 461–4.

Zhao J., Xu K., Song, Y., Liu, Weiguo., Lam W., Liu Y., Xue K., Zhu Y., Yu X., Li Q., “A review on research on replacement of CH<sub>4</sub> in Natural Gas Hydrates by use of CO<sub>2</sub>”. 2012., *Energies*, 5, 399-419.

Zheng X. “Some new development of AVO technique”. *Oil Geophys. Prospect.* 1992, 27 (3), 305–17.

Zhou, X.T., Fan, S.S., Liang, D.Q., Du, J.W. “Replacement of methane from quartz sand-bearing hydrate with carbon dioxide-in-water emulsion”. *Energy Fuels* 2008, 22, 1759–1764.